THE

LONDON, EDINBURGH, AND DUBLIN

# PHILOSOPHICAL MAGAZINE

AND

# JOURNAL OF SCIENCE.

[SEVENTH SERIES.]

*SUPPLEMENT, DECEMBER* 1929.

## LXXXVI. *Impact of Spheres of Soft Metals.*

*By* J. P. ANDREWS, *M.Sc.* *

[Plates XIII. & XIV.]

*Abstract.*

IN the first part of this paper the duration of contact during collision, of two equal spheres of the same material, is investigated with a ballistic pendulum, employing the partial discharge of a condenser to measure the duration. For aluminium, tin, brass, babbitt, and a lead-tin alloy, a law of the form $t = t_0 + a/v^n$ is obtained, where $v$ is the relative velocity at impact, $t_0$, $a$, and $n$ are constants. Zinc follows a similar law, but the constants cannot be accurately determined.

In the second part a description of the flattened areas remaining on the spheres after collision is given, and an explanation of the rim which surrounds them is offered. If $d$ is the diameter of these rims, $d = b(v - v_0)^m$, where $b$, $v_0$, and $m$ are constants different for different spheres. From $v_0$ and the elastic moduli of the materials the least pressure required to start flow is calculated in the various cases, and is found to be of the order $10^9$ dynes/cm.

* Communicated by Prof. C. H. Lees, F.R.S.

*Introduction.*

RESEARCH into the process of collision between two solid bodies has followed two main routes, originally laid down by St. Venant and Hertz respectively. Of these, the wave theory of St. Venant has been found to apply to long bars, and bodies whose dimensions are comparatively large. For bodies whose dimensions in the direction of the motion at impact are small, Hertz's theory of perfectly elastic collision is known to be more in harmony with experiment. No precise criterion can be given, but it is known that where the duration of contact is large compared with the time required for a wave of compression to travel across the body and back again Hertz's theory applies *. Thus, in the case of aluminium, where the velocity of sound is $5{\cdot}1 \times 10^5$ cm./sec., $2l/(5{\cdot}1 \times 10^5)$ has to be small compared with the duration of impact, $l$ being the appropriate linear dimension. This paper is concerned with experiments upon spheres small enough for Hertz's theory to apply if the materials are perfectly elastic.

Investigations of the impact of perfectly elastic spheres have, however, already been carried out, and the formulæ deduced by Hertz for the area of compression and the duration of contact have been verified, first by Hertz himself and then by other investigators †. If $v$ is the relative velocity of two equal spheres of the same material at the moment of collision, and $t$ is the duration of their contact, $tv^{1/5}$ = constant, according to Hertz.

When, however, we employ materials other than the hardest steel the assumption of perfect elasticity is no longer justified, and modifications must be introduced. Assuming a resistance to advance proportional to the square of the velocity, from the moment the spheres touch to the moment they begin to recede, T. Pöschl has shown how to modify the theory of Hertz, and has produced an approximate solution of the problem, which shows that $tv$ = constant in this case ‡. It was the original purpose of this research to discover whether or not this law were obeyed.

*Method of Investigation.*

A good method for investigating this problem was already to hand, and had been used with various modifications by

* *Vide* E. W. Tschudi, Phys. Rev. xviii. p. 423 (1921); J. E. P. Wagstaff, Proc. R. S. cv. p. 544 (1924).

† A. Dinnik, *Jour. d. Russ. Phys. Ges.* xli. p. 57 (1909); W. Müller, *Weiner Ber.* cxxiii. p. 2157 (1914), and others.

‡ T. Pöschl, *Zs. für Phys.* xlvi. p. 142 (1927).

a number of investigators. Only minor improvements have been incorporated here. A condenser is charged, the impact of the metal spheres is allowed to partially discharge it, and the remaining charge is immediately afterwards measured by passing it through a ballistic galvanometer. From a knowledge of the original and final charges and the resistance of the circuit, the time during which the spheres were in contact may be deduced. This method appears to

Fig. 1.

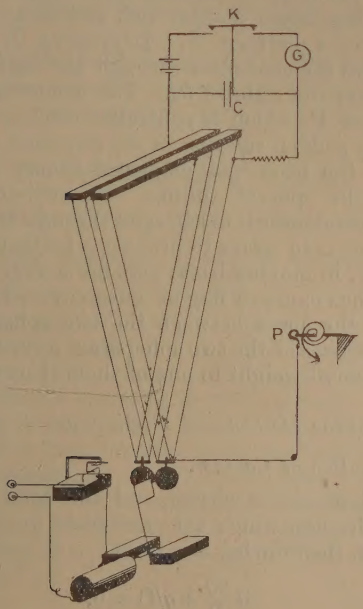


Diagram o Apparatus.

have originated with R. Sabine* in 1876, and has been used, with small differences, by others since, notably by Wagstaff. The chief pitfall to be avoided is the inclusion of appreciable inductance in the circuit, since the formula for calculating the duration of contact then becomes far too complicated. The innovations in the present experiments are the employment of the pendulum suspensions of the spheres as conducting leads and an arrangement enabling the observer to turn the

* R. Sabine, Phil Mag. i. p. 337 (1876)

balls after each collision so as to present a new pair of surfaces at each impact. The spheres were each suspended by four steel wires so as to form pendulums about 180 cm. long, which were so adjusted that the balls were in light contact at points on their equators when at rest. The balls were screwed, as shown, to small bars of brass, to which the suspension wires were soldered. The electrical circuit is represented above. The condenser C is charged by depressing K on the left, while the spheres are separated. This separation is secured by drawing one of the spheres aside by means of a thread passing under a glass rod, and fastened to a hook depending from a platform P. Depressing K to the right then discharges the condenser through the ballistic galvanometer G, producing a throw $\theta_0$. The condenser is charged anew, platform P, which is controlled electro-magnetically, is removed by sudden rotation in the direction of the arrow so as to let the hook and displaced sphere fall perfectly freely, and the spheres collide. Immediately after the collision, the condenser is discharged through G, a deflexion $\theta$ being obtained. In order to prevent a further collision, the second sphere, in moving back, actuates a very easily moved switch, and thus causes a flag of mica covered with soft felt to move into the space between the two spheres, insulating them. The masses of the two spheres are adjusted to equality by adding a small weight to one of them if necessary.

*Theory of the Method and Preliminary Experiments.*

(1) *The Duration of Contact.*

If self-inductance is absent, and the total resistance of the circuit through which the condenser discharges during collision is R, then during this period

$$R\frac{dq}{dt} + q/C = 0,$$

where $q$ is the charge on the condenser. The solution of this equation is

$$q = q_0 e^{-\frac{t}{RC}}, \quad \ldots\ldots\ldots \quad (1)$$

C being the capacity of the condenser. If, however, self-inductance is present, but only to a small extent, such that $\frac{L}{C^2R^2}$ is small, then the equation of motion, which is now strictly

$$L\frac{d^2q}{dt^2} + R\frac{dq}{dt} + \frac{q}{C} = 0,$$

may be written approximately

$$R\frac{dq}{dt} + \left(\frac{1}{C} + \frac{1}{C^2R^2}\right)q = 0$$

since from (1)

$$\frac{d^2q}{dt^2} = \frac{1}{C^2R^2}q,$$

and the new solution is

$$\log q = \log q_0 - \frac{1}{R}\left(\frac{1}{C} - \frac{L}{C^2R^2}\right)t. \quad . \quad . \quad . \quad (2)$$

In actual practice $q$ was measured by discharging through a ballistic galvanometer whose deflexions $\theta$ were proportional to the quantity discharged, so that (2) may be written

$$\log \theta = \log \theta_0 - \frac{1}{R}\left(\frac{1}{C} + \frac{L}{C^2R^2}\right). \quad . \quad . \quad . \quad (3)$$

Hence, provided self-inductance is zero, and there is no other perturbing quantity, $\frac{1}{R}$ will be a linear function of $\log \theta$, the time $t$ being kept constant.

This matter may be tested by separating the balls to the same distance on each occasion, so that the velocity of approach is always the same, and trying the collision experiment with different values of R in the circuit. But a second consideration enters here. When the spheres first touch, the resistance at their junction must be extremely large, then fall rapidly, reaching a minimum, and finally increase to an infinite value. It may be considered as having an unknown average value $r$, which may be a not altogether negligible quantity. Equation (3) ought, therefore, to be written approximately

$$\log \theta = \log \theta_0 - \frac{t}{CR\left(1 + \frac{r}{R}\right)\left(1 - \frac{L}{CR^2}\right)}. \quad . \quad . \quad (4)$$

From the form of this equation, provided a wide range of values of R is considered, the two terms in the brackets cannot always compensate one another unless each is separately unity. An experiment was arranged on these lines, the spheres being rotated through a small angle after each collision, using values of R ranging from 113 to 10,000 ohms, and a perfectly rectilinear graph was obtained when $\frac{1}{R}$ was

plotted against $\log \theta$. It follows that $r = 0$ and $L = 0$ very closely. The usual value of R was about 500 ohms. (See fig. 2.)

(2) *The Velocity of Approach.*

When the bob of a pendulum of length $l$ is withdrawn a horizontal distance $x$, it may be shown that the velocity it

Fig. 2.

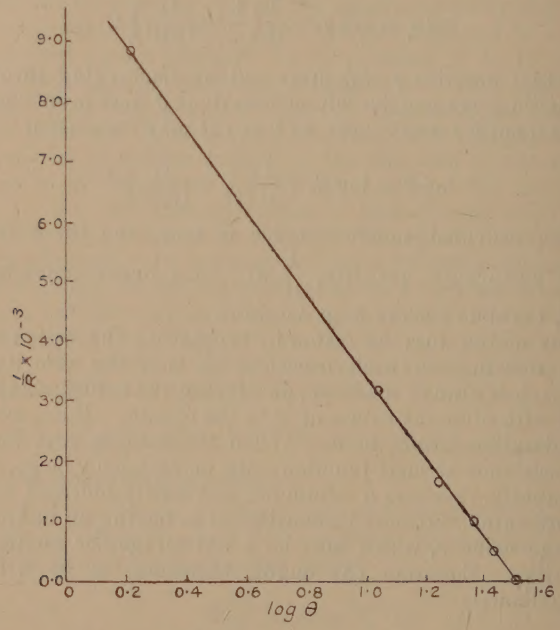


acquires in falling freely to the lowest point of its path is given by

$$v = x\sqrt{\frac{g}{l}}\left\{1+\frac{x^2}{4l^2}\right\},$$

so long as $x$ is small compared with $l$. If appreciable damping occurs, and $\lambda$ is the logarithmic decrement, then the above expression must be multiplied by $\left(1-\frac{\lambda}{2}\right)$, giving finally

$$v = x\sqrt{\frac{g}{l}}\left\{1+\frac{x^2}{4l^2}-\frac{\lambda}{2}\right\}.$$

The value of $x^2/4l^2$ never exceeded 1 per cent., and $\lambda$ varied between 0·012 for aluminium and 0·002 for tin. The corrections were therefore considered negligible.

### *The Initial Separation of the Spheres.*

As it was specially desirable not to contaminate the surfaces of the spheres, the following methods were employed to measure their initial separation. For small separations up to about 20 cm. a large lens was arranged to produce a diminished real image of the spheres, and the horizontal distance between these images was measured in a good travelling microscope. It is estimated that by this means the separation, and therefore the velocity of approach, could be found to about 2 per cent. accuracy, with the exception of the smallest velocities, which were sometimes in error owing to slight draughts. After each set of observations the readings of the microscope were calibrated by observing the apparent length of 10 cm. of a metre scale placed in the position previously occupied by the spheres. For larger distances, where aberration in the lens may have affected the results, the distances were measured directly by a metre scale with stiff paper pointers. For the same degree of accuracy it was only necessary to be certain of the reading to within 4 mm., and it was easy to read it to 1 mm. For simplicity, all the results in this paper are reduced to the microscope scale of the first method.

### *The Condenser employed.*

This was a Siemens Standard 1 mfd., selected because of its small absorption and leakage. In the course of the experiment, as already outlined, the condenser was charged about half a second before the collision, and then discharged about half a second after, so that the chances of any spurious effects due to absorption and leakage were reduced to entirely negligible quantities. The short-circuiting plug of the condenser was inserted for some minutes between collisions. The e.m.f. of the charging battery was carefully watched, and kept at 4 volts.

### *The Galvanometer.*

In the majority of experiments a fluxmeter was employed, this instrument having the advantage of a large periodic time (46 sec.), which enables the ballistic throw to be read off quite accurately. A separate experiment proved that the throw was accurately proportional to the charge suddenly passed through the coil over the whole range employed.

*The Spheres.*

These were first cast and then turned in the Instrument Shop of East London College. The equatorial zone was turned with special care to a truly spherical figure, since here the collision was to take place; and the whole then polished. In some instances the spheres were subsequently annealed, but this was not possible in the case of zinc and aluminium, as non-conducting films were thereby formed. In all cases the spheres were 4·0 cm. in diameter.

## Part I.

*Results.*

Six substances have so far been examined, viz., aluminium, tin, zinc, an alloy of lead and tin containing 60 per cent. tin, and a babbitt alloy. Typical results follow.

### Table I.

*Tin. Expt.* 2.

Temperature of the air 10°·2 C.
Resistance R, including that of the steel leads = 513·2 ohms.
Length of the pendulum = 184·5 cm.
Capacity of condenser = 1 microfarad.
10 cm. of metre scale = 0·785 cm. on microscope.
$\theta_0 = 32{\cdot}77$ cm.

| Separation of spheres, in cm. of microscope, = S. | Throw of galv. $\theta$, cm. | $t$ (sec.) $1{\cdot}18 \log_{10} \frac{\theta_0}{\theta} \times 10^{-3}$. | $v$ = 29·40 S cm./sec. | $t$ calc. sec. $\times 10^{-4}$. |
|---|---|---|---|---|
| 0·050 | 10 35 | 5·91 | 1·47 | 5·91 |
| 0·120 | 12·18 | 5·09 | 3·53 | 5·01 |
| 0·177 | 13·02 | 4·73 | 5·20 | 4·71 |
| 0·285 | 12·95 | 4·76 | 8·38 | 4·38 |
| 0·435 | 14·60 | 4·15 | 12·78 | 4·15 |
| 0·900 | 15·49 | 3·85 | 26·5 | 3·82 |
| 1·420 | 16·15 | 3·62 | 41·8 | 3·65 |
| 1·875 | 16·58 | 3·50 | 55·0 | 3·57 |
| 2·63 | 16·77 | 3·45 | 77·3 | 3·48 |
| 0·032 | 8·85 | 6·71 | 0·94 | 6·49 |

These results and those in Table II. are represented graphically in fig. 3. Curves representing the results for the other materials are also given in figs. 4 and 5.

TABLE II.

*Aluminium. Expt.* 3.

Temperature of the air 18° C.
Resistance R, including that of the steel leads, =525 ohms.
Length of pendulum=182·0 cm.
Capacity of condenser=1 microfarad.
10 cm. of metre scale=0·800 on microscope.
$\theta_0$=19·09 cm.

| Separation of spheres, in cm. of microscope, =S. | Throw of galv. $\theta$, cm. | Observed $t$ (sec.) $=1{\cdot}212\log_{10}\frac{\theta_0}{\theta}\times10^{-3}$. | $v$ =29·0 S cm./sec. | $t$ calc. sec. $\times10^{-4}$. |
|---|---|---|---|---|
| 0·085 | 11·99 | 2·91 | 2·46 | 3·28 |
| 0·150 | 11·53 | 2·65 | 4·50 | 2·47 |
| 0·230 | 13·14 | 1·96 | 6·68 | 2·13 |
| 0·335 | 13·09 | 1·99 | 9·73 | 1·90 |
| 0·515 | 13·66 | 1·76 | 14·96 | 1·71 |
| 0·710 | 14·10 | 1·60 | 20·6 | 1·62 |
| 0·935 | 13·89 | 1·68 | 27·2 | 1·56 |
| 1·180 | 14·73 | 1·37 | 34·3 | 1·51 |
| 1·425 | 14·50 | 1·44 | 41·3 | 1·49 |
| 1·700 | 14·61 | 1·41 | 49·2 | 1·47 |
| 0·100 | 10·20 | 3·30 | 2·90 | 3·04 |
| 0·065 | 8·35 | 5·34 | 1·89 | 3·86 |
| 2·000 | 14·45 | 1·46 | 58·0 | 1·45 |
| 1·020 | 14·00 | 1·60 | 29·6 | 1·54 |

Fig. 3.

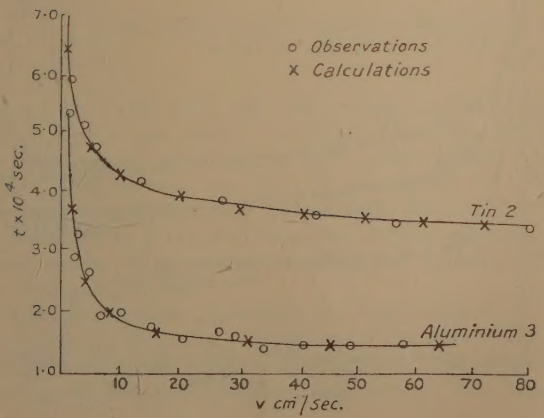

Fig. 4.

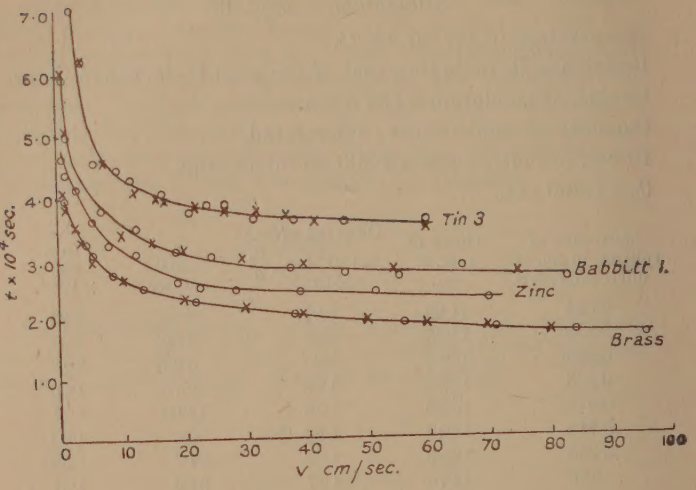
7·0
6·0
5·0
4·0
3·0
2·0
1·0
t x 10⁴ sec.
Tin 3
Babbitt I.
Zinc
Brass
0
10
20
30
40
50
60
70
80
90
100
v cm/sec.

Fig. 5.

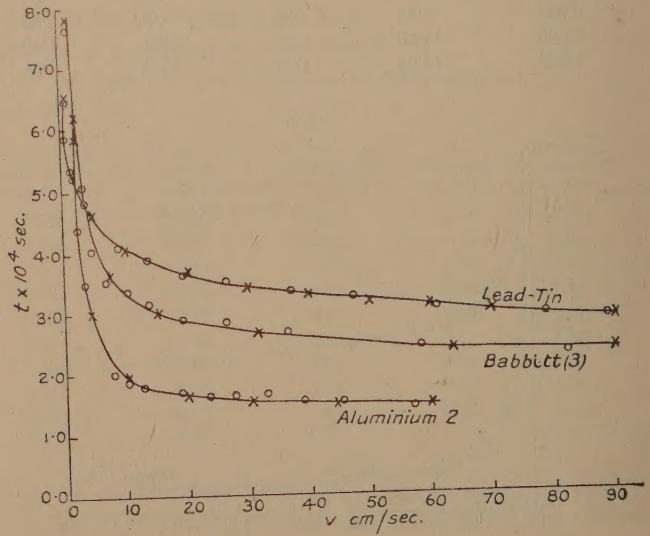
8·0
7·0
6·0
5·0
4·0
3·0
2·0
1·0
0·0
t x 10⁴ sec.
Lead-Tin
Babbitt (3)
Aluminium 2
0
10
20
30
40
50
60
70
80
90
v cm/sec.

The answer to the original question may now be sought, namely, do these results agree with the assumption of a resistance to distortion proportional to the square of the relative velocity? Do they, that is to say, follow a law of the form $tv$=constant?

In no case is this law obeyed. In some instances a law of the form $(t-t_0)v$=constant would be a first approximation; but after an extensive investigation, the best agreement is found to be with a formula of the type

$$t=t_0+a/v^n,$$

where $t_0$, $a$, and $n$ are all constants which differ for the different materials. The values of these constants are

TABLE III.

| Substance. | Expt | $t_0\times10^4$ sec. | $a\times10^4$. | $n$. | Remarks. |
|---|---|---|---|---|---|
| Aluminium ... | 2 | 1·38 | 20·7 | 1·58 | Points scattered. |
| | 3 | 1·34 | 4·52 | 0·92 | Re-turned. |
| Tin ..... | 2 | 2·82 | 3·58 | 0·39 | |
| | 3 | 3·40 | 6·88 | 0·92 | Re-turned. |
| Babbitt ..... | 1 | 1·89 | 3·18 | 0·32 | |
| | 2 | 2·43 | 6·61 | 0·98 | Re-turned. |
| | 3 | 1·93 | 5·88 | 0·59 | Re-turned and annealed. |
| Brass ..... | 1 | 0·16 | 3·79 | 0·19 | |
| Lead–Tin Alloy. | 1 | 1·50 | 5·00 | 0·30 | |
| Zinc ..... | No formula found to cover the whole range, but the curve runs in the same general way. | | | | |

tabulated in Table III., and the crosses on the curves of figs. 3, 4, and 5 are points calculated from the formula to show how nearly they agree with observations. In one instance, that of zinc, no formula was found to cover the whole range, and repetition gave erratic results, which may have been due to marked differences at different parts of the surface, and to the formation on collision of flattened portions of an unusual character.

In calculating these constants, the usual method (as given, for instance, in Running, 'Empirical Formulas') was found to exaggerate small errors at one end of the range. The following method was therefore employed. The slopes of

tangents drawn at chosen points on a smooth curve through the observations were recorded. Then, since

$$\left(\frac{dt}{dv}\right)^2 = n^2a^2v^{2(1-n)},$$

$$2\log\frac{dt}{dv} = \log(n^2a^2) + 2(1-n)\log v,$$

so that (a) if $\log\frac{dt}{dv}$ is a linear function of $\log v$, the formula $t = t_0 + a/v^n$ follows, and (b) $n$ and $a$ are obtained from the slope and intercept of the straight-line graph indicated. These slopes and intercepts, it should be noted, were definitely calculated by the method recently given by J. H. Awbery *.

*Discussion.*

According to the formula, the duration of contact tends towards a steady value $t_0$, which is greater than zero, as the velocity at impact increases. That $t_0$ would be other than zero is to be anticipated, because at high speeds permanent deformation occurs, and during the process of deformation the spheres must be in contact. It appears that at the highest speeds the diminution of the duration of contact which ought to follow from the larger elastic forces called into play on collision is just counterbalanced by the extension of this period, due to the flow of the metal. A conclusion reached by J. H. Vincent †, after experiments in which a steel ball was dropped upon a lead plate, namely, that the time taken by any one sphere to produce a dent was independent of the velocity of impact, is another example of this compensating action.

At very small speeds $t = a/v^n$ very nearly. This is reminiscent of Hertz's formula $tv^{1\cdot5} = \text{constant}$. In one instance, that of brass, $n$ is almost exactly 1/5; while in the cases of lead-tin alloy, babbitt, and tin, the value of $n$ in the first experiments, although greater, is not widely different from 1/5, the difference being possibly due to working on the lathe. Of zinc nothing definite can be said in this respect, while aluminium appears to be so susceptible to mechanical working, and so readily forms a non-conducting layer when annealing is attempted, that the results cannot be regarded as evidence on this point. It therefore seems likely that at very small speeds of approach Hertz's law, or a law very similar to it, may apply. Further experiment is required to

* J. H. Awbery, Proc. Phys. Soc. xli. (1929).

† J. H. Vincent, Proc. Camb. Phil. Soc. x. p. 332 (1898–1900).

establish this point, but it may be noted that some experiments by C. V. Raman * upon slow collisions have shown that the coefficients of restitution for lead, brass, and bronze, all approach unity at small speeds of approach. Similar results have been obtained by Ôkubo † for a number of other substances.

*The Effect of Mechanical Working and Annealing.*

From Table III. it appears, as a rule, that all three constants, $t_0$, $a$, and $n$, increase after the spheres have been re-turned and re-polished; and decrease after annealing. $n$ seems to be the most sensitive in this respect, and $t_0$ the least. These facts may be understood if $t_0$ depends upon the properties of the metal in bulk, while $n$ depends on the properties of the outside layer of the material. This is probably the case, for the theory of Hertz assumes that large stresses occur only in the immediate neighbourhood of the area of contact, and the elastic properties of the surface layers are therefore of prime importance in this theory. The present experiments provide a value of $n$ similar to Hertz's when the temporary deformation is confined to the surface and the surface has not been over worked. As soon, however, as comparatively large permanent deformations appear, metal below the surface, and possibly out of the influence of the lathe tool, begins to have a preponderating effect. This is the region in which $t_0$ is the chief term of the formula.

Finally, these results do not support the view that, after contact is made, the spheres approach one another under a resistance proportional to the square of the velocity.

## Part II.

### *The Permanent Deformation at the Surfaces of the Spheres.*

When the speed of approach is fairly high, small flattened portions, circular in shape, are visible on the surfaces of the spheres. To a cursory view they appear planes, as though a small spherical cap had been cut off; but under the microscope they each appear surrounded by a pronounced rim, higher than the flat portion. A magnified section of the sphere through one of these would probably have the appearance of fig. 6 (*a*) in the majority of cases. When light

* C. V. Raman, Phys. Rev. xii. p. 442 (1918).
† J. Ôkubo, Tohôku Univ. Sci. Rep. p. 454 (1922).

is reflected obliquely from the "flat," it is possible to photograph the rim. Pl. XIII. (*a*) shows this. It is not here a question of one harder sphere imposing a concave impression on the other, for as a rule both spheres exhibit the same deformation. To show this clearly, the four photographs, (*b*), (*c*), (*d*), (*e*) of Pl. XIII. are views of the left and right sides respectively of two "flats" one upon each sphere, formed during a single collision. On some occasions the portion usually plane was itself undulating, probably having a section, as in fig. 6 (*b*). This is illustrated in (*f*) and (*g*) of Pls. XIII. & XIV. These remarks apply to all materials, but the case of zinc requires amplification. Whereas in the other cases the rim was perfectly circular, or only slightly distorted, in the case of zinc it was nearly always irregular, and only roughly circular. The flattened portion within the rim, moreover, was traversed by a network of subsidiary

Fig. 6.


ridges which, although readily seen by the eye, were found difficult to record photographically. (*h*), (*i*), and (*j*) of Pl. XIV. are, however, attempts which do show how regions of the "flat" are cast into shadow when viewed by light reflected obliquely. The irregularity of the outline is, in fact, exaggerated in these pictures, the outside rim, although complete, being partly hidden in shadow. The first thought was that the ridges were boundaries of crystals, but in this case the section would have been as in fig. 6 (*c*), stepped on the flattened part. Illumination from the other side ought then to have made the bright lines dark, and shown up other bright lines. In point of fact the same lines were brought out. The conclusion is that the section must have been as in fig. 6 (*d*).

An explanation on the following lines of these rims and ridges suggests itself. During the beginning of the collision, the metal in the neighbourhood of the point of contact is compressed, the pressure being greatest at the centre *. As

* *Vide* Hertz, 'Miscellaneous Papers,' English ed., p. 173.

the centres of the spheres continue to approach, the pressure becomes so great that, if the initial momentum be sufficient, breakdown occurs. The area over which the metal has "fused" will continue to expand until the balls begin to recede. The continued approach of the centres involves the "fusion" of more material at the centre of the compressed area, and this material has to be forced aside. When the spheres cease to approach, and begin to recede, the pressure on this extruded material is relaxed, and it re-sets. The sharply-defined rim suggests that it has been extruded beyond the area of contact, for here it would solidify on emergence, and immediately be covered by more material, thus building up a projecting ring which would be constrained to lie in the plane of contact until the pressure was released. On relaxation the layers first deposited would recover from the strain of subsequent pressure, pulling the projection into a rim.

It may be asked why, if "fusion" occurs over a common area, the spheres do not adhere. This would be easier to explain than the apparent adhesion of the zinc spheres, for the surfaces are covered with exceedingly fine scratches from the lathe tool, each of which provides an air-film to prevent the coalescing of the two parts. But in the case of zinc transitory adhesion does appear to take place, and the ridges within the rim are probably the lines along which the adhesion was most protracted. This offers a ready explanation of the erratic nature of the results for zinc, but its exceptional behaviour remains unexplained.

A very similar phenomenon has been observed by C. V. Raman * when steel balls are dropped upon a glass surface. He hesitates, however, to ascribe the rim to flow of fused material, owing to the time available being so small. When, however, it is recalled that in my experiments the gradient parallel to the surface, of the normal pressure, is of the order $10^{10}$ dynes per sq. cm. per cm. or more, and the mass of material to be moved of the order $10^{-5}$ gm., it does not seem at all impossible that the required velocity of flow (less than 1000 cm./sec.) could be acquired in a few ten-thousandths of a second, even allowing for powerful forces due to viscous resistance.

### *Size of the Permanent Deformation in Relation to the Velocity at Impact.*

The diameters of the circular rims were measured microscopically, and the results recorded with the velocities of

* C. V. Raman, J. Opt. Soc. Amer. xii. p. 387 (1926).

approach in Table IV., a typical example. These results are plotted in fig. 7, where $d^2$ is taken as the ordinate to bring

TABLE IV.

*Tin Spheres. Exp.* (3).

Diameter of spheres 4·00 cm.
Mass of each sphere 240 gm.

| $v$, cm./sec. | Diameters of rims of deformations. | | | Diameters calculated, cm. |
|---|---|---|---|---|
| | Sphere 1, cm. | Sphere 2, cm. | Means, cm. | |
| 9·2 | 0·083 | 0·160 | 0·095 | 0·081 |
| 11·9 | 0·110 | 0·112 | 0·111 | 0·106 |
| 16·5 | 0·117 | 0·129 | 0·123 | 0·131 |
| 21·0 | 0·153 | 0·145 | 0·149 | 0·150 |
| 23·9 | 0·162 | 0·159 | 0·160 | 0·162 |
| 26·8 | 0·174 | 0·176 | 0·175 | 0·172 |
| 31·8 | 0·192 | 0·199 | | |
| 31·8 | 0·195 | 0·187 | 0·193 | 0·187 |
| 38·6 | 0·205 | 0·208 | 0·206 | 0 205 |
| 46·8 | 0·230 | 0·233 | 0·231 | 0·225 |
| 60·2 | 0·236 | 0·235 | 0·235 | 0·248 |

Fig. 7.

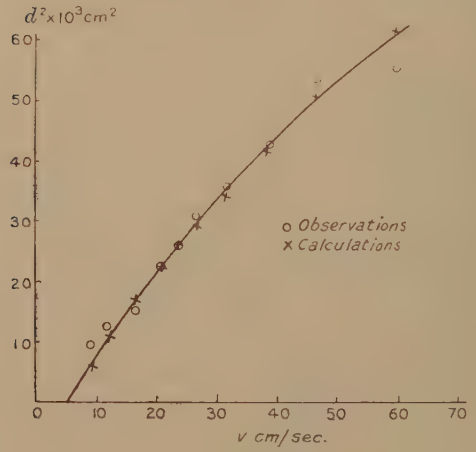


out more clearly the intersection of the curve with the $v$ axis. In some cases the diameters for one sphere of a pair were uniformly a little larger than those for the other, but in all

cases the mean was taken as the most convenient quantity to deal with. The curves for the remaining substances are shown in fig. 8. If the curves may be extrapolated to intersect the axis of $v$, as has been done in the figures, we learn that no permanent deformation is produced until the velocity of approach reaches a definite value $v_0$, which is a characteristic of each material. There is nothing new in this idea, but the observation is a justification for it. The values of $v_0$ are given in Table V. In some instances the diameters could not be measured with sufficient accuracy to

Fig. 8.

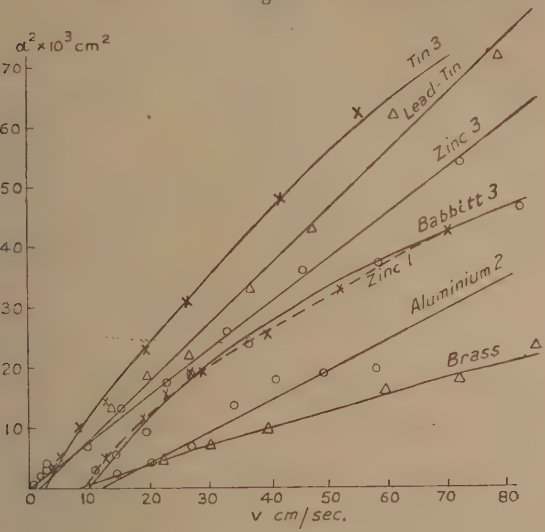


Observations are indicated.

warrant their inclusion here; but, from the reliable sets of observations a formula was sought to represent the results. This was found to be

$$d = b(v - v_0)^m,$$

and Table V. gives the values of the constants $b$, $m$, and $v_0$.

### *Discussion.*

In the cases of aluminium, lead-tin alloy, brass, and zinc after annealing, $m$ is approximately 0·5. Thus $d^4$ is proportional to a quantity of kinetic energy $k(v-v_0)^2$, which, when $v$ is sufficiently large, differs only a little from the expression

for the kinetic energy of the moving sphere at collision. The volume of the small spherical cap whose diameter is $d$ is $\frac{\pi d^4}{64R}$, R being the radius of the sphere. Hence at high speeds we have the rule, originally given by Vincent for the case of spherical indentations in a lead plate, "the volume of the material apparently removed is proportional to the kinetic energy of the moving sphere at impact."

This is, however, no longer true in general for small values of the kinetic energy, and according to these results it is not a principle applicable to all substances. A similar rule might be made for the other substances, but it would be neither so simple nor so suggestive.

TABLE V.

| Substance. | Expt. | $b$. | $v_0$, cm./sec. | $m$. | Remarks. |
|---|---|---|---|---|---|
| Aluminium ... | 3 | 0·023 | 12·0 | 0·5 | Observations rather scattered. |
| Tin ..... | 2 | 0·048 | 2·5 | 0·41 | |
| | 3 | 0·047 | 5 0 | 0·42 | After re-turning. |
| Babbitt ..... | 3 | 0·044 | 10·0 | 0·375 | After re-turning and annealing. |
| Zinc ..... | 1 | 0·045 | 9·0 | 0·37 | |
| | 3 | 0·027 | Very small. | 0·50 | After annealing and then re-turning. |
| Lead–Tin Alloy. | 1 | 0·098 | 2·0 | 0·50 | |
| Extruded Brass. | 1 | 0·020 | 8·0 | 0·47 | |

*The Least Pressure Required to initiate Flow.*

A knowledge of $v_0$ enables us to calculate this pressure for the various substances. The calculation is based on the theory of Hertz, and rests on the assumption that the materials may be regarded as perfectly elastic when $v < v_0$. From the first part of this paper, it will be clear that considerable justification exists for this in the cases of brass, lead-tin alloy, babbitt, and perhaps tin; for zinc and aluminium the case is not so good.

Following Love's version of Hertz's work*, we find that the total thrust over the whole area of contact is given by

$$P = \frac{4}{3\pi} \frac{a^3}{R} \frac{4\pi\mu(\lambda+\mu)}{\lambda+2\mu},$$

* Love, "Elasticity," 4th edn. p. 200. The English translation of Hertz's 'Miscellaneous Papers' contains several serious misprints.

where $a$ is the radius of the compressed area, R the radius of the spheres, $\lambda$ and $\mu$ are elastic moduli commonly employed.

The maximum value attained by $a$ is related to the velocity of impact $v$ thus

$$a_{\max.} = R\left(\frac{v}{c}\right)^{2/5}\left[\frac{5\pi}{16}\frac{(1-\sigma)^2}{1-2\sigma}\right]^{1/5},$$

where $c$ is the velocity of compressional waves in the material of the spheres.

$$c^2 = \frac{\lambda+2\mu}{\rho}; \quad \rho = \text{density of material};$$

$$\sigma = \text{Poisson's Ratio};$$

while the pressure at the centre of the compressed area

TABLE VI.

| Substance. | Expt. | $\phi\times10^{-9}$. | $v_0{}^{2/5}$. | P′, dynes/cm.$^2$. | Tensile strength. dynes/cm.$^2$. |
|---|---|---|---|---|---|
| Aluminium ... | 3 | 2·6 | 2·71 | $7{\cdot}1\times10^9$ | $5{\cdot}4\times10^8$ |
| Tin ..... | 2 | 2·3 | 1·45 | $3{\cdot}3\times10^9$ | $1{\cdot}7\times10^9$ |
| | 3 | 2·3 | 1·90 | $4{\cdot}4\times10^9$ | |
| Babbitt ..... | 3 | 1·7 | 2·51 | $4{\cdot}3\times10^9$ | |
| Zinc..... | 1 | 3·6 | 2·41 | $8{\cdot}7\times10^9$ | $1{\cdot}2\times10^9$ |
| | 3 | 3·6 | Too small to measure. | | |
| Lead–Tin Alloy. | 1 | 2·3 | 1·32 | $2{\cdot}6\times10^9$ | |
| Extruded Brass. | 1 | 4·1 | 2·30 | $9{\cdot}5\times10^9$ | $8\times10^9$ |

(where it is a maximum), is given when $a$ attains its maximum also by

$$P' = \frac{3P}{2\pi a^2}$$

$$= v^{2/5}\left\{\frac{8\lambda(\lambda+\mu)}{\pi(\lambda+2\mu)}\left[\frac{1}{c^2}\frac{5\pi}{16}\frac{(1-\sigma)^2}{1-2\sigma}\right]^{1/5}\right\}$$

$$= v^{2/5}\phi,$$

where the coefficient of $v^{2/5}$ is denoted by $\phi$.

If, now, we insert $v_0$ as the velocity, P′ will be the pressure just capable of starting flow. Table VI. gives the calculated values of these pressures. The necessary elastic constants

for aluminium, zinc, tin, and brass were derived from tables, while those for babbitt and the lead-tin alloy were found from separate experiments on rods of these materials specially cast for the purpose. These pressures may be compared with such quantities as crushing and tensile strengths; but the former are not recorded to any extent except for ferrous metals. The available data on tensile strengths have been added in the last column for comparison. It is interesting to note that these are of the same order as the pressures calculated.

### *Summary of Results.*

#### Part I.

(*a*) The duration of contact is related to the velocity of approach by the law $t = t_0 + \frac{a}{v^n}$.

(*b*) For the alloys brass, lead-tin, and babbitt $n$ is practically 1/5, as in Hertz's formula $tv^{1/5} = \text{constant}$, provided the surface is not mechanically worked to too great an extent.

(*c*) For the metals tin and aluminium $n$ is definitely greater than 1/5, while for zinc no value can be given.

(*d*) Mechanical working of the surface raises the values of $t_0$, $a$, and $n$, while annealing reduces them again.

#### Part II.

(*a*) The circular permanent deformations are found to be bounded by a rim.

(*b*) The diameters of these rims are related to the velocity at impact by the law $d = b(v - v_0)^m$.

(*c*) In the cases of aluminium, lead-tin, and brass $m$ is practically 0·5.

(*d*) In the case of zinc the deformations are irregular in outline and intersected by ridges.

(*e*) The pressures necessary to cause the metal to flow are of the order $10^9$ or $10^{10}$ dynes/cm.$^2$, that is, of the order of the tensile strengths.

In conclusion, this is the first paper upon a research, still in progress, carried out at East London College under the encouragement of Prof. C. H. Lees, to whom I am indebted for many helpful suggestions.

## LXXXVII. *On the 42-Minute Period in the Frequency of the After-Shocks of Earthquakes.* *By* CHARLES DAVISON, *Sc.D., F.G.S.* *

THE time taken by an earthquake-wave to travel from a focus near the surface to its antipodes is almost exactly 21 minutes. As the crust within and near the focus is for some days in a highly sensitive condition, it is possible that the return-pulsation may affect the frequency of the after-shocks, and my object in this paper is to show that a 42-minute periodicity does govern their occurrence. In two earthquakes, the Mino-Owari earthquake of 1891 and the Kwanto earthquake of 1923, I have applied the same methods in the hope of tracing periods of 21 and 84 minutes, but I have not been able to find any decisive evidence of their existence †.

Let us suppose that the crust is on the point of motion in one direction over a certain area, and that a periodic force of strength sufficient to precipitate motion acts upon it in the same direction. The resulting earthquakes would then be subject to a period of the same duration, and the maximum epoch of the period would coincide approximately with that of the variable force. If the latter force were to act in the direction opposite to that in which the crust is about to move, there might still be the same periodicity in the frequency of earthquakes, but the maximum epoch would coincide with the minimum epoch of the variable force. Thus, if the after-shocks of an earthquake are due mainly to a continued exertion of the forces that give rise to the earthquake, then the maximum epoch of the 42-minute period, if it exists, should coincide with the arrival of the return-movement. On the other hand, if most of the after-shocks are due to the settling of the displaced crust, the maximum epoch of the period should occur about 21 minutes after that return.

The only catalogues of after-shocks at my disposal that are full enough for the purpose are those of five Japanese earthquakes from 1891 to 1927, three European earthquakes from 1894 to 1915, and three others depending on personal observations only.

In the following sections the time of occurrence given is that of the initial epoch of the movement. As, however, the duration of a great earthquake may amount to 4 or 5

* Communicated by the Author.

† On this subject, see H. H. Turner, R. Astro. Soc. Monthly Notices, Geoph. Suppl. vol. i. pp. 31–50, 88–99, and vol. ii. pp. 73–76.

minutes, the epoch of the strongest movement may be a minute or two later. In each earthquake, successive intervals of 42 minutes were divided into 14 minor intervals of 3 minutes each, and 7-interval means were taken of the total numbers of after-shocks occurring in corresponding intervals. In the tables the date of the maximum epoch is the number of minutes after the last complete interval of 42 minutes measured from the initial epoch of the earthquakes. In estimating the amplitude the average number of after-shocks in each 3-minute interval is taken as unity.

### *Mino-Owari Earthquake of Oct.* 28, 1891.

The Mino-Owari earthquake occurred at 6.37 A.M. The seismographs at Gifu and Nagoya were at once put out of action, but the first after-shock was recorded at 1.10 P.M. at Nagoya and 1.55 P.M. at Gifu *. In both records the intervals mentioned range from Oct. 28, 2.0 P.M., to Nov. 2, 1.0 P.M., from that date to Nov. 6, 0.12 P.M., and from the latter to Nov. 10, 11.24 P.M.

| Interval. | Gifu. | | | Nagoya. | | |
|---|---|---|---|---|---|---|
| | No. of shocks. | Max. epoch, min. | Ampl. | No. of shocks. | Max. epoch, min. | Ampl. |
| Oct. 28–Nov. 2 ... | 863 | 18½ | ·09 | 507 | 3½ | ·11 |
| Nov. 2–6 ..... | 201 | 9½ | ·22 | 91 | 9½ | ·47 |
| Nov. 6–10 ..... | 177 | 3½ | ·22 | 65 | 21½ | ·41 |

Thus, during the first five days, the minima of the 42-minute period at Gifu, and the maxima at Nagoya, coincided approximately with the return-movements. In the next four days, the series of means were somewhat irregular, and the epochs at both places occupied an intermediate position. In the last four days the epochs were almost reversed, so that the maxima at Gifu and the minima at Nagoya coincided nearly with their return-movements.

The explanation of the opposition in epoch at Gifu and Nagoya is probably to be found in the positions of these places with reference to the great fault-line. Along this fault the crust on the east side was relatively lowered by 10 feet or less, except at one place, Midori, where it was

* F. Omori, Tokyo Imp. Univ. Coll. Sci. Journ. vii. pp. 178–189 (1894).

raised by 20 feet. Gifu lies about 5 miles from the fault-line and 14 miles from Midori. Nagoya lies about 18 miles from the continuation of the fault-line and 34 miles from Midori.

### *Hokkaido Earthquake of Mar.* 22, 1894.

The Hokkaido earthquake occurred at 7.56 P.M., and the after-shocks were recorded at Nemuro (75 miles from the epicentre) without interruption at the start*. The first five days range from Mar. 23, 0.0 A.M., to Mar. 27, 11 P.M , and the next ten days from the latter time to Apr. 6, 9 P.M.

| Interval. | No. of shocks. | Max. epoch, min. | Amplitude. |
|---|---|---|---|
| Mar. 23–27 ..... | 264 | $2\frac{1}{2}$ | ·17 |
| Mar. 27–Apr. 6 ... | 55 | $23\frac{1}{2}$ | ·25 |

Thus, in the first interval, the maxima of the 42-minute period coincided approximately with the return-movements; in the second interval the minimum coincided nearly with those returns.

### *San-riku Earthquake of June* 15, 1896.

The epicentre of this earthquake lay near the foot of the western slope of the Tuscaroora Deep, about 160 miles from the east coast of Japan. It was registered at Tokyo (about 340 miles from the origin) at 7.34 P.M.† During the five days, June 15–19 (36 after-shocks), the maxima of the 42-minute period occurred at $22\frac{1}{2}$ min. after the return-movements (amplitude ·34). After June 19 the recorded shocks are too few in number to determine the existence of the period.

### *Kwanto Earthquake of Sept.* 1, 1923.

The great Kwanto earthquake was recorded at Tokyo at 11 h. 58 m. 44 s., A.M. Most of the seismographs in the central district were overthrown by the shock, but one instrument at Tokyo remained in action throughout. Two lists of after-shocks have been published: one, by A. Imamura and K Hasegawa, of the after-shocks strong enough to be felt in Tokyo from Sept. 1 to Oct. 1; the other, by T. Yasuda, of all

* F. Omori, Imp. Earthq. Inv. Com. Publ. no. 7, pp. 35–51 (1902).
† Brit. Ass. Rep. 1897, pp. 7–8.

the after-shocks recorded in that city from Sept. 1 to Jan. 31, 1924*. The first after-shocks entered in both lists occurred at 0 h. 1 m. 49 s., P.M. on Sept. 1. For the remainder of Sept. 1, Imamura gives the times of 189 shocks and Yasuda of 225. For the whole of September, the corresponding numbers are 720 and 1303.

Making use first of Inamura's list, the maximum epoch for Sept. 1–6 (463 shocks) occurs at 20½ min. with an amplitude of ·13. During the second and third five days (114 and 45 shocks) the existence of the period becomes uncertain, the series of means being irregular. For Sept. 16–30 (84 shocks) the series of means vary regularly, with the maximum epoch at 32½ min. and the amplitude ·30.

The central district is divided by Imamura and Hasegawa into four regions, to each of which belonged its own series of after-shocks. The region A includes most of Sagami Bay and the land to the north; the region B contains the Boso Peninsula and the sea-bed to the east; the region C lies entirely on land to the north of Tokyo; while the region D includes Tokyo and the surrounding country. Of these regions, A and B are by far the most important; the region C was disturbed by comparatively few after-shocks, and the region D by a larger number, usually of slight intensity.

Nearly 24 hours after the great earthquake, at 11 h. 46 m. 55 s., A.M., on Sept. 2, another violent shock, almost as strong as the first, occurred in region B with its epicentre lying about 41 miles to the east. It is probable that most of the after-shocks in this region were connected with this second earthquake, for only one shock on Sept. 1 is assigned to region B.

| Region. | Interval. | No. of shocks. | Max. epoch, min. | Amplitude. |
|---|---|---|---|---|
| A..... | Sept. 1– 6. | 239 | 16 | ·13 |
| ,, ..... | ,, 6–11. | 30 | 41½ | ·83 |
| D ..... | Sept. 1– 6. | 89 | 20½ | ·47 |
| ,, ..... | ,, 6–11. | 48 | 11½ | ·33 |
| B..... | Sept. 2– 7. | 96 | 36 | ·33 |
| ,, ..... | ,, 7 12. | 39 | 23½ | ·36 |

For regions A and D the first five days are reckoned from noon on Sept. 1, the second five from 11 A.M. on

* A. Imamura and K. Hasegawa, Imp. Earthq. Inv. Com. Bull. ii. pp. 72–93 (1928); T. Yasuda, Imp. Earthq. Inv. Com. Rep. no. 100 A, pp. 261–310 (1925).

Sept. 6, and the maximum epoch from 11.59 A.M. on Sept. 1. For region B the first five days are reckoned from noon on Sept. 2, the second five from 11 A.M. on Sept. 7, and the maximum epoch from 11.47 A.M. on Sept. 2.

Thus, in region D, the minima of the period during the first five days coincided closely, and in region A roughly, with the return-movement; during the second five days the maxima in region A coincided closely with those returns. In region B, during the first and second 5-day intervals, the maxima and minima, respectively, coincided roughly with those returns.

Yasuda's list differs from the other in the inclusion of after-shocks imperceptible to human beings in Tokyo. It is also continued for four additional months. The results are as follows :—

| Interval. | No. of shocks. | Max. epoch min. | Amplitude. |
|---|---|---|---|
| Sept. 1– 6 ..... | 755 | 23½ | ·14 |
| „ 6–11 ..... | 288 | 7 | ·14 |
| „ 11–16 ..... | 125 | 13 | ·11 |
| „ 16–30 ..... | 133 | 40 | ·16 |
| Oct. 1–14 ..... | 45 | 41½ | ·38 |
| „ 15–31 ..... | 51 | 2½ | ·22 |

During the intervals Sept. 6–11 and Sept. 11–16 there is no irregularity in the series of means, and the date of the epoch is probably that of the resultant of two periods with maxima near the middle and end of the 42-minute intervals. During November there is no trace of a 42-minute period in either of the intervals Nov. 1–14 and Nov. 15–30. Thus, after two months the throbbing of the earth due to the original displacement seems to have died away.

Lastly, deducting the number of shocks for each interval in Imamura's list from the corresponding number in Yasuda's list, we obtain the numbers of shocks imperceptible to human beings in Tokyo, with the following results :—

| Interval. | No. of shocks. | Max. epoch, min. | Amplitude. |
|---|---|---|---|
| Sept. 1– 6 ..... | 292 | 23½ | ·28 |
| „ 6–11 ..... | 174 | 7 | ·25 |
| „ 11–16 ..... | 79 | 11½ | ·30 |
| „ 16–30 ..... | 49 | 2½ | ·34 |

*Tango Earthquake of Mar. 7, 1927.*

The earthquake occurred at 6.27 P.M. It originated along two faults nearly at right angles to one another. Surveys made in May–June, August–September, and October–November of the same year showed that the movements of the crust continued for at least six months of the earthquake, and not always in the same directions. The after-shocks were recorded at three stations, Maiduru, Kinosaki, and Inemura, about 8, 12, and 13 miles, respectively, from the line of the principal fault*. The first after-shock was recorded at Maiduru at 10.12 P.M. on Mar. 11, and at the other stations on the following day. The first interval in the table (see p. 807) ranges from Mar. 12, 3.12 P.M., to Mar. 16, 11 P.M.

A strong after-shock occurred at 6.7 A.M. on Apr. 1, and this was followed by 191 after-shocks on the same day, so slight that only 12 were recorded at all three stations, 20 at one other station besides Maiduru, and 162 at Maiduru only. The list for the latter station gives the following results :—

| Interval. | No. of shocks. | Max. epoch, min. | Amplitude. |
|---|---|---|---|
| Apr. 1 ..... | 191 | 1½ | ·23 |
| „ 2–3 ..... | 58 | ... | ... |
| „ 4–7 ..... | 53 | 22½ | ·44 |
| „ 8–14 ... | 104 | ... | ... |

The results given in the above tables seem to depend on the complex origin of the principal earthquake. From Mar. 12 to 31 the maximum epoch is at about 30 min., in April at about 28½ min. Then after about seven weeks the epoch is reversed (to 7½ min.) in May. In June the number of shocks recorded is only 17. The list for July seems to contain misprints, and I am unable to make use of it. In August there is no trace of the period. The epochs for Apr. 1 and Apr. 4–7 are reckoned, as before, from the principal earthquake at 6·27 P.M. on Mar. 7. As the interval between the principal earthquakes and the strong after-shock at 6.7 A.M. on Apr. 1 exceeds a multiple of 42 minutes by 20 minutes, it is at first sight doubtful whether the maxima coincide with the return-movements due to the principal earthquake, or the minima with the return-movements from the after-shock.

* N. Nasu, Tokyo Earthq. Res. Inst. Bull. vi. pp. 300-331 (1929).

| Interval. | General. | | | Maiduru. | | | Kinosaki. | | | Inemura. | | |
|---|---|---|---|---|---|---|---|---|---|---|---|---|
| | No. of shocks. | Max. epoch, min. | Ampl. | No. of shocks. | Max. epoch, min. | Ampl. | No. of shocks. | Max. epoch, min. | Ampl. | No. of shocks. | Max. epoch, min. | Ampl. |
| Mar. 12-16... | 142 | 30 | ·28 | 140 | 31½ | ·30 | 115 | 31½ | ·34 | 120 | 28½ | ·36 |
| 16–31... | 196 | ... | ... | 192 | ... | ... | 139 | ... | ... | 158 | ... | ... |
| Apr. 1–14... | 409 | 28½ | ·09 | 408 | 28½ | ·09 | 59 | 28½ | ·50 | 57 | ... | ... |
| 15–30... | 119 | ... | ... | 118 | ... | ... | 50 | 30 | ·31 | 56 | 27 | ·33 |
| May 1–14... | 82 | 7½ | ·27 | 74 | 7½ | ·34 | 53 | 6 | ·27 | 57 | 7½ | ·36 |
| 15–31... | 65 | 7½ | ·31 | 63 | 7½ | ·27 | 33 | 6 | ·23 | 35 | ... | ... |
| Mar. 12–31... | 338 | 31½ | ·13 | 332 | 31½ | ·13 | 254 | 34½ | ·19 | 278 | 34½ | ·23 |
| Apr..... | 528 | 28½ | ·13 | 526 | 28½ | ·13 | 109 | 28½ | ·42 | 113 | 25½ | ·20 |
| May..... | 147 | 7½ | ·38 | 137 | 7½ | ·31 | 86 | 6 | ·25 | 92 | 7½ | ·34 |

That the former alternative is the correct one seems clear from the frequency of the after-shocks during the first three 42-minute periods succeeding the strong after-shock. Taking the number of after-shocks in 3-minute intervals and smoothing the curve by taking for each interval the mean of three successive intervals, the maxima of the curve occur close to the beginning of each of the 42-minute periods. Thus, as the first maximum occurs within a few minutes after the strong after-shock, the period must be connected with the return-movements from the principal earthquake rather than with those (if they existed in sufficient strength) from the after-shock. It follows, therefore, that the movement that gave rise to the after-shock was in the opposite direction to the movement that caused the great earthquake.

### *Locris (N.E. Greece) Earthquakes of Apr. 20 and 27, 1894.*

The first earthquake occurred on Apr. 20 at 6 52 P.M., the second and stronger on Apr. 27 at 9.30 P.M. The after-shocks were recorded at Athens (about 60 miles from the epicentre)*. The first interval ranges from April 20, 7.0 P.M., to Apr. 27, 5.36 P.M., the second from Apr. 27, 9.48 P.M., to May 12, 6.48 P.M.

| Interval. | No. of shocks. | Max. epoch, min. | Amplitude. |
|---|---|---|---|
| Apr. 20–27..... | 21 | 18 | ·52 |
| „ 27–May 12 ... | 31 | 9 | ·23 |

Thus, for the first interval, the maximum epoch agrees nearly with the return-movements.

### *Messina Earthquake of Dec. 28, 1908.*

The earthquake occurred at 5.20 A.M. The first after-shock was recorded at Mileto at 5.36 A.M. and at Catania at 6.4 A.M.†. In the following table the first interval ranges from Dec. 28, 6.0 AM., to Jan. 2, 5.0 A.M., and the second from the latter time to Jan. 12, 3.0 A.M.

* D. Eginitis, *Athènes Obs. Nat. Ann.* ii. pp. 217–229 (1900).

† *Ital. Sism. Soc. Boll.* xv. pt. 2, pp. 566–639 (1911); xvi. pt. 2, pp. 1–50 (1912).

| Record. | Interval. | No. of shocks. | Max epoch, min. | Amplitude. |
|---|---|---|---|---|
| General ... | Dec. 28–Jan. 2. | 107 | 14½ | ·28 |
| „ ..... | Jan 2–12. | 38 | 35½ | ·25 |
| Mileto..... | Dec. 28–Jan. 2. | 58 | 11½ | ·33 |
| „ ... | Jan. 2–12. | 34 | 32½ | ·45 |
| Catania ... | Dec. 28–Jan. 2. | 94 | 14½ | ·36 |

Taking the after-shocks as a whole, the minima of the 42-minute period preceded the return-movements by 6½ min. during the first five days. In the second interval the epoch is reversed. At Mileto the epoch during the first five days preceded the return-movements by 9½ min.; during the next ten days it was reversed. During the months of February and March there is no distinct trace of the period.

### *Marsica Earthquake of Jan.* 13, 1915.

The earthquake occurred at 7.53 A.M. The record of after-shocks at Rocca di Papa (47 miles from the epicentre) is a very full one, the first after-shock being registered at 8.27 A.M. *. The earthquake was unique among those here considered. Though very destructive the area of damage contained only 55 sq. miles and the disturbed area not more than 5700 sq. miles. The first interval of five days (554 after-shocks) gives the maximum epoch at 10 min. and the amplitude as ·06. In succeeding intervals of five, five, and ten days the series of means are somewhat irregular; there is no sign of a reversal of epoch and no certain trace of a 42-minute period after Jan. 18. Making use of shorter intervals, it is clear that the reversal occurred very soon after the earthquake, as follows :—

| Interval. | No. of shocks. | Max. epoch, min. | Ampl. |
|---|---|---|---|
| First six hours (6 hr. 18 m.). | 177 | 19 | ·19 |
| Second „ ..... | 52 | 35½ | ·30 |
| Third „ ..... | 42 | 11½ | ·67 |
| Fourth „ ..... | 32 | 2½ | ·30 |
| Rest of first five days..... | 251 | 40 | ·09 |

* A. Cavasino, *Ital. Sism. Soc. Bol.* xix. pp. 236–291 (1915).

Thus, during the first six hours, the minimum epoch coincided nearly with the return-movement; during the next twelve hours the period seems to be the resultant of two periods with different epochs; in the fourth six hours and during the rest of the first five days the maximum epoch coincided nearly with the return-movement. The early reversal of epoch and the brief duration of the 42-minute pulsations are no doubt connected with the small area affected by the earthquake.

*Hawaiian Earthquakes of Mar.* 28 *and Apr.* 2, 1868.

In these and the remaining earthquakes, the records of after-shocks are non-instrumental. The period considered is, however, too short to be affected materially by the varying conditions of the observers throughout the day.

The first strong earthquake occurred on Mar. 28 at 1.28 P.M., the second and more destructive on Apr. 2 at 3.40 P.M.* The first interval ranges from Mar. 28, 2.6 P.M., to Apr. 1, 6.18 A.M., the second from Apr. 2, 4.12 P.M., to Apr. 7, 4.36 P.M.

| Interval. | No. of shocks. | Max. epoch, min. | Amplitude. |
|---|---|---|---|
| Mar. 28–Apr. 1... | 118 | 24½ | ·23 |
| Apr. 2–7 ..... | 110 | 3½ | ·17 |

Thus, the minima in the first interval and the maxima in the second interval occurred shortly after the return-movements.

*Riviera Earthquake of Feb.* 23, 1887.

The principal earthquake occurred at 6.20 A.M. The first interval ranges from Feb. 23, 9.6 A.M., to Feb. 28, 8.6 A.M., and the second from the latter time to Mar. 10, 6.6 A.M. †.

| Interval. | No. of shocks. | Max. epoch, min. | Amplitude. |
|---|---|---|---|
| Feb. 23–28 ..... | 79 | 20½ | ·38 |
| Feb. 28–Mar. 10 ... | 34 | 5½ | ·45 |

* H. O. Wood, Amer. Seis. Soc. Bull. iv. pp. 178–183 (1914).

† T. Taramelli and G. Mercalli, *Uff. Centr. di Meteor. e Geodin., Annali*, viii. pp. 260–289 (1888).

Thus, in the earlier interval, the maximum epoch occurred at nearly 21 minutes after the return-movements. In the later interval the number of shocks is small, but the epoch tends to agree with those movements. After Mar. 10 there is no trace whatever of the 42-minute period.

### *Zante Earthquake of Apr.* 17, 1893.

The earthquake occurred at 7.4 A.M. The first interval ranges from Apr. 17, 7.0 A.M., to Apr. 22, 6.0 A.M., the second from the latter time to May 2, 4.0 A.M. *

| Interval. | No. of shocks. | Max. epoch, min. | Amplitude. |
|---|---|---|---|
| Apr. 17–22 ..... | 68 | 21½ | ·45 |
| Apr. 22–May 2... | 46 | 30½ | ·34 |

Thus, for the first five days, the minima of the 42-minute period coincided closely with the return-movements.

### *Conclusions.*

(i.) In each of the series of after-shocks examined, there is evidence of the existence of a 42-minute period, connected more or less closely in point of time with the epoch of the earthquake. As a rule, the maxima at first occur about 21 minutes after the returns of the earthquake-movement. This periodicity lasts for about five days—in one earthquake for a few hours and in two others for three or more weeks—but is continued for several weeks longer with a reversal of epoch.

(ii.) The after-shocks of a great earthquake seem to have two distinct origins. Some, including perhaps the stronger, after-shocks result from repetitions of the original movement, transferred in part to other regions and especially to those bordering the area of displacement. Others are due to the settlement of the displaced mass. At first the latter greatly predominate in number, but after about five days the former begin to assert themselves. The reversal of epoch in the 42-minute period is due, not to any change in the variable force, but to the change in the predominating cause of the after-shocks. The change, however, does not take place abruptly, and there are intervals, lasting it may be for some

* *Athènes Obs. Nat. Ann.* ii. pp. 195–196 (1900).

days, in which neither kind of after-shock distinctly predominates. At such times either the maximum epoch occupies an intermediate position, or the series of means is irregular and leads to no definite period *.

(iii.) Three of the earthquakes here considered were followed, after an interval of from one to seven days, by an earthquake of nearly the same, or even greater, intensity. In the Kwanto earthquakes of 1923 and the Hawaiian earthquakes of 1848 the return-movements coincided nearly with the minima of the 42-minute period in the earlier earthquake and with the maxima of the period in the later. In the Locris earthquake of 1894 the change of epoch was less pronounced, but the number of shocks recorded were small (21 and 31). The evidence, so far as it goes, seems to suggest that, when two principal earthquakes occur in one series, the movement causing the earlier is in the opposite direction to that which gives rise to the first after-shocks, while the movement causing the later is in the same direction.

(iv.) So far as I am aware, the 42-minute period is confined to the after-shocks of great earthquakes. I have examined many records of ordinary earthquakes, both for whole years and for single days, but have failed to find any certain trace of the period, except perhaps for a few of the years of the Philippine earthquakes.

(v.) Next to the existence of the 42-minute period, the most interesting point is the length of time for which it lasts. After the great displacement that gives rise to an earthquake, the earth continues to throb for at least ten days, and, in the Kwanto and Tango earthquakes, for not less than two and three months, respectively. Now, during the latter half of the nineteenth century, Milne chronicles 219 destructive earthquakes of the greatest intensity and 368 of the next degree, or, on an average, 12 a year †. As there are many other earthquakes in uninhabited regions of equal or greater strength, it would thus seem possible that the earth is seldom, if ever, entirely at rest from the quivering that follows great earthquake-producing displacements.

* A similar reversal of epoch occurs in the diurnal periodicity of after-shocks (Phil. Mag. xli. pp. 914–915 (1921). Mr. K. Suda has also noticed that, after three or four days, the frequency of the after-shocks of the Kwanto earthquake of 1923 at various stations was somewhat abruptly reduced (Kobe [Japan] Kup. Mac. Obs. Mem. i. pp. 181–186, 1924).

† Brit. Ass. Rep. 1911, pp. 709–740

## LXXXVIII. *The Explosion of Hydrogen-Air Mixtures in a Closed Vessel.*—Part I. *By* B. H. Thorp, *M.Sc* *

### *Introduction.*

DURING the last twenty years several research workers have been measuring the maximum pressures developed in the explosion of gaseous mixtures in closed vessels. The purpose of this paper is to survey the results obtained for mixtures of hydrogen, oxygen, and nitrogen, and to attempt to account for the extraordinary differences between the figures given by various workers. A new diaphragm indicator will also be described, the development of which has emphasized the importance of certain points that have generally been neglected.

As an example of the disagreement which at present exists, the following results may be quoted for a 29·6 per cent. $H_2+14{\cdot}8$ per cent. $O_2+55{\cdot}6$ per cent. $N_2$ mixture exploded at an initial pressure of one atmosphere :—

Table I.

| According to | Ratio of maximum to initial pressure. | Temperature. Initial $t_i°$ C. | Temperature. Maximum $t_m°$ C. | Apparent mean specific heat of steam $t_i°-t_m°$. |
|---|---|---|---|---|
| M. Pier † ..... | 8·38 | 19·4 | 2566 | 10·9 |
| R. W. Fenning ‡ ..... | 7·78 | 51·0 | 2397 | 13·6 |
| Maxwell and Wheeler § .. | 7·97 | 15·0 | 2420 | 12·5 |

The pressure ratios are all corrected to an initial temperature of 15° C. to make them comparable (see Appendix C). These figures have been obtained by interpolation ; the different workers have seldom used mixtures of identical composition, and direct comparison of pressure ratios is difficult. The most convenient method seems to be that of comparing the "apparent mean specific heat" of steam

* Communicated by Prof. W. T. David, Sc.D.

† *Zeit. f. Elektrochem*, xv. p. 536 (1909). The original mixture contained 2·2 per cent. $H_2O$ and a small amount of excess $H_2$ (included in the $N_2$).

‡ Aer. Res. Comm. Report, No. 902, April 1924. This pressure ratio is 2 per cent. higher than that given by Fenning ; in a later paper he says that certain earlier results were 2 per cent. too low, but it is not clear just which.

§ J. C. S. p. 15 (1928). Original mixture contained 1·7 per cent. $H_2O$ (included in the $N_2$).

between 15° C. and the explosion temperature, calculated from each explosion. The method of obtaining these and the figures used for the specific heats of the diluent gases are shown in Appendix A. Allowance has been made in all cases for heat-loss on the basis of actual measurements by Prof. W. T. David (Appendix B). In calculating the apparent mean specific heats, it has been assumed that there was no dissociation of steam or incomplete combustion at maximum pressure. Hence the extent to which they exceed the true mean specific heat of steam is a measure of the amount of energy existing in the gases at maximum pressure in forms other than that of temperature.

In view of this disagreement, it was decided some three years ago to undertake a comprehensive set of explosions under the direction of Professor David in this laboratory, under the best possible conditions and covering a very wide range of $H_2-O_2-N_2$ mixtures. The full results of these will follow in the second part of this paper ; for the present they will only be considered in relation to the results of other workers. With one exception, all the explosions considered in this paper have been made at an initial pressure of one atmosphere.

### *Description of Apparatus employed.*

The explosion vessel is a large cast-steel sphere, 45·4 cm. diameter, with the inner surface silver-plated in order to reduce heat-loss before maximum pressure. It is made in two halves flanged and bolted together ; before each explosion it is opened up and the plating polished with rouge. Extreme care is taken in the drying, mixing, and analysing of the explosive mixtures ; the calculated and observed chemical contractions usually agree to 1 part in 1000 (except where $NO_2$ is formed).

At first a Hopkinson indicator was used, but this was not found suitable for rapid explosions. In these it appears to overshoot, owing either to the inertia of its moving parts or to the pocket below the piston. A new diaphragm indicator (fig. 1) was therefore evolved with a view to overcoming these defects.

A flat diaphragm, 2·8 cm. diameter and 0·75 mm. thick with a solid rim, is turned out of Invar. It is clamped down very firmly on to a seating turned in the wall of the explosion vessel, with only a shallow pocket below it ; the joint is made with a thin ring of soft copper. The glass mirror is stuck on to a small brass pedestal, which is itself soldered on to

the diaphragm at about half the radius; the mirror and pedestal together weigh only 1 gm. A very long beam of light (0·65 m.) is used to obtain a high magnification, and some months were spent in overcoming the optical difficulties involved. The fine, sharp line now obtained enables the deflexions on the films to be measured with an accuracy of 1 in 500.

At first steel diaphragms were used, but it was found that they were giving misleading results, and a large amount of work had to be thrown away. Although protected from the flame by mica they were heated and consequently distorted

Fig. 1.

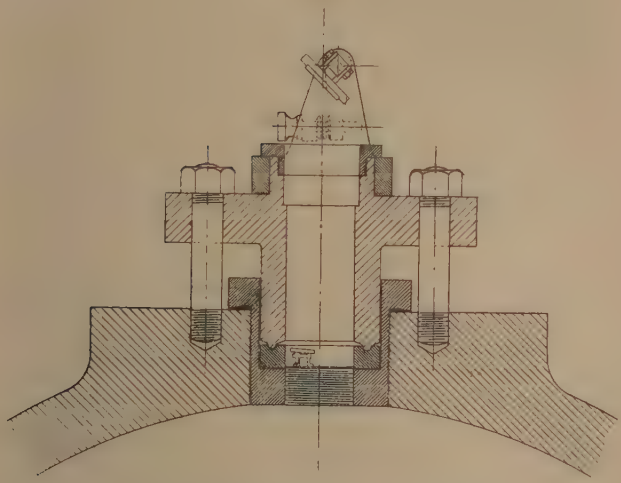

New diaphragm indicator. (Half full size.)

early in the explosion. The distortion due to heating was opposed to that due to increase of pressure inside the vessel, and so the maximum pressure recorded was some 1 per cent. too low. The use of invar has reduced this error to a negligible quantity. Tests on an invar diaphragm in working position showed that a bunsen flame could be held beneath it for at least three seconds before any measurable deflexion took place; whereas with a steel diaphragm a visible deflexion occurred as soon as the flame touched it.

The use of invar had, however, one quite unforeseen effect. While calibrating the indicator it was found that

the temperature of the sphere had a marked influence on the deflexion caused by a given pressure ; a temperature rise of 3° reduced the deflexion 1 per cent. This was at first put down to increase of the modulus of elasticity of invar with temperature, though the data available did not suggest an increase of such magnitude. It was of vital importance to know the cause, as in an average explosion the mean temperature of the diaphragm probably rises some 2° before maximum pressure is reached. If the modulus increases appreciably at the same time, the scale to which the deflexion shall be reckoned is doubtful. The following experiment seemed to show, however, that the modulus does not vary enough to upset the results. During calibration the deflexion produced by a given pressure was determined under the following conditions :—

(*a*) When the diaphragm was at the same temperature as the sphere (15° C.).

(*b*) When some 3 c.c. of half melted snow were dropped on to the diaphragm a couple of seconds before the pressure was applied.

(*c*) When the same was done with water at about 60° C.

No appreciable difference in the deflexions could be measured, and since it can hardly be doubted that the temperature of the diaphragm varied several degrees, it seems clear that it is the temperature of the sphere as a whole whose variations affect the pressure-deflexion scale. It is therefore only necessary to calibrate the indicator over a sufficient range of initial temperatures. The probable explanation is that as the invar diaphragm does not expand thermally along with the sphere as their common temperature rises, but yet is rigidly clamped, it is mechanically stretched and so yields less to the pressure inside the vessel.

Particular care is taken over the calibration of this vessel. The sparking plug is removed from the bottom of the sphere and a tube, passing up through the hole, is screwed into the pocket beneath the diaphragm, the joint being made with a rubber ring. A three-way cock at the bottom of this tube enables the pressure below the diaphragm to be raised suddenly from atmospheric to that of a large tank (170 litres) close by full of compressed air. A record is taken on a film showing the actual jump up of the pressure, the rapidity of which is of the same order as that taking place in an explosion, and the immediate deflexion measured. The

pressure in the tank is measured with a compound mercury gauge to 0·1 per cent., and since it is easy to determine the corrections for such a gauge, the absolute values of the calibration pressures are above suspicion. It is of the utmost importance that the diaphragm should be calibrated in its working position, since the firmness of clamping has a marked effect on the pressure-deflexion scale.

### *Comparison of Experimental Results with those of other Workers.*

Some of the experiments of the following workers have been selected as suitable for comparison with those made here recently :—

M. Pier* (diaphragm indicator ; 40·6 cm. diam. sphere).
R. W. Fenning† (diaphragm indicator ; cylinder 17·8 cm. diam., 20·3 cm. long).
Maxwell and Wheeler‡ (Petavel indicator; 19·7 cm. diam. sphere).
W. Siegel § (diaphragm indicator ; 40·6 cm. diam. sphere).
W. A. Bone ‖ (Petavel indicator ; 7.6 cm. diam. sphere ; 3 atm. initial pressure).

Particulars of these, and the apparent specific heats of steam derived from them, will be found in Table III.

Fig. 2 shows the apparent specific heats plotted against the maximum explosion temperatures for four series of hydrogen-air mixtures—those of Maxwell and Wheeler, Fenning, Bone, and one from this laboratory (Leeds). It is evident that there are considerable differences, and there are good grounds for suggesting that these are chiefly due to the size and shape of vessel used. The Leeds experiments, made in the largest vessel of the four, a sphere 45·4 cm. diameter, give the lowest apparent specific heats—*i. e.* the highest pressure ratios. Maxwell and Wheeler with a sphere 19·7 cm. diameter get intermediate results, while Bone with a very small sphere, only 7·6 cm. diameter, gets the highest apparent specific heat. Fenning, whose results are almost as high as Bone's, used a vessel of about the same size as Maxwell and Wheeler's, but cylindrical in shape. Referring to Table I., it will be seen that Pier with a

* *Loc. cit.* † *Loc. cit.* ‡ *Loc. cit.*
§ *Zeit. f. Phys. Chem.* lxxxvii. p. 641 (1914).
‖ Proc. Roy. Soc. A, cviii. (1925).

40·6 cm. sphere got a much lower apparent specific heat than Maxwell and Wheeler.

Experimental confirmation of this effect of size and shape of vessel on the maximum pressure developed has been obtained in this laboratory. Each mixture was made up in a large tank, drawn off from there to four different vessels (all with rough, black, inner surfaces) and exploded in them under identical conditions. The indicators were calibrated simultaneously, and every precaution taken to ensure strict comparability. Two or more explosions were

Fig. 2.

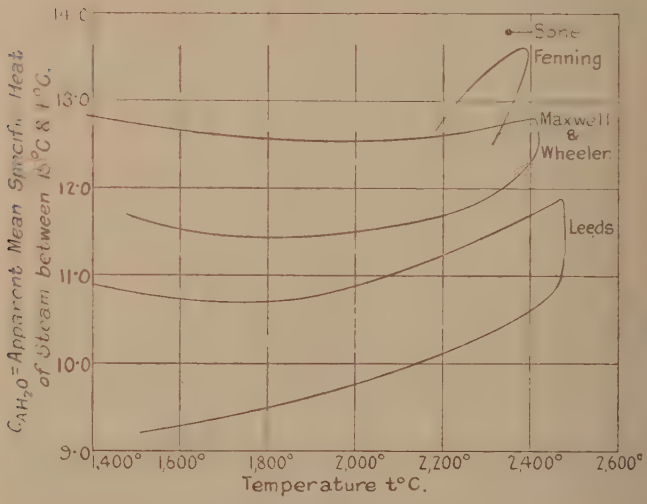


Hydrogen-air mixtures.

made in each vessel for each mixture, and several mixtures were tried. The following results are typical :—

TABLE II.

| Mixture. | Maximum pressure developed in 45·4 cm. sphere. | 30·3 cm. cylinder. | 15·1 cm. sphere. | 15·1 cm. cylinder. |
|---|---|---|---|---|
| 23 % CO+3 % $H_2$+74 % $O_2$... | 7·73 | 7·60 | 7·53 | 7·43 |
| 20 % CO+6 % $H_2$+74 % $O_2$... | 7·69 | 7·46 | 7·58 | 7·36 |

If it be assumed that the absolute rate of heat-loss for a spherical vessel varies as the area of the inner surface (*i. e.* as the diam.$^2$), then the rate of heat-loss, expressed as a percentage of the heat of combustion (which $\propto$ diam.$^3$), varies inversely as the diameter. On the other hand, the time taken to attain maximum pressure varies roughly as the diameter, so that the total percentage heat-loss up to the moment of maximum pressure is almost independent of the diameter. In a cylinder it will be perhaps 50 per cent. greater than in a sphere. But it is believed (on the strength of Professor David's measurements, see Appendix B) that in these rapid explosions it amounts to less than 1 per cent.

Fig. 3.

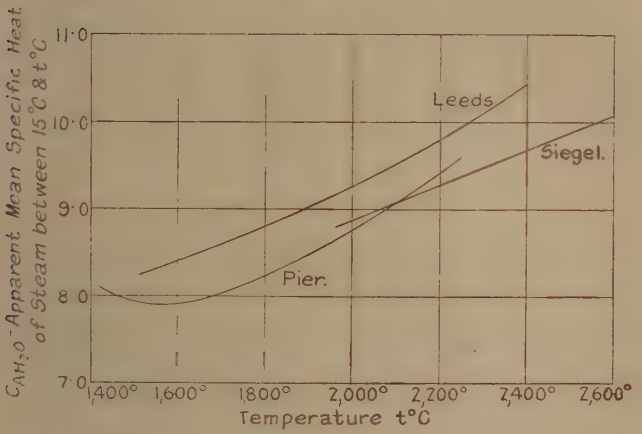


Excess hydrogen-oxygen mixtures.

and that the differences in the pressure ratios must be due to some other far more important factor.

The low pressure ratios recorded by some workers may be partly due to their use of "static" calibration. Pier and Siegel calibrated their indicators by sudden application of compressed air (as is done here), approximating to explosion conditions. The others appear to allow the calibrating pressure to act on the indicator for some time, so that elastic creep may occur before the deflexion is measured. Pier measured this creep and found that it might cause an error of the order of 1 per cent.

Fig. 3 shows apparent specific heat curves derived from

the series of excess hydrogen-oxygen explosions by Pier and Siegel and a third series from this laboratory, all in large spheres of much the same size. It appears that the Leeds experiments are in fair agreement with the others, though they suggest that the maximum pressures recorded by Pier and Siegel are from 1 to 2 per cent. too high. When calibrating they moved their diaphragms to a special vessel (of very small volume, so that it might be filled rapidly to the required pressure with compressed air), and though these may not have been so susceptible to alterations in clamping as the Leeds diaphragms, this throws some doubt on the absolute values of their recorded pressures. They also used steel diaphragms, and our experience has shown (see above) that the distortion of these by heating early in the explosion may cause an error of 1 per cent. either way (depending on the particular diaphragm) in the maximum pressure as calculated from the deflexion. Every care has been taken in this laboratory to obtain very great accuracy in experimenting, and it is believed that the pressures are within $\pm \frac{1}{2}$ per cent. of the true values.

### *Discussion of Results.*

It has been shown how marked an effect the size and shape of the explosion vessel have upon the maximum pressure developed in it for any given mixture of gases, and that this cannot well be explained by heat-loss before maximum pressure. The most likely explanation seems to be that it is due to a time lag in the process of combustion. If the overall reaction $H_2 + \frac{1}{2}O_2 \longrightarrow H_2O + 57{,}290$ cal., after being started in any small volume of gas by the flame travelling through it, takes an appreciable time to complete itself, then the larger the vessel and the more closely it approximates to a sphere with central ignition the more advanced will the reaction be on the average throughout the vessel at the moment of maximum pressure (or at any moment after the flame has reached the walls), and the greater the proportion of the total energy showing itself as temperature and pressure.

There is abundant evidence from other sources to support this theory of "incomplete combustion at maximum pressure," and it will be discussed more fully in the second part of this paper.

TABLE III.

Pier. $x\,\%\ (H_2+\frac{1}{2}O_2)+y\,\%\ H_2+z\,\%\ H_2O$.

| No. | $x\%$. | $z\%$. | Max. temp. $t_m$° C. | $C^{15°,\,t_m°}_{AH_2O}$. |
|---|---|---|---|---|
| 164..... | 13·3 | 2·0 | 1417 | 8·1 |
| 165..... | 15·0 | 2·0 | 1592 | 7·9 |
| 166..... | 17·7 | 1·8 | 1831 | 8·3 |
| 167..... | 20·0 | 1·8 | 2017 | 8·8 |
| 168..... | 23·4 | 2·0 | 2250 | 9·6 |

Siegel. $x\,\%\ (H_2+\frac{1}{2}O_2)+y\,\%\ H_2$.

| No. | $x\%$. | Max. temp. $t_m$° C. | $C^{15°,\,t_m°}_{AH_2O}$. |
|---|---|---|---|
| 78..... | 19·2 | 1963 | 8·8 |
| 75..... | 22·2 | 2205 | 9·3 |
| 76..... | 25·2 | 2428 | 9·7 |
| 79..... | 26·8 | 2535 | 9·9 |
| 77..... | 27·8 | 2593 | 10·1 |

Fenning. $x\,\%\ H_2+y\,\%\ O_2+3{\cdot}9\ y\,\%\ N_2$.

| No. | $x\%$. | Max. temp. $t_m$° C. | $C^{15°,\,t_m°}_{AH_2O}$. |
|---|---|---|---|
| 179..... | 25·2 | 2188 | 12·6 |
| 175..... | 28·0 | 2306 | 13·4 |
| 171..... | 32·3 | 2330 | 12·8 |
| 169..... | 34·6 | 2314 | 12·5 |

Bone, 29·6 % $H_2$ + 14·8 % $O_2$ + 55·6 % $N_2$ at 3 atm. initial pressure, gives

Max. temp. = 2347° C. and $C^{15°,\,t_m°}_{AH_2O} = 13{\cdot}8$.

Maxwell and Wheeler. $x\,\%\ H_2+y\,\%\ O_2+3{\cdot}8y\,\%\ N_2$.

| $x\%$. | Max. temp. $t_m$° C. | $C^{15°,\,t_m°}_{AH_2O}$. |
|---|---|---|
| 14·8 | 1385 | 12·8 |
| 19·1 | 1688 | 12·9 |
| 24·1 | 2090 | 12·2 |
| 28·4 | 2312 | 12·8 |
| 33·5 | 2306 | 12·1 |
| 36·6 | 2258 | 11·7 |
| 38·7 | 2190 | 11·7 |
| 43·6 | 2056 | 11·5 |
| 45·0 | 2010 | 11·6 |
| 53·1 | 1772 | 11·4 |
| 56·2 | 1666 | 11·5 |
| 61·2 | 1477 | 11·7 |

## Appendix A.

*Calculation of Apparent Specific Heat of Steam.*

Let $Q$ = heat of formation of 1 gm. mol. of steam = 57,290 cal.;

$h$ = heat-loss before maximum pressure, as fraction of $Q$;

$x$ = proportion of steam formed;

$w, y, z$ = proportions of steam, $H_2$ and $(N_2+O_2)$ present as diluents;

$t_i$, $t_m$ = initial and maximum temperatures of explosion;

$C_{VH_2}$ = true mean specific heat of hydrogen over the range $t_i$ to $t_m$;

$C_{VN_2}$ = true mean specific heat of $N_2$ and $O_2$ over the range $t_i$ to $t_m$;

$C_{AH_2O}$ = apparent mean specific heat of steam over the range $t_i$ to $t_m$.

Then

$$x.Q(1-h)=(t_m-t_i)[(w+x).C_{AH_2O}+y.C_{VH_2}+z.C_{VN_2}],$$

$$C_{AH_2O}=\frac{x}{w+x}\left[\frac{Q(1-h)}{t_m-t_i}-\frac{y.C_{VH_2}+z.C_{VN_2}}{x}\right].$$

If the original mixture is dry, $w=0$, and this simplifies to

$$C_{AH_2O}=\frac{Q(1-h)}{t_m-t_i}-\frac{y.C_{VH_2}+z.C_{VN_2}}{x}.$$

The mean specific heats of hydrogen, nitrogen, and oxygen are taken from Partington and Shilling's 'Specific Heats of Gases' (1925), and are as follows:—

| | 0° to 1200° | 1600° | 2000° | 2400° | 2800° |
|---|---|---|---|---|---|
| $C_{VH_2}$ ..... | 5·27 | 5·41 | 5·55 | 5·69 | 5·83 |
| $C_{VN_2, O_2}$ ..... | 5·22 | 5·37 | 5·55 | 5·77 | 6·02 |

It should be pointed out that from 1600° upwards these figures have themselves been obtained from explosion experiments. It is, however, improbable that they are so far incorrect (at any rate relatively to each other) as to vitiate the main conclusions reached.

## Appendix B.

### *Heat-loss before Maximum Pressure.*

The heat-loss up to the moment of maximum pressure is calculated from the formula constructed by Prof. W. T. David (Proc. Roy. Soc. A, xcviii. p. 308) from his measurements of loss by radiation and conduction during explosion of coal-gas-air mixtures. It has been assumed that the loss from hydrogen-air explosions is appreciably the same, and that the loss per cent. per second from two different vessels varies directly as the ratio of surface to volume. For the 18 in. sphere the formula becomes

$$\text{Per cent. heat-loss} = \frac{5{\cdot}57 \times (\text{max. temp. }^\circ\text{C.})^{2{\cdot}5} \times \text{time of explosion in secs.}/1000}{10^9 \times \text{per cent. } H_2O \text{ formed}}.$$

For the hydrogen mixtures that have been exploded in the 45·4 cm. diam. sphere the correction varies from 0·3 per cent. for the fastest explosions to 1·4 per cent. for the slowest. For Pier and Siegel's sphere the constant in the formula becomes 6·23, for Maxwell and Wheeler's sphere it is 12·8, for Fenning's cylinder 16·7, for Bone's sphere 10·8 (at three atmospheres, the per cent. loss is assumed inversely proportional to the initial pressure).

This correction has been applied, in calculating the apparent specific heats, by subtracting it from the heat of combustion, which is the only legitimate method. The maximum temperatures given are those actually reached, as calculated from the maximum pressures.

## Appendix C.

### *Correction of Pressure Ratios for Initial Temperature.*

This correction is based on the assumption that two explosions of the same mixture at slightly different initial temperatures, but otherwise under identical conditions, will give the same temperature rise, *i. e.* for two explosions *a* and *b* (if $T_i$, $T_m$ = initial and maximum temps. abs.),

$$(T_m - T_i)_a = (T_m - T_i)_b,$$

$$\frac{T_{ma}}{T_{ia}} = \frac{T_{mb}}{T_{ib}} \times \frac{T_{ib}}{T_{ia}} + 1 - \frac{T_{ib}}{T_{ia}},$$

and, if $P_m$, $P_i$ be the maximum and initial pressures and $e$ the contraction ratio,

$$\frac{P_{ma}}{P_{ia}} = \frac{P_{mb}}{P_{ib}} \times \frac{T_{ib}}{T_{ia}} + e\left(1 - \frac{T_{ib}}{T_{ia}}\right).$$

All the pressure ratios are corrected to 15° C., *i. e.*

$$\left[\frac{P_m}{P_i}\right]_{15°} = \left[\frac{P_m}{P_i}\right]_{T_i} \times \frac{T_i}{288} + e\left(1 - \frac{T_i}{288}\right).$$

This correction neglects the effect of the initial temperature on the mechanism of combustion. Higher initial temperatures probably assist the combustion, but within the limits of these experiments (10° and 23° C.) the effect must be negligible.

---

## LXXXIX. *The Explosion of Hydrogen-Air Mixtures in a Closed Vessel.*—Part II. *By* B. H. Thorp, *M.Sc.**

IN the preceding paper (p. 813) it was shown that the maximum pressure developed in a gaseous explosion is greatly affected by the size and shape of the explosion vessel, large spheres with central ignition giving the highest pressures. It was suggested that combustion lags behind inflammation, and that in the large spheres combustion has, on an average through the vessel, reached a more advanced stage at the moment of maximum pressure, and that therefore a larger proportion of the total energy is making itself felt as pressure.

A new diaphragm indicator was also described, and it was shown that the maximum pressures recorded by this for any particular mixtures in a sphere 45·4 cm. diameter were among the highest found by any workers. Pier and Siegel alone give maximum pressures from 1 to 2 per cent. higher, in a sphere of much the same size, but reasons were mentioned for believing that the results obtained in this laboratory are closer to the true absolute values than theirs.

Our results will now be considered in detail. They consist of six series of explosions at an initial pressure of

* Communicated by Prof. W. T. David, Sc.D.

1 atmosphere. In each series the ratio of nitrogen to oxygen was kept constant, and the resulting "air" was mixed with hydrogen over as wide a range as possible. The ratios of nitrogen to oxygen in the six series were 0, 2, 3·9, 4·9, 6·1 and 6·8. The results are given in Table II.

TABLE I.

The Pressures developed in the Explosion of $x$ per cent. $H_2 + y$ per cent. $O_2 + ay$ per cent. $N_2$ Mixtures.

| % $H_2$. | % $H_2O$ formed. | $\left[\frac{P_m}{P_i}\right]_{15°}$. | Initial Temp. °C. | Maximum Temp. °C. | $C_{A_{H_2}}$. | Time of Explosion in secs./1000 from Spark. | Rise. |
|---|---|---|---|---|---|---|---|
| | | | $N_2/O_2=0$. | | | | |
| 15·0 | 15·0 | 5·46 | 17·6 | 1430 | 12·9 | 51 | 36 |
| 18·9 | 18·9 | 6·33 | 16·0 | 1742 | 12·5 | 34 | 26 |
| 21·1 | 21·1 | 6·76 | 14·1 | 1903 | 12·4 | 25 | 19 |
| 22·7 | 22·7 | 7·07 | 18·5 | 2027 | 12·3 | 15 | 12 |
| 25·3 | 25·3 | 7·49 | 16·9 | 2200 | 12·3 | 15 | 11 |
| — | — | — | — | — | — | — | — |
| 86·5 | 26·1 | 8·13 | 16·0 | 2420 | 10·5 | — | 6 |
| 87·5 | 24·1 | 7·84 | 13·1 | 2292 | 10·1 | 9 | 7 |
| 88·5 | 22·2 | 7·52 | 16·5 | 2165 | 9·7 | — | 8 |
| 89·4 | 20·5 | 7·22 | 14·2 | 2043 | 9·4 | 13 | 10 |
| 90·1 | 19·1 | 6·91 | 18·2 | 1930 | 9·1 | 16 | 12 |
| 90·6 | 18·0 | 6·71 | 17·8 | 1857 | 8·9 | 18 | 14 |
| 91·2 | 16·9 | 6·45 | 14·7 | 1757 | 8·7 | 22 | 16 |
| 91·8 | 15·6 | 6·11 | 17·0 | 1640 | 8·5 | 29 | 21 |
| 92·4 | 14·4 | 5·79 | 18·8 | 1530 | 8·3 | 40 | 28 |
| | | | $N_2/O_2=2$. | | | | |
| 16·3 | 16·3 | 5·95 | 20·5 | 1600 | 11·2 | 41 | 30 |
| 18·4 | 18·4 | 6·44 | 16·3 | 1772 | 11·1 | 34 | 24 |
| 20·3 | 20·3 | 6·82 | 18·2 | 1917 | 11·2 | 23 | 16 |
| 22·5 | 22·5 | 7·22 | 14·8 | 2067 | 11·4 | 16 | 12 |
| 25·2 | 25·2 | 7·63 | 21·4 | 2250 | 11·6 | 12 | 9 |
| 27·4 | 27·4 | 7·94 | 12·8 | 2372 | 11·8 | 11 | 8 |
| — | — | — | — | — | — | — | — |
| 59·3 | 27·3 | 8·19 | 17·5 | 2463 | 10·9 | 8 | 6 |
| 61·6 | 25·8 | 8·02 | 16·4 | 2383 | 10·6 | 9 | 7 |
| 63·8 | 24·3 | 7·82 | 15·4 | 2293 | 10·4 | 10 | 8 |
| 65·9 | 22·9 | 7·58 | 13·3 | 2190 | 10·1 | 11 | 9 |
| 67·4 | 21·8 | 7·44 | 14·9 | 2127 | 9·9 | 12 | 10 |

TABLE I. (*cont.*).

The Pressures developed in the Explosion of $x$ per cent. $H_2+y$ per cent. $O_2+ay$ per cent. $N_2$ Mixtures.

| $H_x$. | $H_2O$ formed. | $\left[\frac{P_m}{P_i}\right]_{15°}$. | Initial Temp.°C. | Maximum Temp.°C. | $C_{A_{H_2}C}$. | Time of Explosion in secs./1000 from Spark. | Rise. |
|---|---|---|---|---|---|---|---|
| | | | $N_2/O_2=2$ (*cont.*). | | | | |
| 69·4 | 20·5 | 7·17 | 15·8 | 2030 | 9·7 | 15 | 12 |
| 72·5 | 18·4 | 6·72 | 14·5 | 1860 | 9·4 | 18 | 14 |
| 74·6 | 17·0 | 6·38 | 13·6 | 1737 | 9·2 | 22 | 18 |
| 76·5 | 15·8 | 6·10 | 16·7 | 1637 | 9·1 | 32 | 22 |
| 78·6 | 14·4 | 5·77 | 18·5 | 1520 | 8·9 | 43 | 30 |
| | | | $N_2/O_2=3·9$. | | | | |
| 15·6 | 16·6 | 6·11 | 14·2 | 1644 | 10·7 | 51 | 35 |
| 17·4 | 17·4 | 6·26 | 18·6 | 1710 | 10·7 | 44 | 30 |
| 20·3 | 20·3 | 6·88 | 15·6 | 1938 | 10·8 | 29 | 20 |
| 22·3 | 22·3 | 7·24 | 18·7 | 2083 | 11·0 | 22 | 16 |
| 25·0 | 25·0 | 7·65 | 18·9 | 2250 | 11·4 | 19 | 14 |
| 27·6 | 27·6 | 8·01 | 16·0 | 2407 | 11·7 | 15 | 12 |
| 29·8 | 28·9 | 8·13 | 20·2 | 2473 | 11·9 | 14 | 11 |
| 32·5 | 27·8 | 8·21 | 16·6 | 2476 | 11·0 | 12 | 10 |
| 35·6 | 26·6 | 8·13 | 13·1 | 2427 | 10·7 | 12 | 10 |
| 38·0 | 25·6 | 7·98 | 17·0 | 2364 | 10·5 | 12 | 10 |
| 41·0 | 24·3 | 7·82 | 12·3 | 2290 | 10·3 | 12 | 10 |
| 44·3 | 23·1 | 7·59 | 17·5 | 2204 | 10·1 | 13 | 10 |
| 49·9 | 20·7 | 7·17 | 15·3 | 2030 | 9·8 | 16 | 13 |
| 51·8 | 19·9 | 7·00 | 17·9 | 1972 | 9·7 | 18 | 14 |
| 53·8 | 19·0 | 6·81 | 16·8 | 1900 | 9·6 | 21 | 16 |
| 56·7 | 17·9 | 6·56 | 16·8 | 1808 | 9·5 | 23 | 19 |
| 59·8 | 16·6 | 6·26 | 14·6 | 1694 | 9·4 | 30 | 24 |
| 62·1 | 15·7 | 6·04 | 18·5 | 1620 | 9·3 | 34 | 28 |
| 64·8 | 14·5 | 5·74 | 18·2 | 1516 | 9·2 | 42 | 32 |
| | | | $N_2/O_2=4·9$. | | | | |
| 12·8 | 12·8 | 5·13 | 15·4 | 1307 | 10·9 | 132 | 95 |
| 15·1 | 15·1 | 5·73 | 20·4 | 1517 | 10·8 | 70 | 50 |
| 17·1 | 17·1 | 6·20 | 17·1 | 1680 | 10·7 | 50 | 35 |
| 19·1 | 19·1 | 6·65 | 17·1 | 1847 | 10·7 | 33 | 28 |
| 21·9 | 21·9 | 7·21 | 18·6 | 2060 | 10·9 | 27 | 22 |
| 24·3 | 24·3 | 7·64 | 13·8 | 2228 | 11·0 | 22 | 20 |
| 25·9 | 25·1 | 7·74 | 16·0 | 2277 | 11·1 | 23 | 18 |
| 27·5 | 24·6 | 7·82 | 15·8 | 2295 | 10·4 | 19 | 17 |
| 28·4 | 24·2 | 7·78 | 14·9 | 2273 | 10·3 | 20 | 17 |
| 31·4 | 23·2 | 7·63 | 16·6 | 2214 | 10·1 | 19 | 17 |

TABLE I. (*cont.*).

| % $H_2$. | % $H_2O$ formed. | $\left[\frac{P_m}{P_1}\right]_{15°}$. | Initial Temp.°C. | Maximum Temp.°C. | $C_{A_{H_2O}}$. | Time of Explosion in secs./1000 from Spark. | Rise. |
|---|---|---|---|---|---|---|---|
| | | | $N_2O_2=4·9$ (*cont.*). | | | | |
| 35·8 | 21·7 | 7·33 | 17·7 | 2097 | 10·0 | 21 | 18 |
| 39·7 | 20·3 | 7·10 | 12·9 | 2003 | 9·8 | 23 | 19 |
| 42·5 | 19·4 | 6·90 | 15·4 | 1926 | 9·7 | 24 | 20 |
| 46·0 | 18·1 | 6·64 | 18·1 | 1833 | 9·6 | 27 | 22 |
| 50·9 | 16·5 | 6·25 | 13·3 | 1685 | 9·4 | 44 | 31 |
| 53·7 | 15·6 | 6·02 | 12·3 | 1605 | 9·4 | — | 40 |
| | | | $N_2/O_2=6·1$. | | | | |
| 13·3 | 13·3 | 5·22 | 19·4 | 1343 | 10·8 | 123 | 83 |
| 15·7 | 15·7 | 5·86 | 19·9 | 1564 | 10·7 | 72 | 52 |
| 17·8 | 17·8 | 6·35 | 16·3 | 1737 | 10·7 | 54 | 40 |
| 19·9 | 19·9 | 6·82 | 18·0 | 1910 | 10·7 | 42 | 30 |
| 22·4 | 21·8 | 7·20 | 18·9 | 2057 | 10·8 | 32 | 27 |
| 24·9 | 21·1 | 7·16 | 15·7 | 2035 | 10·2 | 30 | 25 |
| 27·5 | 20·5 | 7·04 | 17·8 | 1990 | 10·0 | 29 | 22 |
| 29·8 | 19·7 | 6·92 | 19·8 | 1948 | 9·9 | 29 | 23 |
| 34·9 | 18·4 | 6·66 | 15·2 | 1842 | 9·7 | 32 | 25 |
| 39·9 | 17·1 | 6·36 | 16·7 | 1734 | 9·6 | 34 | 28 |
| 44·6 | 15·8 | 6·04 | 17·1 | 1618 | 9·6 | 43 | 34 |
| 49·6 | 14·3 | 5·65 | 19·0 | 1485 | 9·5 | 58 | 45 |
| 52·7 | 13·5 | 5·43 | 18·1 | 1407 | 9·5 | 75 | 56 |
| 54·5 | 13·0 | 5·30 | 17·3 | 1364 | 9·5 | 86 | 64 |
| | | | $N_2/O_2=6·8$. | | | | |
| 14·0 | 14·0 | 5·46 | 16·2 | 1420 | 10·6 | 107 | 80 |
| 14·8 | 14·8 | 5·64 | 16·5 | 1485 | 10·6 | 96 | 70 |
| 15·7 | 15·7 | 5·89 | 17·4 | 1570 | 10·6 | 72 | 53 |
| 17·2 | 17·2 | 6·23 | 18·0 | 1696 | 10·6 | 62 | 48 |
| 17·9 | 17·9 | 6·40 | 18·5 | 1757 | 10·6 | 59 | 45 |
| 20·2 | 20·2 | 6·93 | 14·4 | 1943 | 10·6 | 43 | 35 |
| 22·3 | 20·0 | 6·95 | 16·9 | 1957 | 10·1 | 39 | 32 |
| 24·6 | 19·5 | 6·86 | 17·8 | 1920 | 9·9 | 38 | 30 |
| 26·2 | 19·0 | 6·77 | 19·4 | 1890 | 9·8 | 36 | 29 |
| 29·0 | 18·3 | 6·63 | 11·0 | 1827 | 9·7 | 35 | 28 |
| 33·1 | 17·2 | 6·39 | 14·5 | 1740 | 9·6 | 37 | 30 |
| 36·4 | 16·3 | 6·18 | 17·6 | 1667 | 9·6 | 42 | 35 |
| 40·2 | 15·4 | 5·95 | 15·4 | 1584 | 9·5 | 55 | 45 |
| 44·4 | 14·3 | 5·66 | 17·8 | 1487 | 9·5 | 75 | 60 |

Fig. 1.

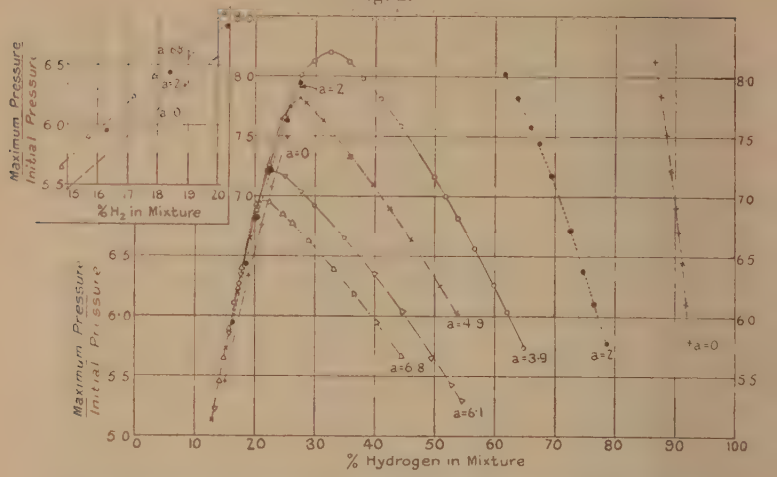


The ratios of maximum to initial pressure ($P_m/P_i$) are all corrected to an initial temperature of 15°C., and the "apparent mean specific heat" of steam ($C_{\Delta_{H_2O}}$) between

Fig. 2.

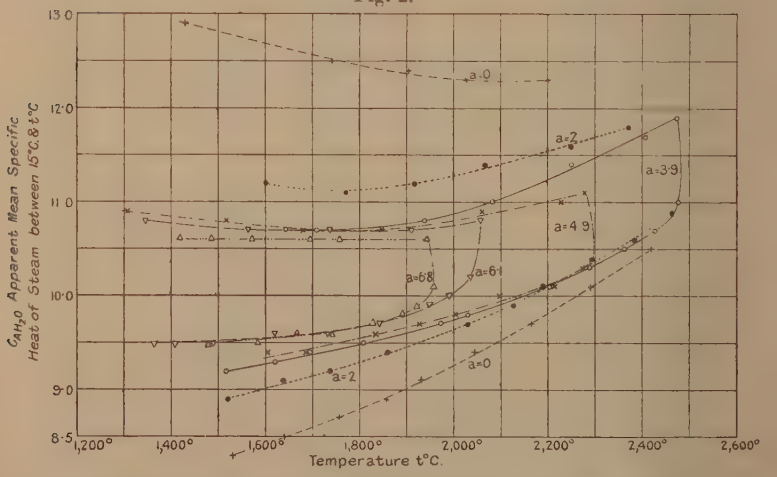


the initial and maximum temperature is calculated for each explosion (see Appendices to previous paper). These apparent specific heats are shown plotted against the

maximum temperatures in fig. 2, curves being drawn through the points belonging to each series. There are three striking features :—

1. It will be noticed that each curve consists of two almost parallel lines, the points on the lower line being obtained from mixtures containing an excess of hydrogen, and those on the upper line from mixtures containing an excess of " air."

2. In the case of mixtures containing excess hydrogen, the replacement of part of that hydrogen by nitrogen causes a great increase in the apparent specific heat of steam, or, in other words, reduces the maximum pressure.

3. In the case of mixtures containing excess oxygen, the replacement of part of that oxygen by nitrogen causes a great decrease in the apparent specific heat of steam, *i. e.* it increases the maximum pressure.

Considering 1, three possible explanations might be put forward :—

(*a*) That there is greater dissociation of steam at maximum pressure in the excess oxygen than in the excess hydrogen mixtures ; or,

(*b*) That the chemical process $H_2+\frac{1}{2}O_2 \rightarrow H_2O+57290$ cals. is further from completion at the moment of maximum pressure in the excess oxygen than in the excess hydrogen mixtures ; or,

(*c*) That, contrary to general belief, the specific heat of oxygen is much higher than that of hydrogen at high temperatures.

As mixtures containing very little excess oxygen or hydrogen differ nearly as much as those containing large excesses (*c*) may be ruled out. For the series in which the nitrogen/oxygen ratio is 6·8 the highest temperatures reached are only about 1950°C., and since " dissociation " in the strict sense of the word is negligibly small at temperatures below 2000°C. this cannot account for the missing energy. It seems probable therefore that there is extensive " incomplete combustion " (defined in the sense

described in (*b*) above) at the moment of maximum pressure in all the mixtures containing excess oxygen, and that at the higher temperatures (over 2000°C.) dissociation occurs as well.

The second feature may be readily explained on the principle of mass action, but the third is directly opposed to that principle, and apparently some process is taking place which completely swamps the mass action effect. Comparing for example the mixtures :—

20 per cent. $(H_2+\frac{1}{2}O_2)+70$ per cent. $O_2$ giving a maximum pressure of 6·55 atm.,

20 per cent. $(H_2+\frac{1}{2}O_2)+13{\cdot}3$ per cent. $O_2+56{\cdot}7$ per cent. $N_2$ giving a maximum pressure of 6·76 atm.,

20 per cent. $(H_2+\frac{1}{2}O_2)+1{\cdot}3$ per cent. $O_2+68{\cdot}7$ per cent. $N_2$ giving a maximum pressure of 6·82 atm.,

it is evident that here the presence of nitrogen has a beneficial effect on the overall process of combustion.

It is possible that $H_2O_2$ is a primary product in those explosions where there is a large excess of $O_2$; it would reduce the maximum pressure both through having a higher heat of formation than steam, and also through increasing the chemical contraction.

It has been felt that some attempt should be made to find out whether chemical equlibrium is established at the moment of maximum pressure. If the exploded gases could be very rapidly cooled just after maximum pressure has been reached, analysis might show whether chemical reaction is still in progress.

An arrangement has been made whereby a valve in the wall of the explosion vessel may be suddenly opened and closed again at any desired points during the explosion. Through this valve carbon dioxide may be injected in large quantities into the exploded gases, cooling them down suddenly to 200° or 300°C. Alternatively the valve may be opened to allow a large fraction (20 per cent.) of the hot gases to be injected into cool carbon dioxide or any desired reagent. This apparatus is still in the trial stage and no definite results can yet be given.

It is proposed to continue these experiments at higher initial densities, and a start has already been made with explosions at three atmospheres.

*Calculation of the Extent of Incomplete Combustion for any mixture.*

If several mixtures which develop the same maximum explosion temperature give different values for the apparent mean specific heat of steam between 15°C. and that temperature, it may be supposed that there is least incomplete combustion at the moment of maximum pressure in the mixture which gives the lowest value for the mean specific heat. It is possible to calculate how much more incomplete combustion there is in the other mixtures than in that one, but not to obtain absolute values from the data here available.

Fig. 2 shows that the lowest values for the apparent specific heat of steam come from mixtures containing hydrogen only as diluent. It will be assumed for the present that these are the true values, and on that basis the amount of incomplete combustion in any other mixture may be calculated as follows :—

Let $Q$ = the heat of formation of 1 gm.mol. of $H_2O$ = 57290 cal.,

$a$ = proportion of incomplete combustion at maximum pressure,

$x$ = proportion of $H_2O$ formed by the end of the explosion,

$t_i$, $t_m$ = initial and maximum temperatures of explosion,

$C_{H_2O}$ = true mean specific heat of steam over the range $t_i$ to $t_m$,

$C_d$ = true mean specific heat of the diluent $N_2$, $H_2$ & $O_2$ between $t_i$ & $t_m$.

Then $$x \,.\, Q(1-a) = (t_m - t_i)[x \,.\, C_{H_2O} + (1 - 3x/2).C_d]$$

$$1 - a = \frac{t_m - t_i}{Q}\left(C_{H_2O} + \frac{2-3x}{2x} \,.\, C_d\right),$$

or $$a = 1 - \frac{t_m - t_i}{Q}\left(C_{H_2O} + \frac{2-3x}{2x} \,.\, C_d\right).$$

It must be observed that the calculated maximum temperature

$$t_m = t_i \times \frac{P_m}{P_i} \times \frac{1}{1-\frac{1}{2}(1-a)x}$$

depends on the proportion of incomplete combustion. For the case $x=0{\cdot}2$, $t_m$ will be 0·6 per cent. lower when the incomplete combustion $a=0{\cdot}05$ than when $a=0$, *i. e.* erhaps 12° in 2000°C. This will only be so if "incomplete combustion" means that some of the $H_2$ and $O_2$ molecules that should have combined to form $H_2O$ still exist as $H_2$ and $O_2$ molecules at maximum pressure, so that chemical contraction is also incomplete. If, however, incomplete combustion is not chemical in nature, or if it means that some intermediate endothermic product such as $H_2O_2$ is in existence at maximum pressure, the chemical contraction may be complete by this time. It has therefore been considered advisable to neglect the possible effect on the maximum temperature.

TABLE II.

Percentage Incomplete Combustion at Maximum Pressure.

| Maximum Temp. °C. | Ratio $N_2/O_2$ = | 0 | 2 | 3·9 | 4·9 | 6·1 | 6·8 |
|---|---|---|---|---|---|---|---|
| **Excess Hydrogen Mixtures.** | | | | | | | |
| 1600 ... ... ... | | 0 | 1·6 | 2·2 | 2·7 | 3·1 | 3·1 |
| 1800 ... ... ... | | 0 | 1·8 | 2·1 | 2·2 | 2·7 | 3·1 |
| 2000 ... ... ... | | 0 | 0·9 | 1·6 | 1·7 | 2·8 | — |
| 2200 ... ... ... | | 0 | 0·7 | 1·2 | 1·2 | — | — |
| 2400 ... ... ... | | 0 | 0·7 | 0·7 | — | — | — |
| **Excess "Air" Mixtures.** | | | | | | | |
| 1600 ... ... ... | | 11·2 | 7·4 | 6·6 | 6·6 | 6·6 | 5·8 |
| 1800 ... ... ... | | 11·4 | 7·2 | 6·0 | 6·0 | 6·0 | 5·3 |
| 2000 ... ... ... | | 10·6 | 7·1 | 5·6 | 5·4 | 5·0 | — |
| 2200 ... ... ... | | 9·3 | 6·6 | 5·5 | 4·3 | — | — |
| 2400 ... ... ... | | — | 6·0 | 5·5 | — | — | — |

These are minimum figures in that they are based on the assumption that there is no incomplete combustion in mixtures of oxygen with excess hydrogen.

### *Conclusions.*

It has been shown from the experiments carried out in this laboratory on mixtures of hydrogen, oxygen and nitrogen, that :—

(*a*) There seems to be extensive incomplete combustion at the moment of maximum pressure in mixtures containing excess oxygen.

(*b*) Probably the same is true in a lesser degree for mixtures containing excess hydrogen ; hence the specific heat of steam, as calculated from the maximum pressures developed in explosion experiments, must always be rather too high.

(*c*) By taking the lowest apparent specific heat of steam found for a given temperature as the true specific heat, the extent of incomplete combustion at maximum pressure in other mixtures giving that same maximum temperature may be estimated.

(*d*) For mixtures containing excess hydrogen, the gradual replacement of that hydrogen by nitrogen causes a steady decrease in the maximum pressure, *i. e.*, an increase in the amount of incomplete combustion.

(*e*) For mixtures containing excess oxygen, the gradual replacement of that oxygen by nitrogen causes a steady increase in the maximum pressure, *i. e.* a decrease in the amount of incomplete combustion.

I should like to express my indebtedness and gratitude to Professor David for his invaluable direction and advice during the progress of this work, and for permission to use the results of other workers in this laboratory of the Engineering Department, Leeds University (see Part I, Table 2 ; they have also taken a considerable part in the development of the new diaphragm indicator).

I should also like to thank the Department of Scientific and Industrial Research for maintenance grants during the two years 1925-27, which enabled me to begin this work.

XC. *The Characteristic Numbers of the Mathieu Equation with Purely Imaginary Parameter.* *By* H. P. MULHOLLAND *and* S. GOLDSTEIN *.

METHODS are known for calculating the characteristic numbers of integral order of the Mathieu equation

$$\frac{d^2y}{dx^2}+(4\alpha-16q\cos 2x)y=0, \quad . \quad . \quad . \quad . \quad (1)$$

and tables have been given † for real $q$. We have calculated the first eight characteristic numbers for purely imaginary $q$, and the results are given in Tables I. *a* and I. *b* (p. 839).

The notation is the usual one ‡. $\alpha_n$ and $\beta_n$ correspond to the functions $ce_n$ and $se_n$ respectively.

The equation with purely imaginary parameter is of importance in the physical problem of the alternating flow of electricity along conducting elliptic cylinders. In addition, it has considerable theoretical interest.

### *Numerical Example and Tabular Values.*

As an example we shall give the calculation of $\beta_2$ (corresponding to the function $se_2(x)$, odd in $x$ and $\frac{1}{2}\pi-x$) for $q=1{\cdot}8i$.

If
$$se_2(x,q)=\sum_{r=1}^{\infty}\mathrm{B}_{2r}\sin 2rx, \quad . \quad . \quad . \quad . \quad . \quad (2)$$

$$i\mathrm{B}_{2+r2}/\mathrm{B}_{2r}=u_r, \quad . \quad . \quad . \quad . \quad . \quad . \quad . \quad . \quad . \quad (3)$$

and
$$q=is, \quad . \quad . \quad . \quad . \quad . \quad . \quad . \quad . \quad . \quad (4)$$

then the recurrence relations for the B lead to the formula

$$u_{r-1}=\frac{2s}{r^2-\alpha+2su_r} \quad (r>1) \quad . \quad . \quad . \quad . \quad (5)$$

and the equation

$$\mathrm{L}=1-\alpha+2su_1=0. \quad . \quad . \quad . \quad . \quad . \quad (6)$$

* Communicated by Prof. E. L. Ince.

† Ince, Proc. Roy. Soc. Edin. xlvi. pp. 20–29 (1925); xlvi. pp. 316–322 (1926); xlvii. pp. 294–301 (1927). Goldstein, Trans. Camb. Phil. Soc. xxiii. pp. 303–336 (1927).

‡ See the papers cited above, or Whittaker and Watson's 'Modern Analysis,' Chap. xix. The parameters $a=4\alpha$ and $\theta=8q$ are also employed sometimes

The method of calculation is to take $u_r = 0$ for a sufficiently large value of $r$, and to find the required zero of L by Newton's rule. A first approximation, $\alpha$, to the zero is found by methods to be given later, and a second approximation is given by $\alpha + \delta\alpha$, where

$$\delta\alpha = -\mathrm{L}/\frac{\partial \mathrm{L}}{\partial \alpha}. \quad . \quad . \quad . \quad . \quad . \quad . \quad . \quad (7)$$

To calculate $\partial \mathrm{L}/\partial\alpha$ we first differentiate (5), obtaining

$$\frac{\partial}{\partial \alpha}(2su_{r-1}) = u^2{}_{r-1}\left[1 - \frac{\partial}{\partial \alpha}(2su_r)\right], \quad . \quad . \quad . \quad (8)$$

by repeated applications of which we arrive at the convenient formula :

$$-\partial \mathrm{L}/\partial\alpha = 1 - u_1{}^2 + u_1{}^2u_2{}^2 - u_1{}^2u_2{}^2u_3{}^2 + \ldots \quad . \quad . \quad (9)$$

For $q$ equal to $1{\cdot}8i$, we choose $3{\cdot}6829 - 3{\cdot}1779i$ as first approximation to $\beta_2$ (see p. 838). It is sufficient to take $u_8$ equal to zero.

Then

$$u_7 = \frac{3{\cdot}6}{60{\cdot}3171 + 3{\cdot}1779i} = 0{\cdot}060 - 0{\cdot}003i,$$

$$u_6 = \frac{3{\cdot}6}{45{\cdot}3171 + 3{\cdot}1779i + 3{\cdot}6(0{\cdot}060 - 0{\cdot}003i)}$$

$$= 0{\cdot}0787 - 0{\cdot}0055i,$$

$$u_5 = \frac{3{\cdot}6}{32{\cdot}3171 + 3{\cdot}1779i + 3{\cdot}6(0{\cdot}0787 - 0{\cdot}00551i)}$$

$$= 0{\cdot}10949 - 0{\cdot}01060i,$$

and so on until we get

$$u_2 = 0{\cdot}4702\ 3365 - 0{\cdot}2213\ 5931i,$$

$$u_1 = \frac{3{\cdot}6}{0{\cdot}3171 + 3{\cdot}1779i + 3{\cdot}6(0{\cdot}4702\ 3365 - 0{\cdot}2213\ 5931i)}$$

$$= 0{\cdot}7452\ 61814 - 0{\cdot}8828\ 48342i,$$

and

$$\mathrm{L} \equiv 1 - \alpha + 2su_1 = 0{\cdot}0000\ 4253 - 0{\cdot}0003\ 5403i.$$

Also

$$-\partial L/\partial\alpha = 1 - u_1^2 + u_1^2u_2^2 - u_1^2u_2^2u_3^2 + \ldots = 0{\cdot}9380 + 1{\cdot}1374i,$$

Hence we take

$$\delta\alpha = \frac{0{\cdot}0000\ 4253 - 0{\cdot}0003\ 5403i}{0{\cdot}9380 + 1{\cdot}1374i} = -0{\cdot}000167 - 0{\cdot}000175i.$$

Our next approximation to $\alpha$ is therefore

$$\alpha = 3{\cdot}682733 + 3{\cdot}178075i,$$

and with this value of $\alpha$ we find

$$L = -0{\cdot}0000\ 0002 - 0{\cdot}0000\ 0001i.$$

It is to be noticed that the ratios of the coefficients in the Fourier series are found in the process of finding the characteristic numbers, so that the calculation of the functions themselves is a simple matter.

The series of Mathieu * suffice to show that, for sufficiently small $s$, $\alpha_{2m}$ and $\beta_{2m}$ are real. We find that $\alpha_0$ and $\alpha_2$ become equal when $s = 0{\cdot}1836\ldots$. For larger values of $s$, up to $2{\cdot}0$, the tables show $\alpha_0$ and $\alpha_2$ as conjugate complex numbers. It will be seen later that a certain asymptotic expansion gives good numerical approximations to $\alpha_0$ for the larger values of $s$ here considered, and unless this ceases to hold with increasing $s$, $\alpha_0$ remains complex, and $\alpha_0$ and $\alpha_2$ remain conjugate.

Similar remarks apply to $\beta_2$ and $\beta_4$.

We have found $\alpha_4$ and $\alpha_6$ and $\beta_6$ and $\beta_8$ to behave in a similar way. The numerical values suggest the theorem that $\alpha$, as a function of $q$, has an infinite number of branch-points on the imaginary axis in the $q$ plane.

In the neighbourhood of the point where $\alpha_0$ and $\alpha_2$ become equal, Newton's method fails. Hence, having taken $u_r$ as zero for some sufficiently large value of $r$, we must write out the equation $L = 0$ in full, and use another method for finding the roots in question—say Horner's method for real roots and the root-squaring method of Dandelin, Lobachevsky, and Graeffe for complex ones. [The process was employed to find $\alpha_0$ and $\alpha_2$ for $s = 0{\cdot}2$. It was sufficient to solve a quintic, and it was quicker to find the real roots by Horner's method and divide out than to use the root-squaring method.]

$\alpha_{2m+1}$ and $\beta_{2m+1}$ are conjugate complex numbers.

* *Journ. de Math.* (2) xiii. pp. 137–203 (1868).

### *Asymptotic Expansions.*

Numerical values show that, as $s$ increases, $\alpha_0$ and $\alpha_2$ approach $\alpha_1$ and $\beta_1$, and $\beta_2$ and $\beta_4$ approach $\alpha_3$ and $\beta_3$.

Now $\alpha_0$ and $\alpha_2$ being given on the real axis, their values on the imaginary axis beyond the branch-point will depend on the path taken from a point on the real axis (or, alternatively, on the cuts made in the $q$-plane). A full discussion of the singularities of $\alpha$ as a function of $q$ is beyond the scope of this paper, but for the sake of clarity it is desirable to be able to distinguish between $\alpha_0$ and $\alpha_2$. We shall therefore suppose the path in the $q$-plane so chosen that along the imaginary axis, for the sufficiently large values of $s$ to be considered, $\alpha_0$ is nearly equal to $\beta_1$. Similarly we shall suppose that $\alpha_3$ is nearly equal to $\beta_4$.

Now when $q$ is real and positive,

$$\alpha_m \sim \beta_{m+1} \sim \mathrm{A}_m{}^*, \quad . \quad . \quad . \quad . \quad . \quad (10)$$

where

$$\mathrm{A}_m \equiv -\tfrac{1}{8}k^2 + \tfrac{1}{4}m'k - \frac{m'^2+1}{2^5} - \frac{m'(m'^2+3)}{2^8 k}$$
$$- \frac{54m'^4+34m'^2+9}{2^{12}k^2} - \frac{m'(33m'^4+410m'^2+405)}{2^{16}k^3}$$
$$- \frac{63m'^6+1260m'^4+2943m'^2+486}{2^{18}k^4}$$
$$- \frac{m'(527m'^6+15617m'^4+69001m'^2+41607)}{2^{22}k^5} - \ldots$$
$$. \quad . \quad . \quad (11)$$

Here $$k = +(32q)^{\frac{1}{2}}, \quad \text{and} \quad m' = 2m+1 \quad . \quad . \quad . \quad (12)$$

Also †

$$\beta_{m+1} - \alpha_m \sim \mathrm{B}_m \quad . \quad . \quad . \quad . \quad . \quad . \quad (13)$$

where

$$\mathrm{B}_m \equiv \tfrac{1}{2}\left(\frac{k}{\pi}\right)^{\frac{1}{2}} \frac{(8k)^{m+1}}{m!}\, e^{-2k}\left(1 + \frac{c_1}{k} + \frac{c_2}{k^2} + \ldots\right), \quad . \quad (14)$$

* Ince, *loc. cit.*; Goldstein, *loc. cit.*

† Goldstein, Proc. Roy. Soc. Edin. xlix. pp. 210–223 (1929). The numerical results given here were obtained about the same time as the above formula, and provided at first a strong incentive to finding the formula, and later a valuable check on its accuracy, since it was obtained by a formal process only.

and it has been found empirically from numerical results for real $q$ that when $m$ is 0, $c_1$ is $-0{\cdot}45$, and when $m$ is 1, $c_1$ is $-1{\cdot}698$.

We had not proceeded far with the calculation when we noticed that the following asymptotic expressions would give good numerical approximations when $q$ is a positive imaginary:

$$\alpha_0 \sim \beta_1 \sim A_0 \quad . \quad . \quad . \quad . \quad . \quad . \quad (15)$$

and

$$\alpha_3 \sim \beta_4 \sim A_1, \quad . \quad . \quad . \quad . \quad . \quad . \quad (16)$$

where arg $q$ is given its principal value in interpreting the $q^{\frac{1}{2}}$ involved.

We found similarly that the formulæ

$$\beta_1 - \alpha_0 \sim B_0 \quad . \quad . \quad . \quad . \quad . \quad . \quad (17)$$

and

$$\beta_4 - \alpha_3 \sim B_1 \quad . \quad . \quad . \quad . \quad . \quad . \quad (18)$$

held for the larger values of $s$ considered.

(The obvious extensions of these formulæ are

$$\alpha_{4m} \sim \beta_{4m+1} \sim A_{2m}, \quad \alpha_{4m-1} \sim \beta_{4m} \sim A_{2m-1}, \quad . \quad (19)$$

and

$$\beta_{4m+1} - \alpha_{4m} \sim B_{2m}, \quad \beta_{4m} - \alpha_{4m-1} \sim B_{2m-1}.) \quad . \quad (20)$$

When $q$ is real and positive, $A_m$ is a better approximation to $\frac{1}{2}(\alpha_m + \beta_{m+1})$ than to either $\alpha_m$ or $\beta_{m+1}$. Numerical values show similar results for $A_0$ and $A_1$ when $q$ is imaginary, so that we have compared $A_0$ with $\frac{1}{2}(\alpha_0 + \beta_1)$ and $A_1$ with $\frac{1}{2}(\alpha_3 + \beta_4)$ (see Table II. *a*, p. 840). Also $\beta_1 - \alpha_0$ is compared with $B_0$, and $\beta_4 - \alpha_3$ with $B_1$ (Table II. *b*, p. 840). The values of $c_1$ are the same as for real $q$ for $m$ equal to 0 and 1 respectively.

Finally, we point out how an approximate value of $\alpha$ is found to start the main calculation. First, when $s$ is sufficiently small, we use the series of Mathieu previously mentioned. When $s$ is moderately large, we take $A_0 - \frac{1}{2}B_0$ as an approximation to $\alpha_0$, and when $\alpha_0$ has been calculated, take $\alpha_0 + B_0$ as an approximation to $\beta_1$. Similarly we take $A_1 - \frac{1}{2}B_1$ as an approximation to $\alpha_3$, and $\alpha_3 + B_1$ as an approximation to $\beta_4$. In this way the approximation to $\beta_2$ (which is conjugate to $\beta_4$) when $s$ is 1·8, namely $3{\cdot}6829 - 3{\cdot}1779i$, was obtained. As examples we may note that when $s$ is as low as 0·4 we get $0{\cdot}603 - 0{\cdot}990i$ as an approximation to $\alpha_0$, and $0{\cdot}5286 - 0{\cdot}9395i$ as an approximation to $\beta_1$—both very good approximations indeed, with which we have no difficulty in completing the calculation.

TABLE I. *a*.

| $\varepsilon$. | $a_0$. | $a_2$. |
|---|---|---|
| 0·02 | 0·003209 | 0·997324 |
| 0·04 | 0·012947 | 0·989185 |
| 0·06 | 0·029567 | 0·975226 |
| 0·08 | 0·053740 | 0·954772 |
| 0·10 | 0·086618 | 0·926663 |
| 0·12 | 0·130223 | 0·888869 |
| 0·14 | 0·188444 | 0·837489 |
| 0·16 | 0·270636 | 0·763155 |
| 0·18 | 0·422320 | 0·620331 |

TABLE I. *b*.

| $\varepsilon$. | $a_0$. | $\beta_1$. |
|---|---|---|
| 0·2 | $0{\cdot}526248-0{\cdot}217463\,i$ | $0{\cdot}328562-0{\cdot}416728\,i$ |
| 0·4 | $0{\cdot}599837-0{\cdot}992788\,i$ | $0{\cdot}528852-0{\cdot}940749\,i$ |
| 0·6 | $0{\cdot}705302-1{\cdot}640667\,i$ | $0{\cdot}713982-1{\cdot}602207\,i$ |
| 0·8 | $0{\cdot}821211-2{\cdot}306374\,i$ | $0{\cdot}838783-2{\cdot}299441$ |
| 1·0 | $0{\cdot}931317-2{\cdot}995455\,i$ | $0{\cdot}939893-2{\cdot}999885\,i$ |
| 1·2 | $1{\cdot}030380-3{\cdot}699973\,i$ | $1{\cdot}032031-3{\cdot}704884\,i$ |
| 1·4 | $1{\cdot}119646-4{\cdot}413499\,i$ | $1{\cdot}118567-4{\cdot}416182\,i$ |
| 1·6 | $1{\cdot}201620-5{\cdot}132870\,i$ | $1{\cdot}200182-5{\cdot}133715\,i$ |
| 1·8 | $1{\cdot}278205-5{\cdot}856723\,i$ | $1{\cdot}277220-5{\cdot}856638\,i$ |
| 2·0 | $1{\cdot}350591-6{\cdot}584391\,i$ | $1{\cdot}350120-6{\cdot}584019\,i$ |

| $\varepsilon$. | $a_3$. | $\beta_2$. | $\beta_4$. |
|---|---|---|---|
| 0·2 | $2{\cdot}211411-0{\cdot}016747\,i$ | 1·053942 | 3·978050 |
| 0·4 | $2{\cdot}130732-0{\cdot}141334\,i$ | 1·223940 | 3·903906 |
| 0·6 | $2{\cdot}143946-0{\cdot}406823\,i$ | 1·544119 | 3·742990 |
| 0·8 | $2{\cdot}294532-0{\cdot}719887\,i$ | 2·162533 | 3·346121 |

| | | $\beta_4$. |
|---|---|---|
| 1·0 | $2{\cdot}541327-1{\cdot}065650\,i$ | $2{\cdot}895037-0{\cdot}906426\,i$ |
| 1·2 | $2{\cdot}852994-1{\cdot}475122\,i$ | $3{\cdot}063353-1{\cdot}538181\,i$ |
| 1·4 | $3{\cdot}181293-1{\cdot}974374\,i$ | $3{\cdot}255211-2{\cdot}088545\,i$ |
| 1·6 | $3{\cdot}472882-2{\cdot}543309\,i$ | $3{\cdot}464373-2{\cdot}627919\,i$ |
| 1·8 | $3{\cdot}718564-3{\cdot}138044\,i$ | $3{\cdot}682733-3{\cdot}178075\,i$ |
| 2·0 | $3{\cdot}935301-3{\cdot}737708\,i$ | $3{\cdot}901859-3{\cdot}746215\,i$ |

NOTE.—$\beta_1$ and $a_3$ are conjugate to $a_1$ and $\beta_3$ respectively, and $a_0$ and $\beta_4$ when complex, are conjugate to $a_2$ and $\beta_2$ respectively.

TABLE II *a*.

| $\varepsilon$. | $\frac{1}{2}(a_0+\beta_1)$. | $A_0$. |
|---|---|---|
| 0·2 | 0·427405 − 0·317095 $i$ | 0·381560 − 0·346229 $i$ |
| 0·4 | 0·564344 − 0·966768 $i$ | 0·567214 − 0·963367 $i$ |
| 0·6 | 0·709642 − 1·621437 $i$ | 0·709697 − 1·622127 $i$ |
| 0·8 | 0·829997 − 2·302907 $i$ | 0·829848 − 2·302867 $i$ |
| 1·0 | 0·935605 − 2·997670 $i$ | 0·935618 − 2·997634 $i$ |
| 1·2 | 1·031205 − 3·702428 $i$ | 1·031215 − 3·702430 $i$ |
| 1·4 | 1·119106 − 4·414840 $i$ | 1·119107 − 4·414843 $i$ |
| 1·6 | 1·200901 − 5·133292 $i$ | 1·200900 − 5·133292 $i$ |
| 1·8 | 1·277712 − 5·856680 $i$ | 1·277712 − 5·856680 $i$ |
| 2·0 | 1·350356 − 6·584205 $i$ | 1·350356 − 6·584205 $i$ |
| $\varepsilon$. | $\frac{1}{2}(a_3+\beta_4)$. | $A_1$. |
| 1·0 | 2·7182 − 0·9860 $i$ | 2·6720 − 0·9759 $i$ |
| 1·2 | 2·9582 − 1·5067 $i$ | 2·9593 − 1·5014 $i$ |
| 1·4 | 3·2183 − 2·0315 $i$ | 3·2234 − 2·0309 $i$ |
| 1·6 | 3·4686 − 2·5856 $i$ | 3·4693 − 2·5874 $i$ |
| 1·8 | 3·7006 − 3·1581 $i$ | 3·7001 − 3·1585 $i$ |
| 2·0 | 3·9186 − 3·7420 $i$ | 3·9183 − 3·7418 $i$ |

TABLE II. *b*.

| $\varepsilon$. | $\beta_1-a_0$. | $B_0$. |
|---|---|---|
| 0·2 | −0·20 −0·20 $i$ | −0·14 −0·17 $i$ |
| 0·4 | −0·0710 +0·520 $i$ | −0·0712 +0·0533 $i$ |
| 0·6 | +0·0087 +0·0385 $i$ | +0·0089 +0·0382 $i$ |
| 0·8 | +0·01757 +0·00693 $i$ | +0·01754 +0·00686 $i$ |
| 1·0 | +0·008576 − 0·004430 $i$ | +0·008542 − 0·004439 $i$ |
| 1·2 | +0·001651 − 0·004911 $i$ | +0·001640 − 0·004902 $i$ |
| 1·4 | −0·001079 − 0·002683 $i$ | −0·001081 − 0·002678 $i$ |
| 1·6 | −0·001438 − 0·000845 $i$ | −0·001436 − 0·000842 $i$ |
| 1·8 | −0·000985 + 0·000085 $i$ | −0·000983 + 0·000085 $i$ |
| 2·0 | −0·000471 + 0·000372 $i$ | −0·000470 + 0·000372 $i$ |
| $\varepsilon$. | $\beta_4-a_3$. | $B_1$ |
| 1·0 | +0·35 +0·16 $i$ | +0·33 +0·18 $i$ |
| 1·2 | +0·210 −0·063 $i$ | +0·215 −0·062 $i$ |
| 1·4 | +0·0739 −0·1142 $i$ | +0·0731 −0·1149 $i$ |
| 1·6 | −0·0085 −0·0846 $i$ | −0·0082 −0·0842 $i$ |
| 1·8 | −0·03583 − 0·04003 $i$ | −0·03568 − 0·03988 $i$ |
| 2·0 | −0·03344 − 0·00851 $i$ | −0·03336 − 0·00849 $i$ |

# XCI. *Measurement of the Flow of Heat.* By A. F. Dufton, *M.A., D.I.C., and* W. G. Marley *.

[Plates XV. & XVI.]

1. THE method recently described † of recording the flow of heat across the surface of a wall is only applicable when the flow of heat is toward the wall. It requires, moreover, the insertion of thermocouples in the surface of the wall, and cannot be used at a glass surface such as a window. Simpler apparatus has now been devised which does not suffer from these limitations and the transfer of heat by radiation and by convection can be recorded as separate items.

2. The instrument shown in Pl. XV. is designed to measure radiation. It comprises 40 sheets of tinfoil (0·5 in. × 0·3 in.) connected in series by wire alternately of 40 s.w.g. constantan ½ in. long and of 46 s.w.g. copper. Alternate sheets are cemented together, with paper insulation in the overlap, to form panels (2 in. × ½ in.) and the terminals are connected to a recording galvanometer. The obverse of one panel and the reverse of the other are sprayed with carbon black.

3. The radiation instrument was calibrated upon a wall, the flow of heat to which was measured by the method referred to above. The heating was contrived so that the temperature of the air was automatically kept equal to that of the wall surface : the heating was purely radiant.

An E.M.F. of 743 microvolts was recorded by the instrument when the flow of heat was 10 B.Th.U. per square foot per hour.

This calibration was checked by exposing the instrument between blackened copper surfaces, one of which was at room temperature. Table I. shows the measured values together with the radiation between surfaces of emissivity 0·92 calculated from Stefan's Law ($\sigma = 5\ 7 \times 10^{-5}$ erg cm.$^{-2}$ sec.$^{-1}$ deg.$^{-4}$).

4. The instrument shown in Pl. XVI. is designed to measure convection. It comprises short lengths of 40 s.w.g. wire, alternately of copper and of constantan, soldered together to form 16 junctions touching the wall surface and 16 junctions 5·0 mm. from the wall. The terminals are connected to a recording galvanometer.

* Communicated by the Authors.

† Journ. of Scientific Inst. iv. p. 446 (1927).

5. The convection instrument was calibrated upon a wall, the convection of heat to which was recorded as the difference

TABLE I.

| Temperature difference °C. | Radiation (B.Th.U./sq. ft./hour). | |
|---|---|---|
| | Measured. | Calculated. |
| 3·4 | 5·8 | 5·6 |
| 4·0 | 6.6 | 6·6 |
| 4·7 | 8·1 | 7·8 |
| 5·5 | 9·2 | 9·2 |
| 7·1 | 11·9 | 11·9 |
| 8·0 | 13·5 | 13·5 |
| 12·6 | 21·1 | 21·7 |
| 14·6 | 24·8 | 25·4 |

Fig. 1.

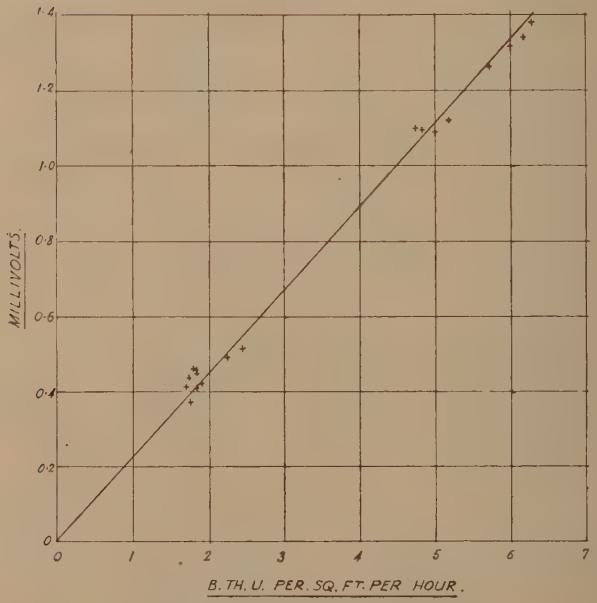


Calibration of convection instrument.

between the total flow and the radiant heat measured as described above.

The measurements show that the convected heat is proportional to the 1·07th power of the E.M.F. recorded by the instrument. Although the relationship is not linear, it is clear from fig. 1 that for the range required the error in "making it so" is negligible.

6. The radiation and convection instruments can be combined to record the total flow of heat. Simultaneous records of the flow from a room to a wall by the original method and by the new instrument are shown in fig. 2. It will be

Fig. 2.

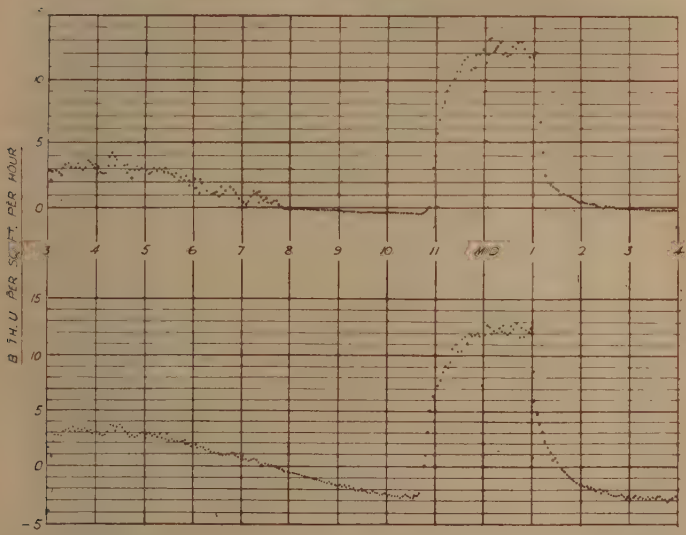


The flow of heat from a room to a wall simultaneously recorded by the original method (above) and by the new instrument.

seen that the original method ceased to measure when the flow became zero and when the uncovered surface of the wall became cooler than the surface covered by the square foot of cork. On resumption the record was inaccurate for a short period until the square foot had regained uniformity with the remainder of the wall.

### *Note on the Convection of Heat.*

In the calibration of the convection instrument the convection of heat to a wall was recorded as the difference

between the total flow of heat and the radiant heat. A record was also made of the temperature difference between the air (at 5·0 cm. from the wall) and the wall surface. Corresponding values are plotted in fig. 3.

Previous experimenters, using small bodies, have found the convection of heat per unit area to be approximately proportional to the 5/4th power of the temperature difference and to be a function of the size of the body.

Fig. 3.

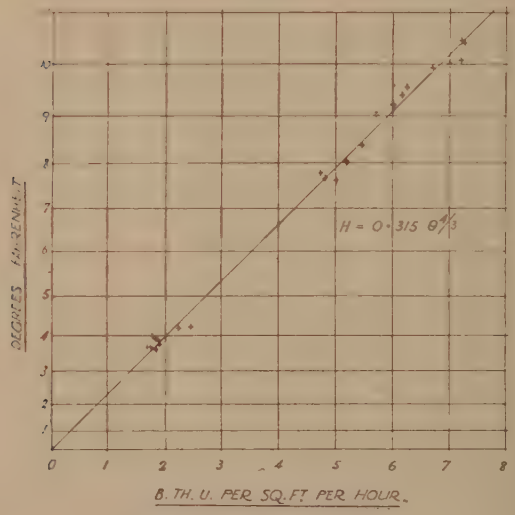


Heat transfer by convection.

Considerations of Similitude * show that if the convection per unit area were independent of the size of the body it would be proportional to the 4/3rd power of the temperature difference.

The present measurements show the convection of heat to a wall to be proportional to the 4/3rd power of the temperature difference and equal to 0·315 B.Th.U. per sq. ft. per hour for a temperature difference of 1° Fahrenheit.

Building Research Station,
Garston, Herts.

* Dict. of Applied Physics, i. p. 477.

## XCII. *The K-Absorption Discontinuities of Manganous and Chromate Ions.* *By* Don M. Yost, *Fellow of the National Research Council and International Education Board* *.

IT is known that the wave-length of the X-ray absorption discontinuity of an element is influenced not only by the valence of the element, but also by the nature of the crystal in which the element occurs. Thus the wave-length of the K-absorption discontinuity of chloride ion in crystalline sodium chloride is different from that found in the case of potassium chloride †. It was thought that similar effects might be found when the discontinuity for ions in aqueous solution was compared with that for the same ions present in a crystal.

The solutions of the salts used were placed in fine quartz capillary tubes. The outside diameters of the tubes varied from 0·04 mm. to 0·1 mm., the inside diameter being about six-tenths of the outside diameter. To fill the tubes it was only necessary to dip one end into the solution, the capillary action causing the liquid to rise in them. The longer-filled tubes were cut into sections of about one centimetre in length, and the ends of the latter carefully sealed with a bit of hard wax. The tubes, before being used, were placed in a spectrograph, which was then evacuated. After some fifteen minutes the tubes were examined and the defective ones rejected. They were also examined at the end of an experiment to make sure that no leaks had developed.

In an absorption experiment a tested tube was placed directly in a V-shaped slit in such a way that the walls of the tube were tangent to the walls of the slit. Two small bits of soft wax served to hold the tube securely in place. The vacuum spectrograph used was of the conventional Siegbahn type. A piece of 20-$\mu$ red-coloured goldbeater's skin was employed as a window between the body of the spectrograph and the X-ray tube to prevent the light emitted by the filament from fogging the photographic plate. Both filament and anticathode were of tungsten. The tension used was about twice that corresponding to the wave-length of the absorption discontinuity; the electron current varied from 25 to 100 milliamperes, and the length of the exposures from 4 to 8 hours. The analysing crystal was of calcite.

* Communicated by the Author.

† See Siegbahn's 'Spectroscopy of X-rays' Oxford Univ. Press, (1925). Also Otto Stelling, 'Ueber den Zusammenhang zwischen chemischer Konstitution und K-Röntgenabsorptionsspectra.' Thesis from Lund University, Sweden.

Preliminary experiments showed that for the region of longer wave-lengths (3·5 A and greater) the absorption of the quartz itself was so great that satisfactory photograms could not be obtained in a reasonable length of time. The final experiments were carried out with solutions of manganous chloride and potassium chromate, the ions of interest being manganous ion and chromate ion. The small amount of material actually present in the path of the beam of X-rays made it necessary to use concentrations of at least 0·7 molal, since with lower concentrations the lack of photographic contrast at the absorption edge made it impossible to measure the plates with any accuracy.

In the following table are presented some representative results. The values there given are the distances in millimetres between the absorption edges and a standard reference line photographed on the same plate. The corresponding measurements for the solid salts are also given, and were obtained with the same spectrograph.

Results of the Absorption Measurements.

Radius of spectrograph : 176·27 mm.
Analysing crystal : Calcite.

| Substance. | Concentration. | Std. line. | Dist. of edge from std. line. | Distance of white line from std. line. |
|---|---|---|---|---|
| $MnCl_2$ ... | Solid. | $FeK\alpha_1$ | 2·58 mm. | — |
| $MnCl_2$ ... | 1·399 m. | „ | 2·61 „ | — |
| $MnCl_2$ ... | 0·699 m. | „ | 2·64 „ | — |
| $K_2CrO_4$... | Solid. | „ | 7·81 „ | 8·13 mm. |
| $K_2CrO_4$... | 1·681 m. | „ | 7·78 „ | 8·08 „ |

Within the limits of experimental error the absorption discontinuities of manganous and chromate ions in solution have the same wave-lengths as the corresponding ions in crystalline salts. It is possible that differences might be observed in the region of longer wave-lengths, say for the case of chlorides ; the experimental difficulties to be overcome are rather formidable, however. It is to be especially noted that the fine structure of the chromate edge (designated as a white line in the table) observed in the case of the solid salts is also observed unchanged in the spectra obtained with solutions. Moreover, it was also found that no observable reduction of the chromate to lower valence forms had taken place. In this case, at least, the fine structure is to be

attributed to the chromate chromium itself, and not to reduced forms arising as a result of the action of the X-radiation.

I wish to express here my appreciation of Prof. M. Siegbahn's kindness in allowing me to make use of the facilities of his laboratory at Uppsala. I am also indebted to him for suggesting and providing the capillary tube.

Uppsala,
June 1929.

---

XCIII. *The Scattering of Beta-Particles by Light Gases and the Magnetic Moment of the Electron.* *By* MALCOLM C. HENDERSON, *Ph. D., Trinity College, Cambridge* *.

## 1. *Introduction.*

IN 1925 Uhlenbeck and Goudsmit † showed that the multiplet structure of line spectra could be interpreted if it were postulated that the electron is not merely a point charge of electricity, but possesses also an angular momentum of $\frac{1}{2} \cdot \frac{h}{2\pi}$ due to its own rotation and a magnetic moment equal to one Bohr magneton. This postulate provides a theoretical basis for the fourth quantum number. The problem then arises as to the effect the magnetic moment will have when two electrons collide with one another.

If an electron possesses at all times a magnetic field, such as is necessarily associated with a magnetic moment, the collisions between it and a $\beta$-particle, that is, between two electrons, should be profoundly modified. For example, it may be calculated simply from the law of force between magnets in the "end-on" position ($6MM'/r^4 = e^2/r^2$, where $M = M' = 9{\cdot}2 \times 10^{-21}$ Gauss-cms.) that the distance at which the electrostatic force equals the magnetic force is about $5 \times 10^{-11}$ cm. As usually calculated from the electrostatic force alone, the closest possible approach in a head-on collision between a 344,000 volt $\beta$-ray and an electron is about $8{\cdot}3 \times 10^{-13}$ cm.,

* Communicated by Dr. J. Chadwick. The material in this paper formed part of a Thesis submitted for the degree of Doctor of Philosophy at the University of Cambridge.

† Uhlenbeck & Goudsmit, *Naturwiss.*, xiii. p. 953 (1925); 'Nature,' cxvii. p. 264 (1926).

that is, about 1/60 as much. At less than $5 \times 10^{-11}$ cm. the magnetic force of attraction will exceed the electrostatic force of repulsion, since it varies as a higher negative power of the distance. The deflexion experienced by a $\beta$-ray on passing an electron at 60 times the minimum possible distance of approach is about half a degree. All deflexions larger than this amount should be greatly influenced by the magnetic force. The angle through which a particle is deflected for a given nearness of approach should be widely different from the deflexion as calculated from the inverse square law only. Consequently the manner in which the number of particles scattered varies with their deflexion should also be different from the calculated distribution. It may be noted in passing that an inverse fourth power orbit is unstable and under some conditions the electrons might theoretically coalesce.

The other kind of magnetic deflexion, namely, that experienced by a charged particle moving in a magnetic field, is eliminated by the assumption that the particles come at once into the end-on position. The motion is then entirely along the lines of force and the equation $H\rho = mv/e$ no longer applies. If this assumption is not made, a rough calculation shows that the maximum distance at which the two forces may be equal is about $8 \times 10^{-12}$ cm.

From the theory of single scattering, as developed in detail by Darwin*, it can easily be shown that for small angles the ratio of the nuclear to the electronic scattering is $N^2 : N$, where N is the atomic number of the scattering element. Hence for hydrogen and helium the electronic scattering will be respectively $\frac{1}{2}$ and $\frac{1}{3}$ of the total. For these elements a discrepancy in electronic scattering should therefore be expected to show most markedly. By comparing the scattering of $\beta$-rays by these two gases with the scattering by nitrogen and argon it should be possible to determine whether the electrons do in fact possess some field of force in addition to their normal electrostatic field.

Of the solid elements in which the scattering of $\beta$-rays has been studied, aluminium is the lowest in atomic number. For small angles the electrons of this element cause, theoretically, about 8 per cent. of the total scattering.

* C. G. Darwin, Phil. Mag. xxvii. p. 499 (1914).

In previous investigations * the interest was in the nuclear scattering and a correction was made for the scattering by the electrons. The agreement between the experimental results when corrected and those expected from theory suggests that the electronic scattering is in fact not very different from 8 per cent. But the correction is too small, compared to the total scattering, for this evidence to be conclusive. From observations of $\beta$-ray tracks in a Wilson expansion chamber, Bothe † found the electronic scattering in air to be of about the expected amount, but the small number of collisions observed leaves something to be desired statistically.

Accordingly, some preliminary measurements were made with hydrogen, helium, nitrogen, and argon in a simple form of scattering chamber. Use was made of a familiar principle, namely, the reduction in the number of particles in a beam caused when some of them are deflected through more than a fixed angle. The results suggested an increased scattering in hydrogen and helium. The following more accurate investigation was therefore undertaken.

## 2. *Apparatus and Method.*

The scattering chamber used was of the "annular ring" type. It was similar to the one used by Rutherford and Chadwick‡ for measuring the scattering of $\alpha$-particles in helium.

The dimensions are shown in the figure (see p. 850). The diaphragms were originally of graphite, but the natural effect when the chamber was evacuated was much too high. The diaphragms were therefore backed with 2 mm. of lead (not shown in the figure) and the central disks were joined and supported by a brass rod only slightly smaller in diameter than the disks. The support for the rod was a thin sheet of graphite. The scattering from this support is unavoidable. It amounted, however, together with other residual scattering, to less than $\frac{1}{8}$ of the total current and was deducted from the readings. The average angular limits of the scattering were 9·2 and 29·7 degrees, and the thickness of the scattering layer was 3 cm.

The gases measured were hydrogen, helium, nitrogen, argon, and air. The first four were drawn from cylinders of

* Chadwick and Mercier, Phil. Mag. l. p. 208 (1925); and others.
† Bothe, *Zeit. f. Phys.* xii. p. 117 (1922).
‡ Rutherford and Chadwick, Phil. Mag. iv. p. 605 (1927).

the compressed gas. Every gas passed over phosphorus pentoxide before entering the scattering chamber, and the hydrogen and helium were in addition passed through two charcoal tubes cooled in liquid air. A test experiment showed no difference between hydrogen that was thus purified and that which was taken directly from the cylinders. Nevertheless it was always thus purified. The nitrogen was taken directly from the cylinders. Any impurity was presumably air, and since the ratio of the theoretical scatterings of air and nitrogen is 69·6 : 65·8, an impurity of this kind would be quite negligible. The argon used was about 99·5 per cent. pure.

The source of $\beta$-rays was a deposit of radium E on a nickel button 3 mm. in diameter. The deposit was

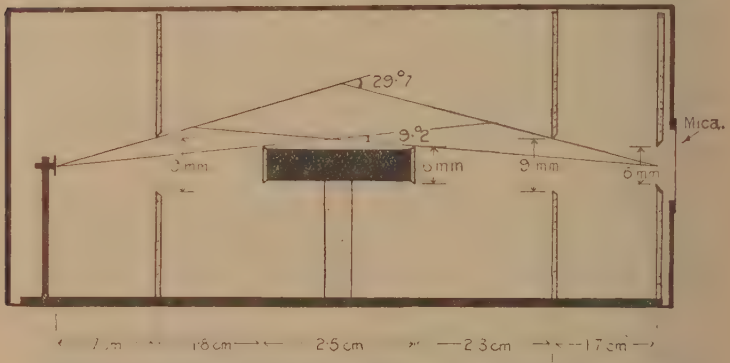


obtained by stirring the button for some time in a hot solution of radium D, E, and F. The initial strength of the source was equivalent to about $\frac{3}{4}$ mg. of radium, as measured on a $\beta$-ray electroscope. The amount of radium D on the button was less than 1 per cent.

The $\beta$-rays from radium E are heterogeneous and their velocity varies over rather a large range. The average energy is in the neighbourhood of 344,000 volts*, $\beta=0{\cdot}8$. The deflexion which any particle experiences in a given encounter varies inversely as the square of its energy. This fact is not important as long as only the relative scattering by different elements is measured. A possible source of error is that hydrogen may scatter, for example, the low velocity rays relatively more strongly than the

* Ellis and Wooster, Proc. Roy. Soc. A, cxvii. p. 109 (1927).

high velocity rays in comparison with argon. Such a selective effect would mean that the scattering varies with the energy of the rays according to a different law for different atomic numbers. For such a departure from theory there is no experimental evidence.

The measurements were made with a Dolezalek electrometer with a sensitivity of about 3000 mm. per volt. During each experiment the electrometer was held at its zero position by a charge induced on a small condenser forming part of the insulated system. A measure of the ionization current was afforded by the time required for the voltage on the outer casing of the condenser to change by a fixed amount while holding the electrometer stationary. The ionization chamber was cylindrical, 10 cm. in diameter and 14 cm. deep. The outer casing was maintained at 200 volts. Guard rings protected the insulated system from leakage across the insulation of the ionization chamber and condenser.

### 3. *The Theoretical Scattering Power.*

In the original annular scattering chamber* the scattering substance was in the form of foil. A term $t \sec \phi/2$ entered the integrand of the expression for the scattering because the foil was not perpendicular to the incident beam of particles. In the chamber as modified for gases $t$ is measured along the incident beam and is approximately constant. The expression for the scattering by the nuclei then becomes :

$$\nu_n = \frac{Qnt\,N^2}{8r^2}\left(\frac{e^2}{mv^2}\right)^2 \int_{\phi_1}^{\phi_2} \operatorname{cosec}^3\frac{\phi}{2}\cdot\cos\frac{\phi}{2}\cdot\frac{d\phi}{2}$$

$$= \frac{Qnt\,N^2}{16r^2}\left(\frac{e^2}{mv^2}\right)^2 \left[-\operatorname{cosec}^2\frac{\phi}{2}\right]_{\phi_1}^{\phi_2}.$$

$\nu_n$ is the number of particles received per unit area of the final diaphragm perpendicular to the axis of the chamber, Q is the number of particles in the incident beam, $n$ is the number of atoms of the gas per c.c., N is the atomic number of the scatterer, $m$ is the mass and $v$ the velocity of the $\beta$-particle, and $r$ is the average distance from the source to the scattering layer. This expression differs only slightly, in numerical value, from the more complex formula in the original paper.

* Chadwick, Phil. Mag. xl. p. 734 (1920).

If we consider an electron in the atom to be at rest before the encounter and take its mass equal to that of the incident $\beta$-particle, then the amount of the electronic scattering will be given by

$$\nu_e = N\frac{Qnt}{4r^2}\left(\frac{e^2}{mv^2}\right)^2\left[-\operatorname{cosec}^2\phi\right]_{\phi_1}^{\phi_2}.$$

The number of electrons projected between the angles $\phi_1$ and $\phi_2$ will be

$$N\frac{Qnt}{4r^2}\left(\frac{e^2}{mv^2}\right)^2\left[\sec^2\phi\right]_{\phi_1}^{\phi_2}.$$

For the values of $\phi_1$ and $\phi_2$ used in these experiments the projected electrons are relatively so few in number that they will be neglected in the calculations which follow.

The sum of these expressions gives the total scattering by the gas.

However, as shown by C. G. Darwin *, each of these expressions must be corrected for the change in the orbit caused by the variation of the mass of the $\beta$-particle with its velocity, the so-called relativity correction. For the nuclear scattering this takes the form

$$\left[\frac{\beta\operatorname{cosec}\psi}{\cot\frac{\phi}{2}}\right]^2, \quad \text{where} \quad \beta\cot\psi = \tan\left[\pi - \cos\psi\left(\frac{\phi+\pi}{2}\right)\right].$$

The mean value of this correcting factor was calculated to be 1·2 for the conditions of the present experiments.

The corresponding correcting factor for the electronic scattering has not been worked out. However, elementary considerations show that it will have a value less than one, that is, it will serve to reduce the calculated amount of electronic scattering, for in the encounter with an electron the $\beta$-particle will be retarded in its motion, not accelerated as in an encounter with the positive nucleus. The correction will in general be small and it has been omitted in the following calculations.

Adding the above expressions for the nuclear and electronic scattering and simplifying:

$$\nu = \frac{Qnt}{4r^2}\left(\frac{e^2}{mv^2}\right)^2\left[\frac{1}{4}N^2\operatorname{cosec}^2\frac{\phi}{2}\cdot\left[\frac{\beta\operatorname{cosec}\psi}{\cot\frac{\phi}{2}}\right]^2 + N\operatorname{cosec}^2\phi\right]_{\phi}^{\phi_1}.$$

* C. G. Darwin, Phil. Mag. xxv. p. 201 (1913).

Substituting the values for the experimental conditions, viz.,

$$\phi_2 = 29°{\cdot}7\,; \quad \phi_1 = 9°{\cdot}2\,; \quad \left[\frac{\beta \operatorname{cosec} \psi}{\cot \frac{\phi}{2}}\right]^2 = 1{\cdot}2$$

$$\nu = k\left[\mathrm{N}^2 \cdot \frac{143{\cdot}2}{4} \cdot 1{\cdot}2 + 35{\cdot}3\,\mathrm{N}\right],$$

where $k = \frac{\mathrm{Q}nt}{4r^2}\left(\frac{e^2}{mv^2}\right)^2$,

or, to a sufficiently exact approximation.

$$\nu = 35{\cdot}8k(1{\cdot}2\,\mathrm{N}^2 + \mathrm{N}).$$

As shown by this formula the number of scattered particles should be proportional to $1{\cdot}2\mathrm{N}^2 + \mathrm{N}$ when there are the same number of atoms present per c.c. The values entered in column 2 of Table II are calculated from this expression.

### 4. *Experimental Results.*

In each experiment readings of the ionization current were taken for different pressures of the various gases: hydrogen, helium, nitrogen, argon, and air. When the pressure is plotted against the ionization current the points lie approximately on straight lines, indicating the predominance of single scattering, up to a pressure of about 2 cm. for argon, 6 cm. for nitrogen, 50 cm. for helium and 70 cm. for hydrogen. There is a tendency toward upward curvature as plural scattering becomes more prominent *. The observed values of the ionization current in two experiments, corrected for natural effect, with the corresponding pressures are shown in columns 2 and 3 of Table I. The ionization current divided by the pressure gives a constant for each gas, and the ratios of these constants to each other are the ratios of the scattering powers. The quotients of the figures in column 2 divided by those in column 3 are entered in column 4.

Table II. gives the collected results of the last five experiments. In column 2 are the theoretical values of

* It may be noted that the scattering ceases to be single at about the point indicated by Wentzel's criterion. For example, the scattering in nitrogen is single up to a pressure of about 6 cm., for which $4\omega$ under the conditions of these experiments was about 4·8°, while $\phi$ varies from 9° to 30°. (*Cf.* Wentzel, *Ann. d. Phys.* lxix. p. 335, 1922.)

the relative scattering power of the gas concerned (see section 3), in column 3 are the theoretical percentage

TABLE I.

Showing the pressures and corresponding ionization currents for various gases and the resulting relative scattering powers.

| 1 | 2 P. | 3 I. | 4 I./P. | 5 Av. | |
|---|---|---|---|---|---|
| N ... ... | 5·01 | 23·3 | 4·65 | | |
| | 4·23 | 20·5 | 4·84 | 4·64 | |
| | 3·23 | 14·4 | 4·46 | | $\frac{4\cdot64}{23_4} = \frac{65\cdot8}{3\cdot32} = \frac{N_2}{H_2}$ |
| $H_2$ ... ... | 73·50 | 17·2 | ·234 | | |
| | 55·00 | 12·9 | ·235 | ·234 | |
| | 67·15 | 19·0 | ·283 | | $\frac{4\cdot64}{27_7} = \frac{65\cdot8}{3\cdot92} = \frac{N_2}{He}$ |
| He ... ... | 37·30 | 10·1 | ·271 | ·277 | |
| A ... ... | 2·57 | 48·1 | 18·7 | | |
| | 1·90 | 37·9 | 19·9 | 19·4 | |
| | 1·21 | 23·9 | 19·7 | | $\frac{19\cdot4}{8\cdot4} = \frac{203}{88} = \frac{A}{Air}$ |
| Air ... ... | 2·05 | 16·9 | 8·25 | | |
| | 4·14 | 35·8 | 8·65 | 8·4 | |
| | 6·12 | 50·5 | 8·25 | | |

TABLE II.

Collected Results.

| 1 Gas. | 2 Theoretical scattering power $1\cdot2N^2+N$ | 3 Theoretical percentage electronic contribution. | 4 Experimental scattering powers. A=203. | 5 Ratio experimental to theoretical. |
|---|---|---|---|---|
| $H_2$ ..... | 2·2 | 45 | 4·0 | 1·8 |
| He ..... | 3·4 | 29 | 4·8 | 1·4 |
| $N_2$ ..... | 65·8 | 10·6 | 79 | 1·2 |
| Air ..... | 69·6 | 10·4 | 84 | 1·2 |
| A ..... | 203 | 4·4 | 203 | 1 |

contributions by the electrons to that scattering power, in column 4 are the experimentally determined scatterings all reduced to 203 for argon (the ratio of nitrogen to air is taken as normal, that is, equal to 65·8 : 69·6), in column 5

are the ratios of experimental to theoretical scattering power.

### 5. *Discussion.*

The results in Table II. show that the lighter gases possess a scattering power for $\beta$-rays in excess of that calculated from the expression $1{\cdot}2N^2+N$. This excess scattering may be attributed to the orbital electrons, since it increases with decreasing atomic number in about the same manner as does the theoretical electronic scattering. An attempt was made to fit the expression $1{\cdot}2N^2+kN$ to the observed scatterings by using various values of $k$. When $k=3{\cdot}3$ the relative values of this expression lie within eight per cent. of the observed scatterings in the gases measured.

In the collisions between nucleus and $\beta$-particle it is usually assumed that the magnitude of the velocity of the $\beta$-particle is unchanged by the encounter, unless there is radiation. On the other hand its velocity is reduced in an encounter with another electron because of the energy imparted to the latter. Calculation of a special case shows that when a $\beta$-particle of velocity $\cdot 8c$ is scattered by an electron through an angle of 11·2 degrees, its velocity is reduced to $\cdot 79c$ and the projected electron moves with a velocity of $\cdot 25c$ in a direction at 76·7° with the incident particle. The loss of velocity suffered by the $\beta$-particle is thus small. No correction has therefore been made for this effect in these experiments.

As calculated in section 1, if the magnetic moment of the electron is one Bohr magneton, the maximum distance at which the magnetic and electric forces between two electrons become equal is $5\times 10^{-11}$ cm. This is about 60 times the minimum apsidal distance for collisions between the average radium E $\beta$-particle and an electron, calculating the apsidal distance in the usual way for a purely electrostatic field. The theoretical deflexion for an impact parameter of 60 times the minimum apsidal distance is about half a degree. For larger angles of scattering the magnetic force should be the more important factor in determining the final path of the particles. It would appear that under the conditions adopted in the present experiments the electronic scattering should be determined almost completely by the magnetic forces. A rough calculation on these lines shows that the amount

of scattering should be very different from that actually found, and it therefore seems unlikely that the electron can have a magnetic moment as large as one Bohr magneton. The fact that an increase in the number of particles was observed, roughly proportional to the relative importance of the electron in the atoms, suggests, however, that there is an additional field of force present in collisions between electrons. Without measurements over other ranges of angle the nature of this field of force cannot be inferred.

From the nature of magnetic force the force between two magnetons must depend both in sign and magnitude upon the orientation of the axes of the particles with respect to each other. The magnetons will also in general exert a torque upon each other tending to bring them into the position of greatest attraction. If, however, the magnetic moment is the result of an actual spin, the two particles will merely precess about the line of centres. The force between them will not then be increased by their rotation toward the end-on position. Calculation of the orbits described under such conditions is difficult. Hicks * and Wessel † have made calculations of this nature for the somewhat simpler conditions of a fixed magneton and a non-magnetic moving particle. Bothe ‡ also has calculated the orbits of a $\beta$-particle about a nucleus, using a somewhat different assumption. He considers that the magnetic $\beta$-particle is moving in the inhomogeneous magnetic field of the nucleus. In this case there are two possible orientations. The axes of the particles may be either parallel or anti-parallel.

An objection to the conception of an electron as possessing spin and consequent magnetic moment is the relative complexity of this model compared to the point charge. Dirac § has shown how to avoid the necessity for a magnetic electron by a more complete solution of the fundamental equations. The electron according to his theory is still a point charge but it displays a duplex character, in many respects resembling the behaviour of a magneton. Iwanenko and Landau ¶ have shown by an

* Hicks, Proc. Roy. Soc. A, xc. p. 356 (1914).
† Wessel, *Ann. d. Phys.* lxxviii. p. 757 (1925).
‡ Bothe, *Zeit. f. Phys.* xliv. p. 543 (1927).
§ Dirac, Proc. Roy. Soc. A, cxvii. p. 610 (1928) : cxviii. p. 351 (1928).
¶ Iwanenko and Landau, *Zeit. f. Phys.* xlviii. p. 340 (1928).

entirely different method that the assumptions of wave mechanics lead to the same result. The problem of the collision of a $\beta$-particle with an electron has not yet been examined on the basis of Dirac's equations, and although it seems possible that the duplex character of an electron in an orbit may be interpreted to give a magnetic field effective in collisions, the magnitude of the effect cannot be estimated without a laboured calculation. When such calculations are available it may be possible to give an adequate explanation of the results obtained in the present experiments, without any further hypotheses.

In the experiments performed heretofore on $\beta$-ray scattering, additional fields of force, usually magnetic, have often been postulated to explain increased scattering, but they have always been discarded later after more exact investigation. Whether the increased scattering found in the present work must finally be explained by that postulate is a matter for further investigation to decide.

## Summary.

The hypothesis of the magnetic electron put forward by Uhlenbeck and Goudsmit in 1925 raises the question as to the effect which the magnetic field of the electron will have upon the collisions between $\beta$-particles and electrons in their orbits. Experiments upon the scattering power of light gases for $\beta$-particles have therefore been carried out to determine whether there is any such effect.

The experiments with the $\beta$-particles from radium E show that hydrogen and helium possess a scattering power, measured between 10° and 30°, about 80 and 40 per cent., respectively, in excess of that to be expected from the usual theory. The variation in scattering power with atomic number (N) is fitted within 8 per cent. by the expression $aN^2+kN$, where $a$ is the relativity correction and $k$ is 3·3 instead of the theoretical value slightly less than unity. Although this result suggests that the electron possesses a field of force in addition to the normal electrostatic field, it apppears unlikely that it can have a magnetic moment as large as one Bohr magneton.

The author is indebted to Professor Sir Ernest Rutherford and to Dr. J. Chadwick for their advice and interest during this investigation.

XCIV. *The Thermal Expansion of Liquids according to van der Waals.* *By* J. E. Verschaffelt, *Professor in Physics at the University of Ghent* *.

THE Philosophical Magazine has published recently a paper by Mr. V. N. Thatte †, in which the author intended to show that from van der Waals's equation of state,

$$p+\frac{a}{v^2}=\frac{RT}{v-b}, \quad \ldots \ldots \quad (1)$$

taken at temperatures so low that the vapour pressure $p$ may be neglected against the pressure of cohesion $\frac{a}{v^2}$, a formula may be derived for the relative coefficient of cubical expansion $c=\frac{1}{v}\frac{dv}{dT}$ of the liquid similar to that of Davies. Putting $p=0$ in the equation (1), one finds

$$\frac{1}{c}=\frac{a}{R}-2T, \quad \ldots \ldots \quad (2)$$

and this relation is indeed similar to the formula of Davies when we suppose, as Mr. Thatte does, that the term $\frac{a}{vR}$ is (at least nearly) a constant proportional to the critical temperature $T_c$; only the coefficients are different. Determining the coefficient of $T_c$ by using experimental data, Mr. Thatte finds

$$\frac{1}{c}=2{\cdot}5\ T_c-2T.$$

I wish to say that I do not quite agree with this result. I do not see why Mr. Thatte deduces the value of the term $\frac{a}{vR}$ from experiment, instead of deriving it from the equation of state, by which it is completely determined; that seems to me illogical. Now we know that at very low temperatures that equation gives $v=b$, and it is known also that, according to the same equation,

$$\frac{a}{bR}=\frac{27}{8}T_c; \quad \ldots \ldots \quad (3)$$

* Communicated by the Author.

† V. N. Thatte, "Coefficient of Cubical Expansion of Liquids and Critical Temperature," Phil. Mag. vii. p. 887 (May 1929).

so it results from the equation itself that the term $\frac{a}{vR}$ is really proportional to $T_c$, but the coefficient of proportionality is $\frac{27}{8} = 3{\cdot}4$ instead of being 2·5.

But this is only a limit value. One must not overlook the fact that the term $\frac{a}{vR}$ may not be considered as constant, because $v$ is a function of temperature, and this circumstance modifies also the value of the coefficient of T. In order to find this coefficient, we write equation (2) in the form

$$\frac{1}{c} = \frac{a}{R}\delta - 2T = T_c\left(\frac{a}{3bRT_c}\cdot\frac{\delta}{\delta_c} - 2\,\frac{T}{T_c}\right) = T_c\left(\frac{9}{8}\cdot\frac{\delta}{\delta_c} - 2\frac{T}{T_c}\right), \quad . \quad . \quad . \quad . \quad (4)$$

where $\delta = \frac{1}{v}$ is the (molecular) density; for according to van der Waals's equation.

$$\delta_c = \frac{1}{3b}. \quad . \quad . \quad . \quad . \quad . \quad . \quad . \quad . \quad (5)$$

Now values of $\frac{\delta}{\delta_c}$ corresponding to different values of $\frac{T}{T_c}$ have been calculated by J. P. Dalton *. From his table and equation (4) we deduce the following one :—

| $\frac{T}{T_c}$ | $\frac{\delta}{\delta_c}$ | $\frac{1}{c}$ |
|---|---|---|
| $=0$ | $=3{\cdot}00$ | $=3{\cdot}375\,T_c$. |
| 0·1 | 2·91 | 3·07 |
| 0·2 | 2·81 | 2·76 |
| 0·3 | 2·70 | 2·44 |
| 0·4 | 2 59 | 2·11 |
| 0·5† | 2 46 | 1·76 |

and from this it is easily seen that we may put approximately :

$$\frac{1}{c} = 3{\cdot}4\,T_c - 3{\cdot}2\,T. \quad . \quad . \quad . \quad . \quad . \quad . \quad (6)$$

But according to van Waals the relation between $\frac{1}{c}$ and T is not really linear, as in Davies's formula, deduced from the

* See J. P. Kuenen, 'Die Zustandsgleichung der Gase und Flüssigkeiten, p. 94 (1907).

† Up to this value of $\frac{T}{T_c}$ the vapour pressure remains negligible. See Kuenen, *loc. cit.*

law of the rectilinear diameter. The exact relation is to be found by substitution in (4) of the function $\frac{\delta}{\delta_c}$ determined by the equation :

$$\frac{a}{v^2} = \frac{RT}{v-b} \quad \text{or} \quad a\delta = \frac{RT}{1-b\delta},$$

which may be put in the reduced form :

$$3\frac{\delta}{\delta_c}\left(3-\frac{\delta}{\delta_c}\right) = 8\frac{T}{T_c}. \quad . \quad . \quad . \quad . \quad . \quad . \quad (7)$$

The greatest root of this quadratic equation must be taken. By developing it in a series, one finds

$$\delta = 3\delta_c(1-x-x^2-2x^3- \ldots \ldots), \quad . \quad . \quad . \quad (8)$$

with

$$x = \frac{8}{27}\frac{T}{T_c}, \quad . \quad . \quad . \quad . \quad . \quad . \quad . \quad . \quad (9)$$

and consequently

$$\frac{1}{c} = \frac{27}{8}T_c\,(1-3x-x^2-2x^3- \ldots \ldots), \quad . \quad . \quad (10)$$

or

$$c = \frac{8}{27T_c}(1+3x+10x^2+35x^3+ \ldots \ldots), \quad . \quad . \quad (11)$$

which last relation may be deduced directly from (8) by observing that

$$c = \frac{1}{v}\frac{dv}{dT} = \frac{d\log v}{dT} = -\frac{d\log \delta}{dT}.$$

The relation (11), however, is less useful than (10) on account of its less rapid convergency.

It is obvious that form (6) does not agree well with the experimental data; only Davies's formula does for normal substances at low temperatures (at which the density of the vapour is nearly zero). Even Thatte's formula, partly deduced from experiment, is in disagreement, save for $T = \pm\frac{1}{2}T_c$, at which temperature both the formulæ of Davies and Thatte give $\frac{1}{c} = 1{\cdot}5\ T_c$. It may, moreover, be remarked that van der Waals's equation does not give a quite different value.

Natuurkundig Laboratorium,
Ghent, Aug. 1929.

## XCV. *On the Operational Solution of Linear Differential Equations and an Investigation of the Properties of these Solutions.* By Balth. van der Pol, *D.Sc.* *

### 1. *Introduction.*

In a former paper † the rules for solving operationally linear differential equations with constant coefficients and with an arbitrary second member were considered. Arbitrary given initial conditions could be taken care of. The best-known case is that for which the system is originally fully at rest, while at the instant $t=0$ a unit force is suddenly impressed upon the system.

It is the purpose of the present paper (i.) to consider some general rules in connexion with the operational calculus, (ii.) to outline a method similar to the one used in the former paper for the solution of linear differential equations with variable coefficients, and (iii.) to consider simple operational methods for the investigations of the properties of the functions defined by those equations.

Though the subject matter is relatively new in physics ‡ the idea of fractional differentiation and integration, which forms an important part of the operational calculus, was worked out by Riemann ('Werke,' p. 331), a report of which is to be found in Pincherle's article on "Funktional-operationen und -Gleichungen" in the *Enz. der Math. Wiss.* ii. A. 11, where again, however, no mention is made of Heaviside's important contributions to the subject §.

As in our former paper, we will here again take as a basis of the development the integral equation of Carson ‖, of which Bromwich's well-known integral ¶ is the solution.

* Communicated by the Author.

† Balth. van der Pol, "A Simple Proof and an Extension of Heaviside's Operational Calculus for Invariable Systems." Phil. Mag. vii. p. 1153 (1929).

‡ *E. g.* we do not find any reference to it either in the new edition of Riemann–Weber, 'Die Differential-gleichungen der Physik' (1927) or in Courant–Hilbert, 'Mathematische Physik,' i. (1924).

§ The same is true for the article by A. Voss, "Integralrechnung," *Enz. der Math. Wiss.* ii. A. 2, p. 116, where, also, fractional differentiation is considered.

‖ J. R. Carson, 'Electric Circuit Theory and the Operational Calculus (McGraw-Hill, New York, 1926).

¶ T. J. I'a. Bromwich, Proc. London Math. Soc. xv. p. 401 (1916). In this paper arbitrary initial conditions are already considered in the operational solution of differential equations. See also H. Jeffreys, 'Operational Methods in Mathematical Physics' (Cambridge University Press, London, 1927).

In order to expound our method as clearly as possible we insert various examples, mostly taken from Bessel functions, spherical harmonics, and other functions. It is found to be a relatively simple matter, once the operational representations of these functions have been obtained, to write down, almost at a glance, many relations between those functions, of which several may be new. In particular we refer to the parallelism between the familiar relations which exist between Bessel functions of different order on the one hand and the well-known similar relations between spherical harmonics on the other hand. It will, for instance, be shown that the one set of relations can directly be derived from the other. Further, three new expressions will be derived for the derivative of Bessel functions with respect to their order. In this respect a new function,

$$\mathrm{Ji}(x) = \int_{\infty}^{x} \frac{\mathrm{J}_0(x)}{x} dx, \quad . \quad . \quad . \quad . \quad . \quad (1)$$

which is analogous to

$$\mathrm{Ci}(x) = \int_{\infty}^{x} \frac{\cos x}{x} dx, \quad . \quad . \quad . \quad . \quad . \quad (2)$$

will be shown to play an important part. It looks to the writer as if the shortest way to expound and explore the properties of Bessel functions, for example, is by the powerful method of operators. Finally, at the end of the paper a list is given of the symbolic representations of many functions, of which several may here be given for the first time. Throughout, the notations of the well-known tables of Jahnke–Emde * will be adhered to.

## 2. *Some General Theorems.*

We assume the symbolic or operational representation $f(p)$ of a function $h(x)$ of $x$ to be defined by Carson's integral:

$$f(p) = p \int_0^{\infty} e^{-px} h(x)\, dx. \quad . \quad . \quad . \quad . \quad . \quad (3)$$

Thus, on the one hand, when the function $h(x)$ is given its operational representation $f(p)$ is found by an integration. On the other hand, when the operational expression $f(p)$ of the unknown function $h(x)$ is given, (3) represents an integral equation for the unknown function $h(x)$. The

* Jahnke–Emde, 'Funktionentafeln' (Teubner, Leipzig und Berlin).

solution of the integral equation is given by the following complex integral, first obtained by Bromwich :—

$$h(x) = \frac{1}{2\pi i}\int_{c-i\infty}^{c+i\infty} \frac{f(p)}{p}\rho^{px}\,dp, \quad . \quad . \quad . \quad . \quad (4)$$

where $c > 0$; this was pointed out by Lévy * and March †.

Now from the definition (3) of the operational representation $f(p)$ of a function $h(x)$ a set of theorems has been derived by Carson. As we shall make frequent use of these relations, they will here be summarized without proof. The proofs can be found in the above-mentioned treatise of Carson.

Thus, if $f(p) \doteqdot h(x)$ ‡,

then
$$f\left(\frac{p}{s}\right) \doteqdot h(sx) \qquad (s = \text{constant}), \quad . \quad . \quad . \quad (5)$$

$$pf(p) \doteqdot \frac{d}{dx}h(x) \qquad (\text{provided } h(0) = 0), \quad (6)$$

$$\frac{1}{p}f(p) \doteqdot \int_0^x h(x)\,dx, \quad . \quad . \quad . \quad . \quad . \quad . \quad . \quad . \quad (7)$$

$$\frac{p}{p+\alpha}f(p+\alpha) \doteqdot e^{-\alpha x}h(x), \quad . \quad . \quad . \quad . \quad . \quad . \quad . \quad . \quad (8)$$

$$e^{-\lambda p}f(p) \doteqdot \begin{cases} 0 & \text{for } x < \lambda \\ h(x-\lambda) & \text{for } x > \lambda \end{cases} \quad (\lambda > 0), \quad (9)$$

$$e^{+\lambda p}f(p) \doteqdot h(x+\lambda)\ \S, \qquad (\lambda > 0). \quad . \quad (10)$$

when $h(x) = 0$ for $0 < x < \lambda$.

To this list the following relations may be added :—

$$\left(-p\frac{d}{dp}\right)^n f(p) \doteqdot \left(x\frac{d}{dx}\right)^n h(x), \qquad (n > 0), \quad . \quad (11)$$

$$p\left(-\frac{d}{dp}\right)^n \left\{\frac{f(p)}{p}\right\} \doteqdot x^n . h(x), \qquad (n > 0), \quad . \quad (12)$$

$$\int_p^\infty \frac{f(p)}{p}\,dp \doteqdot \int_0^x \frac{h(x)}{x}\,dx, \quad . \quad . \quad . \quad . \quad . \quad . \quad (13)$$

$$\int_0^p \frac{f(p)}{p}\,dp \doteqdot \int_0^\infty \frac{h(x)}{x}\,dx, \quad . \quad . \quad . \quad . \quad (13\,a)$$

* P. Lévy, 'Le Calcul symbolique de Heaviside' (Gauthier-Villars, Paris, 1926).

† H. W. March, "The Heaviside Operational Calculus," Bull. Am. Math. Soc. xxxiii. p. 311 (1927).

‡ When $f(p)$ is the operational representation of $h(x)$, as defined by (3), we use the symbol $\doteqdot$, and write $f(p) \doteqdot h(x)$.

§ See also Jeffreys, *l. c.* p. 18.

$$\int_0^\infty \frac{f(p)}{p}\,dp = \int_0^\infty \frac{h(x)}{x}\,dx. \quad . \quad . \quad . \quad . \quad . \quad (14)$$

$$\operatorname*{Lim}_{p\to\infty} f(p) = \operatorname*{Lim}_{x\to 0} h(x), \quad . \quad . \quad . \quad . \quad . \quad . \quad (15)$$

$$\operatorname*{Lim}_{p\to 0} f(p) = \operatorname*{Lim}_{x\to\infty} h(x), \quad . \quad . \quad . \quad . \quad . \quad . \quad (15\,a)$$

provided the definite integrals and limits have a meaning, *i.e.* they can be extended to the limits 0 and $\infty$.

If, further,

$$f_1(p) \doteqdot h_1(x)$$

and

$$f_2(p) \doteqdot h_2(x),$$

then

$$p\left\{h_1\left(-\frac{d}{dp}\right)\right\}\cdot\left[\frac{f_2(p)}{p}\right] = p\left\{h_2\left(-\frac{d}{dp}\right)\right\}\cdot\left[\frac{f_1(p)}{p}\right] \doteqdot h_1(x).h_2(x), \quad . \quad . \quad . \quad (16)$$

provided either $h_1(x)$ or $h_2(x)$ can be expanded in a series of positive powers of $x$.

Finally, we have the very important theorem

$$f_1(p).f_2(p).\frac{1}{p} \doteqdot \int_0^x h_1(\xi).h_2(x-\xi).d\xi = \int_0^x h_2(\xi).h_1(x-\xi).d\xi. \quad . \quad (17)$$

As the theorems (11)–(16) were not given by Carson, the proof will be indicated here.

To prove (11) differentiate both sides of (5) with respect to $s$ and then put $s=1$. We obtain

$$-p\frac{df(p)}{dp} \doteqdot x\frac{dh(x)}{dx}. \quad . \quad . \quad . \quad . \quad . \quad (11\,a)$$

A repeated differentiation with respect to $s$ thus yields (11). When, further, (11$a$) is multiplied by $p^{-1}$, which, according to (7), means integration on the right-hand side between zero and $x$, we obtain

$$-\frac{df(p)}{dp} \doteqdot \int_0^x x.\frac{dh(x)}{dx}dx = xh(x) - \int_0^x h(x)\,dx$$

or

$$-\frac{df(p)}{dp} + \frac{f(p)}{p} = -p\frac{d}{dp}\left(\frac{f(p)}{p}\right) = x.h(x),$$

from which (12) follows.

To demonstrate (13) an integration of both members of (5) can be effected between the limits zero and unity. If the same integration is taken between the limits zero and infinity (14) is obtained, while the subtraction of (13) and (14) yields (13 *a*). Further, (15) follows from (3) when it is remembered that

$$\underset{\substack{x\geqq 0\\ p\to\infty}}{\mathrm{Lim.}}\, pe^{-px} = \delta(x)$$

is a function of the type as used by Dirac* in atomic theory, and called by him a $\delta$ function. It has the property

$$\int_{-\infty}^{+\infty} \delta(x)\, dx = 1,$$

and is zero everywhere except at $x=0$, where it is infinite.

These functions have the property

$$\int_{-\infty}^{+\infty} \delta(x).h(x)\, dx = h(0),$$

and thus (15) follows. It is interesting to remark that these $\delta$-functions were recognized and used extensively by Heaviside † already thirty-five years ago. He called them "impulsive" functions.

Thus

$$1 \doteqdot [1],$$
$$p \doteqdot \delta(x),$$
$$p^2 \doteqdot \delta'(x),$$
$$p^3 \doteqdot \delta''(x),$$
$$\cdot \quad \cdot \quad \cdot \quad \cdot$$

with the general property

$$\int_{-\infty}^{+\infty} f(x).\overset{(n)}{\delta}(x).\, dx = \overset{(n)}{f}(0).$$

Further, (16) can be demonstrated with the aid of (12). When one of the functions $h_1(x)$ or $h_2(x)$ can be expanded as a power series (8) is thus seen to be a special case of (16), because we have

$$f_1(p) = \frac{p}{p+\alpha} \doteqdot e^{-\alpha x} = h_1(x),$$

$$f_2(p) \doteqdot h_2(x),$$

* See, *e.g.*, Proc. Roy. Soc. A, cxiii. p. 625 (1926).

† See, *e.g.*, Heaviside, 'Electromagnetic Theory, ii. p. 92.

and applying (15), we find

$$p\,e^{\alpha\frac{d}{dp}}\left(\frac{f_2(p)}{p}\right) = p\left(1+\alpha\frac{d}{dp}+\frac{\alpha^2}{2!}\frac{d^2}{dp^2}+\ldots\right)\frac{f_2(p)}{p}$$

$$= \frac{p}{p+\alpha}\cdot f_2(p+\alpha) \doteqdot e^{-\alpha x}h_2(x).$$

Finally (17), which is the most important theorem of all, is frequently used by Carson. It is of the type of a "produit de composition," as defined by Volterra, and it is on the basis of this theorem that Lévy * builds up the operational calculus. This expression was also at the base of Riemann's investigation †. Further, this theorem was given by Borel ‡, and is closely related to Borel's "associated function" § and his "sommation exponentielle" of divergent series. Moreover, it expresses the well-known Hopkinson–Boltzmann's superposition principle, and it is used and demonstrated in a special case by Lord Rayleigh in his 'Theory of Sound,' i. p. 74. It will be of frequent use further on.

### 3. *Examples illustrating the General Theorems.*

After having obtained a rather complete set of theorems, or working rules, we will now consider some examples of application of these rules. From the definition of the $\Pi(n)$ functions

$$\Pi(n) = \int_0^\infty e^{-u}.u^n.du,$$

where $\Pi(n) = n!$ for $n =$ positive integer,

it follows at once from (3) that

$$\frac{1}{p^n} = \frac{x^n}{\Pi(n)}, \quad \ldots\ldots \quad (18)$$

which is valid for all values of $n$ for which $n > -1$, fractional values of $n$ included.

Similarly, we have

$$\frac{p}{p+1} \doteqdot e^{-x}, \quad \ldots\ldots \quad (18\alpha)$$

* *Loc. cit.*

† *Enz. der Math. Wiss.* ii. A. 11, p. 771.

‡ E. Borel, 'Leçons sur les Séries divergentes,' (Gauthier-Villars, Paris, 1928).

§ See, *e. g.*, Whittaker and Watson, 'Modern Analysis,' p. 140.

$$\frac{p}{p^2+1} \doteqdot \sin x, \quad \ldots\ldots \quad (18\,b)$$

$$\frac{p^2}{p^2+1} \doteqdot \cos x. \quad \ldots\ldots \quad (18\,c)$$

These expressions can easily be verified by series expansion. *E. g.* :

$$\frac{p^2}{p^2+1} = 1-\frac{1}{p^2}+\frac{1}{p^4}-\ldots \doteqdot 1-\frac{x^2}{2!}+\frac{x^4}{4!}-\ldots = \cos x.$$

Consider (9). Let again $f(p) \doteqdot h(x)$. As (3) only considers the values of $h(x)$ in the region 0 to $\infty$, it cannot give any information as to the behaviour of $h(x)$ in the region $x < 0$. In connexion with (9) it is, therefore, appropriate to consider all our functions to be zero for $x<0$.

This is demonstrated in fig. 1. A factor $e^{-\lambda p}$ therefore shifts $h(x)$ over a distance to the right, while a factor $e^{+\lambda p}$ shifts it over the same distance to the left, but in the last case a part of the function is moved through an imaginary vertical cut along the $y$-axis and slipped under a rigid cover, which keeps the function equal to zero whenever $x<0$. That this is the only consistent interpretation follows directly from the integral (3). For

$$e^{-\lambda p}.f(p) = p\int_0^\infty e^{-p(x+\lambda)}h(x)\,dx = p\int_A^\infty e^{-ps}.h(s-\lambda)\,ds,$$

or

$$e^{-\lambda p}.f(p) = p\int_\lambda^\infty e^{-px}.h(x-\lambda)\,dx.$$

When $\lambda$ is positive this would be the representation of $h(x-\lambda)$ if the lower limit of the last integral were zero. This can be obtained if $h(x-\lambda)$ is taken to be zero in the region $0<x<\lambda$, as represented in fig. 1 *b*. Again, if $\lambda$ is negative and $\lambda=-\lambda'$, the lower limit of the integral can again be made zero if $h(x+\lambda')$ is taken to be zero in the region $x<0$, *i. e.*, if the function starts as indicated in fig. 1 *c*.

That the function $e^{-\lambda p}.f(p)$ is rightly interpreted above can also be proved simply by theorem (17), when $e^{-\lambda p}$ is interpreted as being unity for $x>\lambda$ and zero for $x<\lambda$.

Let us consider an instance.

$h(x)=x$ is represented symbolically by $\frac{1}{p}$, or $\frac{1}{p} \doteqdot x$ (see

fig. 2 *a*); fig. 2 *b* represents $e^{-\lambda p}.\frac{1}{p}$; fig. 2 *d*, $e^{+\lambda p}.\frac{1}{p}$. If, however, $e^{-\lambda p}.\frac{1}{p}$ were developed as

$$\left(1-\frac{\lambda p}{1!}+\frac{\lambda^2 p^2}{2!}-\ldots\right)\frac{1}{p},$$

Fig. 1 *a*.

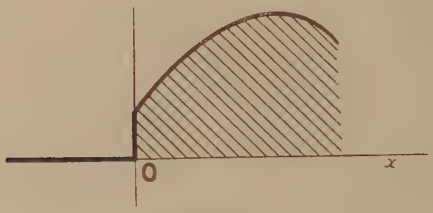


$h(x) \div f\ p$

Fig. 1 *b*.

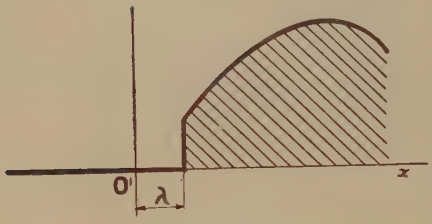


$e^{-\lambda p} f(p)$.

Fig. 1 *c*.

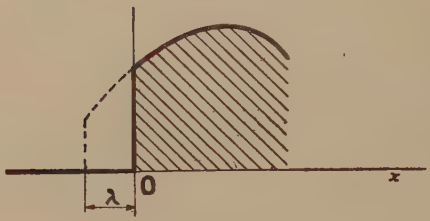


$[e^{+\lambda p} f(p)]$.

and the positive powers of $p$ were rejected, we should obtain

$$\frac{1}{p}-\lambda \doteq x-\lambda,$$

Fig. 2 *a*.

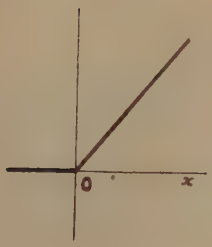


$h(x) \doteqdot \frac{1}{p} \doteqdot x$

Fig. 2 *b*.

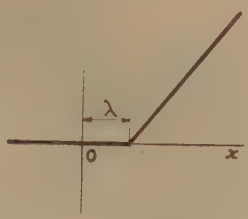


$e^{-\lambda p} \cdot \frac{1}{p}$.

Fig. 2 *c*.

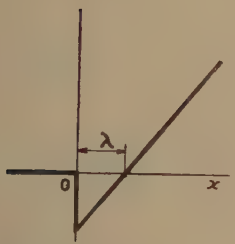


$\left[e^{-\lambda p} \cdot \frac{1}{p}\right] = \frac{1}{p} - \lambda = x - \lambda.$

Fig. 2 *d*.

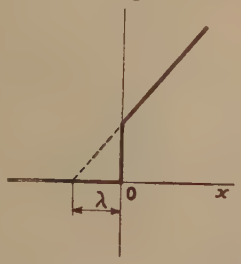


$\left[e^{+\lambda p} \cdot \frac{1}{p}\right] \begin{cases} = x+\lambda & \text{for } x>0, \\ = 0 & \text{for } x<0. \end{cases}$

Fig. 2 *e*.

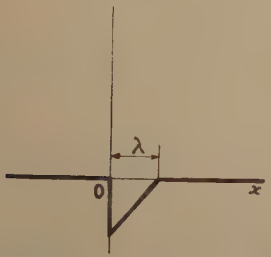


$$-\left[\left[e^{-\lambda p} \cdot \frac{1}{p}\right]\right] = \frac{1}{p}\left\{\frac{\lambda^2 p^2}{2!} - \frac{\lambda^3 p^3}{3!} + \frac{\lambda^4 p^4}{4!} - \dots\right\}.$$

as represented in fig. 2 *c*, which is erroneous. It is, however, interesting to note that

$$\left[e^{-\lambda p}\frac{\Pi(n)}{p^n}\right] \doteq (x-\lambda)^n$$

if $n$ is a positive integer, and when the brackets [ ] are understood to mean the omission of all positive powers of $p$. Therefore the difference

$$[[e^{-\lambda p}.f(p)]] = e^{-\lambda p}.f(p) - [e^{-\lambda p}.f(p)],$$

(where the double brackets symbolize the retention of the positive powers of $p$ only, the zero'th power excluded) yields (see fig. 2 *e*)

$$[[e^{-\lambda p}.f(p)]] \doteq \left\{ \begin{matrix} -h(x-\lambda), & 0<x<\lambda \\ 0, & x<0 \text{ or } x>\lambda \end{matrix} \right\}. \quad (18\,d)$$

In the same way it follows that

$$[[e^{+\lambda p}.f(p)]] = 0, \qquad 0<x<\infty,$$

for the factor $e^{+\lambda p}$ shifts the function to the left as explained above, there being no positive region at present where the function is continuously zero.

These considerations are obviously only valid when $h(x)$ can be developed as a series of positive powers of $x$. Later on, in the treatment of the Legendre functions, we shall come back to these properties. The relation of these properties with a Laurent development has not yet been investigated.

Returning to the meaning of $e^{-\lambda p}$, it follows at once from the development of

$$\frac{1}{2}\left\{1+\coth\frac{hp}{2}\right\} = \frac{1}{1-e^{-hp}} = 1+e^{-hp}+e^{-2hp}+e^{-3hp}+\ldots$$

that

$$\frac{1}{2}\left\{1+\coth\frac{hp}{2}\right\}$$

means the "staircase"-function depicted in fig. 3 *, because each following term adds discontinuously unity to the function.

Again

$$\frac{1}{2}\tanh\frac{hp}{2} = \frac{1}{2} - e^{-hp}+e^{-2hp}-e^{-3hp}+\ldots$$

represents the meander-function of fig. 4 †.

* See Heaviside, ' Electromagnetic Theory,' ii. p. 90.
† Heaviside, *loc. cit.* ii. p. 97.

As an instance of (13) we take

$$f(p) = \frac{p}{p^2+1} \doteqdot \sin x = h(x).$$

Applying (13), we find on the one hand

$$\int_p^\infty \frac{f(p)}{p}\,dp = \int_p^\infty \frac{dp}{p^2+1} = \tan^{-1}p \Big|_p = \cot^{-1}p.$$

On the other hand we have

$$\int_0^x \frac{h(x)}{x}\,dx = \int_0^x \frac{\sin x}{x}\,dx = \mathrm{Si}(x),$$

Fig. 3.

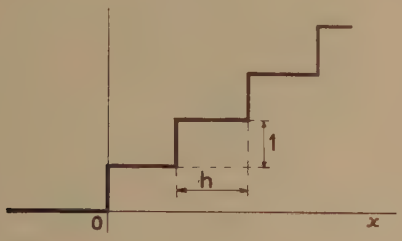


Fig. 4.


and thus we find, as the operational expression for the integral sine,

$$\cot^{-1}p \doteqdot \mathrm{Si}(x) = \int_0^x \frac{\sin x}{x}\,dx \quad . \quad . \quad . \quad (19)$$

Applying theorem (14) to this result, we find at once

$$\int_0^\infty \frac{\sin x}{x}\,dx = \operatorname*{Lim.}_{p\to 0} \cot^{-1}p = \frac{\pi}{2}.$$

Again, let us consider

$$f(p) = \frac{p^2}{p^2+1} \doteqdot \cos x = h(x).$$

The application of (13 *a*) yields, on the one hand,

$$\int_0^p \frac{p\,dp}{p^2+1} = \log \sqrt{p^2+1}.$$

On the other hand, by definition we have

$$\int_x^\infty \frac{\cos x}{x}\,dx = -\mathrm{Ci}(x),$$

and thus we find as the operational expression for the integral cosine

$$\log \frac{1}{\sqrt{1+p^2}} \doteqdot \mathrm{Ci}(x) = \int_\infty^x \frac{\cos x}{x}\,dx \quad . \quad . \quad (20)$$

In the same way we can treat

$$\mathrm{Ei}(x) = \int_\infty^{-x} \frac{e^{-x}}{x}\,dx.$$

For, with (13), (13 *a*), and (14), we find

$$\int_\infty^{-x} \frac{e^{-x}}{x}\,dx = \int_\infty^x \frac{e^{-x}}{x}\,dx + \int_x^0 \frac{e^{-x}}{x}\,dx + \int_0^x \frac{e^{+x}}{x}\,dx$$

$$\doteqdot -\int_0^p \frac{dp}{p+1} - \int_p^\infty \frac{dp}{p+1} + \int_p^\infty \frac{dp}{p-1} = \log \frac{1}{p-1},$$

and thus

$$-\log(p-1) \doteqdot \mathrm{Ei}(x) = \int_\infty^{-x} \frac{e^{-x}}{x}\,dx. \quad . \quad . \quad (21)$$

As another example of the application of (14), we take the Frullani integral *

$$\int_0^\infty \frac{e^{-ax} - b^{-bx}}{x}\,dx.$$

Writing this integral operationally, we obtain

$$\int_0^\infty \left(\frac{1}{p+a} - \frac{1}{p+b}\right) dp = \log \frac{b}{a},$$

and thus we have found operationally

$$\int_0^\infty \frac{e^{-ax} - e^{-bx}}{x}\,dx = \log \frac{b}{a}.$$

Before taking up our main subject, the solution of linear differential equations, attention may first be drawn to the

* Bromwich, 'Infinite Series,' p. 488.

operational representation of $\log x$. Here we first follow Heaviside's example *.

Above we found from (1)

$$\frac{1}{p^n} \doteqdot \frac{x^n}{\Pi(n)}. \quad . \quad . \quad . \quad . \quad . \quad . \quad . \quad (18)$$

Now differentiate both members with respect to $n$. We thus obtain

$$\frac{1}{p^n}\log\frac{1}{p} \doteqdot \frac{x^n}{\Pi(n)}\{\log x - \psi(n)\}, \quad . \quad . \quad . \quad (18e)$$

where

$$\psi(n) = \frac{d}{dn}\{\log \Pi(n)\}\dagger. \quad . \quad . \quad . \quad . \quad (18f)$$

We therefore have the special cases

$$\left.\begin{aligned}
&\log\frac{1}{p} \doteqdot \log x - \psi(0) = \log x + \mathrm{C},\\
&\frac{1}{p}\log\frac{1}{p} \doteqdot \frac{x}{1!}(\log x + \mathrm{C} - 1),\\
&\frac{1}{p^2}\log\frac{1}{p} \doteqdot \frac{x^2}{2!}(\log x + \mathrm{C} - 1 - \tfrac{1}{2}),\\
&\quad . \quad . \quad . \quad . \quad . \quad . \quad . \quad . \quad . \quad . \quad .\\
&\frac{1}{p^n}\log\frac{1}{p} \doteqdot \frac{x^n}{n!}\left(\log x + \mathrm{C} - 1 - \tfrac{1}{2} - \tfrac{1}{3} \ldots - \frac{1}{n}\right),
\end{aligned}\right\} \quad (18g)$$

where $$\mathrm{C} = 0{\cdot}57722\ldots.$$

With the aid of (18*g*) we can now easily expand, *e.g.*, (20). Thus,

$$\log\frac{1}{\sqrt{1+p^2}} = \log\frac{1}{p} - \frac{1}{2}\log\left(1+\frac{1}{p^2}\right)$$

$$= \log\frac{1}{p} - \frac{1}{2}\left(\frac{1}{p^2} - \frac{1}{2p^4} + \frac{1}{3p^6} - \ldots\right)$$

$$\doteqdot \log x + \mathrm{C} - \frac{1}{2}\cdot\frac{x^2}{2!} + \frac{1}{4}\cdot\frac{x^4}{4!} - \frac{1}{6}\cdot\frac{x^6}{6!} + \ldots = \mathrm{Ci}(x).$$

* Heaviside, *loc. cit.* ii. p. 358.

† Here our notation for $\psi(n)$ differs from that of Jahnke-Emde, 'Funktionentafeln,' but agrees with that of Schafheitlin, 'Die Theorie der Besselschen Funktionen' (Teubner, Berlin, 1908). As $\Pi(n)$ coincides with $n!$ for $n$ = integer, we believe that it is advisable to use $\Pi$-functions instead of $\Gamma$-functions. Thus, instead of defining

$$\psi(n) = \frac{d}{dn}(\log\Gamma(n)),$$

we use the definition (18*f*).

4. *Linear Differential Equations* : (a) *with Constant Coefficients.*

Suppose the following simple differential equation be given :—

$$\dot{y}+\alpha y=[\cos\omega t],$$

where the sign [ ] bracketing $\cos\omega t$ means that the force as expressed by the right-hand member is zero for $t<0$ and is $\cos\omega t$ for $t>0$. Let the initial condition be $y(0)=0$, from which it follows that $y(0)=\dot{y}(0)=\ddot{y}(0)=\ldots=0$.

To solve our equation operationally we must obtain the expression for

$$f(p)=p\int_0^\infty e^{-pt}y(t)\,dt. \quad . \quad . \quad . \quad . \quad . \quad (3)$$

Hence we proceed as in our former paper *, multiply throughout with $e^{-pt}$, and integrate between zero and infinity. Integration by parts of the first member yields

$$(p+\alpha)\mathrm{X}(p)=\int_0^\infty e^{-pt}\cos\omega t\,.\,dt=\frac{p}{p^2+\omega^2}, \quad . \quad (22)$$

where $$\mathrm{X}(p)=\int_0 e^{-pt}\,.\,y(t)\,dt.$$

As $$f(p)=p\,.\,\mathrm{X}(p),$$

we can write at once, from (21),

$$f(p)=\frac{p^2}{(p^2+\omega^2)\,.\,(p+\alpha)}\doteqdot y(t). \quad . \quad . \quad . \quad (23)$$

The same result would have been obtained if we had simply replaced $\frac{d}{dt}$ by $p$ and had written the symbolic expression for $\cos\omega t$ for the second member. It may be remarked that the result (23) would also have been obtained if the original differential equation had been symbolically

$$(p^2+\omega^2)\,.f(p)=\frac{p^2}{p+\alpha},$$

or, written in $t$,

$$\ddot{y}+\omega^2y=\frac{d}{dt}[e^{-\alpha t}].$$

Hence the operational method enables us often easily to write down several differential equations which have the

* Phil. Mag. vii. p. 1153 (1929).

same solution. It also answers the following question: let a right-hand member [1], representing the sudden application of a constant force, be given to the equation

$$\ddot{y}+y=0,$$

what must be done in order to have no transient phenomena? It is easily seen that a second-order impulse, i. e., $p^2$, must also be impressed on the system; for if

$$(p^2+1)\,.\,f(p)=1+p^2,$$

then $$f(p)=1, \quad \text{or} \quad y(t)=[1].$$

Let us take another example. The solution of

$$\dot{y}+y=0, \quad \text{with} \quad y=y(0) \text{ for } t=0,$$

is easily found to be

$$f(p)=y(0)\cdot\frac{p}{1+p}\doteq y(0)\,.\,e^{-t}.$$

Now let the equation be multiplied with $(t-a)$, and the solution again be sought for the same initial condition. We have

$$(t-a)(\dot{y}+y)=0, \quad . \quad . \quad . \quad . \quad . \quad (24)$$

or

$$t\dot{y}-a\dot{y}+ty-ay=0. \quad . \quad . \quad . \quad . \quad (24\,a)$$

Again multiply by $e^{-pt}$ and integrate. The first term thus becomes

$$\int_0^\infty e^{-pt}\,.\,t\frac{dy}{dt}\,dt=-\frac{d}{dp}\int_0^\infty e^{-pt}\frac{dy}{dt}dt$$

$$=-\frac{d}{dp}\left\{-y(0)+p\int_0^\infty e^{-pt}\,.\,y(t)\,dt\right\}$$

$$=-\frac{d}{dp}(p\mathrm{X})=-\frac{d}{dp}f(p).$$

A similar reduction of the other terms of $(24\,a)$ yields

$$\frac{df}{dp}+a(f-y(0))+\frac{d}{dp}\left(\frac{f}{p}\right)+a\frac{f}{p}=0,$$

or

$$(p+1)\frac{df}{dp}+\left(ap+1-\frac{1}{p}\right)f=a\,y(0)\,p\,; \qquad (24\,a)$$

$$\therefore \qquad f(p)=y(0)\frac{p}{p+1}+\mathrm{C}e^{-ap}\,.\,\frac{p}{p+1} \quad . \quad . \quad . \quad (25)$$

The interpretation of the first term is simply

$$y(0) \cdot \frac{p}{p+1} \doteq y(0) \cdot e^{-t},$$

but the second term must be explained with (9) as

$$(e^{-ap} \cdot \frac{p}{p+1} \doteq \begin{cases} 0 & \text{for } t < a, \\ Ce^{-(t-a)} & \text{for } t > a, \end{cases} \quad \text{or}$$

so that the complete solution is

$$y(t) = \begin{cases} y(0)e^{-t} & \text{for } t < a, \\ y(0)(1+Ce^{a})e^{-t} & \text{for } t > a, \end{cases} \quad \text{or}$$

meaning that in (24), through the multiplication by $t-a$ the initial condition determines the solution up to the time $t=a$. At that moment, however, the multiplier $t-a=0$, and thus leaves the other factor in (24), $\dot{y}+y$, free to take any value ; thus our operational solution shows that at that moment the amplitude may discontinuously be increased by the arbitrary value C, and after that instant the effect of the initial condition is lost If we had made $a=0$, *i. e.*, if (24) had the multiplier $t$, instead of $t-a$, the initial conditions would have been lost from the beginning. As the example shows, we could have taken $y(0)=0$ from the start and solved (24 *a*) simply with the second member equal to zero. Later on, in (25), the integration constant C could have been adjusted to the initial conditions, and thus the right solution would have been obtained in a simple way. Obviously the multiplication of the original differential equation by $t$ simply brings in a differentiation $\frac{d}{dp}$ throughout in the operational expression; similarly a factor $t^2$ causes $\frac{d^2}{dp^2}$, etc. Very often it is, therefore, much simpler to take

$$y(0)=\dot{y}(0)=\ddot{y}(0)=\ldots=0$$

from the beginning.

### 5. *Linear Differential Equations* : (b) *with Variable Coefficients.*

Our last example brought us already from the domain of equations with constant coefficients to those with variable

coefficients, and to the latter we will now turn our attention. Let us consider the equation for the Bessel functions,

$$\frac{d^2z}{du^2}+\frac{1}{u}\frac{dz}{du}+\left(1-\frac{n^2}{u^2}\right)z=0. \quad . \quad . \quad . \quad (26)$$

Substitute

$$z=u^{-n}y, \quad \text{and} \quad u^2=4x;$$

thus (26) becomes

$$x\frac{d^2y}{dx^2}+(1-n)\frac{dy}{dx}+y=0. \quad . \quad . \quad . \quad . \quad (27)$$

Now multiply (27) again by $e^{-px}$ and integrate between 0 and $\infty$ in order to find

$$\mathrm{X}=\int_0^\infty e^{-px}\,.\,y(x)\,.\,dx,$$

from which

$$f(p)=p\mathrm{X}\doteqdot y(x).$$

As integrations by parts are mostly necessary, we can, beforehand, make a list as follows. Through the integration

$$\left.\begin{array}{lll}
y & \text{becomes} & \mathrm{X}, \\
xy & \text{,,} & -\dfrac{d\mathrm{X}}{dp}, \\
x^2y & \text{,,} & \dfrac{d^2\mathrm{X}}{dp^2}, \\
\cdot\ \cdot\ \cdot\ \cdot\ \cdot\ \cdot\ \cdot\ \cdot\ \cdot & & \\
\dfrac{dy}{dx} & \text{,,} & -y(0)+p\mathrm{X}, \\
x\dfrac{dy}{dx} & \text{,,} & -\dfrac{d}{dp}(p\mathrm{X}), \\
x^2\dfrac{dy}{dx} & \text{,,} & \dfrac{d^2}{dp^2}(p\mathrm{X}), \\
\cdot\ \cdot\ \cdot\ \cdot\ \cdot\ \cdot\ \cdot\ \cdot\ \cdot & & \\
\dfrac{d^2y}{dx^2} & \text{,,} & -y'(0)-py(0)+p^2\mathrm{X}, \\
x\dfrac{d^2y}{dx^2} & \text{,,} & y(0)-\dfrac{d}{dp}(p^2\mathrm{X}), \\
x^2\dfrac{d^2y}{dx^2} & \text{,,} & \dfrac{d^2}{dp^2}(p^2\mathrm{X}), \\
\cdot\ \cdot\ \cdot\ \cdot\ \cdot\ \cdot\ \cdot\ \cdot\ \cdot & &
\end{array}\right\} \quad . \quad . \quad (28)$$

Applying the transformations (28) to (27) we can now at once write down (taking $y(0)=0$)

$$p \cdot \frac{d(pX)}{dp} + \left(n - \frac{1}{p}\right) pX = 0,$$

or

$$pX = f(p) = Cp^{-n} \cdot e^{-\frac{1}{p}}.$$

Adjusting C to the ordinary normalization of the Bessel functions, we thus have found

$$x^{\frac{n}{2}} \cdot J_n(2\sqrt{x}) \doteqdot p^{-n} \cdot e^{-\frac{1}{p}}, \quad . \quad . \quad . \quad (29)$$

which is valid for $n > -1$. Thus the development of the second member as a power series in $p^{-1}$ gives us the familiar series for Bessel functions.

Now that the operational representation has been obtained, we can, with the aid of our theorems (5) to (17), write down, almost at a glance, several properties of $J_n$.

(*a*) Differentiate the left-hand member of (29), *i. e.*, multiply the right-hand member by $p$. Thus we find

$$\frac{d}{dx}\left(x^{\frac{n}{2}} \cdot J_n(2\sqrt{x})\right) \doteqdot p^{-n+1} \cdot e^{-\frac{1}{p}} \doteqdot x^{\frac{n-1}{2}} \underset{n-1}{J}(2\sqrt{x}),$$

or

$$\frac{n}{x} J_n(x) + J_n'(x) = \underset{n-1}{J}(x), \quad . \quad . \quad . \quad . \quad (30)$$

a familiar relation.

(*b*) Again, multiplication of (29) by $p^n$ yields

$$\frac{d^n}{dx^n}\left(x^{\frac{n}{2}} \cdot J_n(2\sqrt{x})\right) \doteqdot p^n \cdot p^{-n} \cdot e^{-\frac{1}{p}} = e^{-\frac{1}{p}} \doteqdot J_0(2\sqrt{x}),$$

or

$$\left(\frac{d}{x\,dx}\right)^n (x^n \cdot J_n(x)) = J_0(x), \quad . \quad . \quad . \quad . \quad (31)$$

which is also a well-known relation. However, operationally it still has a meaning when $n$ is *not* an integer.

(*c*) Now apply (11) in the form

$$-p \frac{df(p)}{dp} \doteqdot x \frac{dh(x)}{dx},$$

which easily gives

$$\frac{n}{x} J_n(x) - J_n'(x) = \underset{n+1}{J}(x), \quad . \quad . \quad . \quad . \quad (32)$$

(*d*) Next apply (12) in the form

$$-p \frac{d}{dp}\left(\frac{f(p)}{p}\right) \doteqdot x \cdot h(x),$$

which yields, after reduction,

$$\mathrm{J}_{n+1}(x)+\mathrm{J}_{n-1}(x)=\frac{2n}{x}\cdot \mathrm{J}_n(x). \quad . \quad . \quad . \quad (33)$$

(*e*) If we further apply (9), we obtain

$$e^{-\lambda p}\cdot p^{-n}\cdot e^{-\frac{1}{p}}=(x-\lambda)^{\frac{n}{2}}\cdot \mathrm{J}_n(2\sqrt{x-\lambda}), \quad (x>\lambda),$$

where the development of the first member yields

$$\left(\frac{1}{p^n}-\frac{\lambda}{p^{n-1}}+\frac{\lambda^2}{2!\,p^{n-2}}-\ldots\right)e^{-\frac{1}{p}}.$$

Each term represents a function of the form

$$\frac{\lambda^m}{m!}\cdot x^{\frac{n-m}{2}}\cdot \mathrm{J}_{n-m}(2\sqrt{x}),$$

and thus, after an obvious transformation, we obtain

$$\sum_{r=0}^{r=\infty}\frac{1}{\Pi(r)}\left(\frac{-a^2}{2x}\right)^r\cdot \mathrm{J}_{n-r}(x)$$

$$=\left(1-\frac{a^2}{x^2}\right)^{\frac{n}{2}}\cdot \mathrm{J}_n(\sqrt{x^2-a^2}) \qquad (x>a). \quad . \quad (34)$$

(*f*) Next consider

$$e^{-\frac{a}{p}}\cdot p^{-n}\cdot e^{-\frac{1}{p}}=p^{-n}\left(1-\frac{a}{p}+\frac{a^2}{2!\,p^2}-\ldots\right)e^{-\frac{1}{p}}=p^{-n}\cdot e^{-\frac{1+a}{p}},$$

and interpret the series as a series of Bessel functions. This series becomes

$$x^{\frac{n}{2}}\mathrm{J}_n(2\sqrt{x})-ax^{\frac{n+1}{2}}\cdot \mathrm{J}_{n+1}(2\sqrt{x})+\frac{a^2}{2!}x^{\frac{n+2}{2}}\cdot \mathrm{J}_{n+2}(2\sqrt{x})-\ldots$$

$$=\frac{1}{(1+a)^n}\{(1+a)\cdot x\}^{\frac{n}{2}}\cdot \mathrm{J}_n(2\sqrt{(1+a)x}),$$

which, with

$$\sqrt{1+a}=y \quad \text{and} \quad 2\sqrt{x}=s,$$

and replacing $s$ again by $x$, becomes

$$\sum_{r=0}^{r=\infty}\frac{1}{\Pi(r)}\cdot\left\{(1-y^2)\frac{x}{2}\right\}^r\cdot \mathrm{J}_{n+r}(x)=y^{-n}\mathrm{J}_n(yx), \quad . \quad (35)$$

being the theorem for the multiplication of the argument of a Bessel function.

(*g*) Further, let us apply (14). This theorem gives

$$\int_0^\infty p^{-(n+2)} \cdot e^{-\frac{1}{p}} \cdot dp = \int_0^\infty x^{\frac{n+1}{2}} \cdot \frac{J_{n+1}(2\sqrt{x})}{x}\, dx,$$

or, after the substitution $2\sqrt{x}=s$, and replacing $s$ again by $x$,

$$\Pi(n) = \frac{1}{2^n}\int_0^\infty x^n \cdot J_{n+1}(x)\, dx \qquad (n>-1) \qquad (36)$$

(*h*) Next, with the definition (3), we can at once write down the integral

$$p^{-n} \cdot e^{-\frac{1}{p}} = p\int_0^\infty e^{-px} \cdot x^{\frac{n}{2}} \cdot J_n(2\sqrt{x})\, dx,$$

which, after an obvious transformation, becomes

$$\int_0^\infty e^{-\alpha x} \cdot x^n \cdot J_{n-1}(2\alpha x)\, dx = \frac{1}{2\alpha} \cdot e^{-\alpha} \qquad (\alpha > 0). \qquad (37)$$

(*j*) As

$$e^{\frac{i}{p}} \doteqdot J_0(2\sqrt{-ix}) = \mathrm{ber}\,(2\sqrt{x}) + i\ \mathrm{bei}\,(2\sqrt{x}),$$

and

$$e^{-\frac{i}{p}} \doteqdot J_0(2\sqrt{+ix}) = \mathrm{ber}\,(2\sqrt{x}) - i\ \mathrm{bei}\,(2\sqrt{x}),$$

we obtain at once the operational expressions for Kelvin's "ber" and "bei" functions as

$$\left.\begin{aligned} \mathrm{ber}\,(2\sqrt{x}) &\doteqdot \cos\frac{1}{p}, \\ \mathrm{bei}\,(2\sqrt{x}) &\doteqdot \sin\frac{1}{p}. \end{aligned}\right\} \quad . \quad . \quad . \quad (29\,a)$$

(*k*) Let us finally make use of the very fertile theorem (17) of the "produit de composition." Taking, *e. g.*,

$$f_1(p) = p^{m-n} \doteqdot \frac{x^{n-m}}{\Pi(n-m)}, \qquad (n-m>-1)$$

$$f_2(p) = p^{1-m} \cdot e^{-\frac{1}{p}} \doteqdot x^{\frac{m-1}{2}} \cdot J_{m-1}(2\sqrt{x}), \quad (m>0),$$

we find

$$f_1(p) \cdot f_2(p) \cdot \frac{1}{p} = p^{-n} \cdot e^{-\frac{1}{p}} \doteqdot x^{\frac{n}{2}} \cdot J_n(2\sqrt{x}).$$

The application of (17) thus at once gives

$$\frac{1}{\Pi(n-m)}\int_0^x (x-\xi)^{n-m}\,.\,\xi^{\frac{m-1}{2}}\,.\,\underset{m-1}{\mathrm{J}}(2\sqrt{\xi})\,.\,d\xi = x^{\frac{n}{2}}\,.\,\mathrm{J}_n(2\sqrt{x})$$

or

$$\frac{2^{m-n}}{\Pi(n-m)}\cdot\int_0^x (x^2-\xi^2)^{n-m}\,.\,\xi^m\,.\,\underset{m-1}{\mathrm{J}}(\xi)\,.\,d\xi = x^n\mathrm{J}_n(x) \quad (38)$$

$$(n-m->1, \quad m>0)$$

Taking in (38),

$$m=\tfrac{1}{2}, \qquad \xi = x\sin\omega,$$

and making use of

$$\xi^{\frac{1}{2}}\mathrm{J}_{-\frac{1}{2}}(\xi) = \sqrt{\frac{2}{\pi}}\cos\xi,$$

(38) becomes

$$\int_0^{\pi/2} (\cos\omega)^{2n}\,.\cos(x\sin\omega)\,d\omega = \sqrt{\pi}\,.\,2^{n-1}\,.\,\Pi(n-\tfrac{1}{2})\,.\,x^{-n}\mathrm{J}_n(x)$$

$$(n>-\tfrac{1}{2}),$$

which for $n=0$ gives the familiar integral definition of the zero'th Bessel function

$$\frac{2}{\pi}\int_0^{\pi/2} \cos(x\sin\omega)\,d\omega = \mathrm{J}_0(x). \quad . \quad . \quad . \quad (39)$$

The results (30–39), which could easily be still further extended, were all obtained with the aid of the operational expression for

$$x^{\frac{n}{2}}\mathrm{J}_n(2\sqrt{x}).$$

In order to obtain another operational expression for a Bessel function we return to the differential equation (26). After the substitution $z=u^{-n}y$, and writing $x$ for $u$, we obtain

$$x\frac{d^2y}{dx^2} + (1-2n)\frac{dy}{dx} + xy = 0. \quad . \quad . \quad . \quad (26\,a)$$

Now we transform (26 $a$) again operationally by multiplying it with $e^{-px}$ and integrating; this is simplified by the use of table (28). Hence we can write at once

$$(p^2+1)\frac{d\mathrm{X}}{dp} + (2n+1)p\mathrm{X} = 0, \quad . \quad . \quad . \quad (26\,b)$$

where, as explained above, we took $y(0)=0$, and where again

$$\mathrm{X}(p) = \int_0^\infty e^{-px}\,.\,y(x)\,dx.$$

The solution of (26 *b*) is easily found to be

$$f(p)=pX(p)=\frac{Cp}{(p^2+1)^{n+\frac{1}{2}}},$$

and again, after adjustment of the integration constant to the usual normalization of the Bessel function, we find a new operational expression

$$\frac{\Pi(2n)}{2^n\Pi(n)}\cdot\frac{p}{(p^2+1)^{n+\frac{1}{2}}}=\frac{2_n\Pi(n-\frac{1}{2})}{\sqrt{\pi}}\cdot\frac{p}{(p^2+1)^{n+\frac{1}{2}}}\doteq x^n\,.\,J_n(x), \quad . \quad . \quad . \quad (40)$$

which is valid for $n>-\frac{1}{2}$. As particular instances we note, for $n=0$ and $n=\frac{1}{2}$,

$$\frac{p}{\sqrt{p^2+1}}\doteq J_0(x), \quad . \quad . \quad . \quad . \quad . \quad . \quad (41)$$

$$\sqrt{\frac{2}{\pi}}\frac{p}{p^2+1}\doteq x^{\frac{1}{2}}\,.\,J_{\frac{1}{2}}(x). \quad . \quad . \quad . \quad . \quad . \quad (42)$$

The last relation (42) can be interpreted by (18 *b*), giving the familiar result,

$$x^{\frac{1}{2}}\,.\,J_{\frac{1}{2}}(x)=\sqrt{\frac{2}{\pi}}\,.\sin x. \quad . \quad . \quad . \quad . \quad . \quad (43)$$

Of course (40) can again be developed as a series in $p^{-1}$, thus yielding the expansion of $J_n(x)$ in a series of positive powers of $x$. Obviously one could, as in the former case, apply several of the theorems (5)–(17) to (40) again. We will, however, only derive a new relation with the aid of (17), in the following way.

Take

$$f_1(p)=\frac{p}{(p^2+1)^{n+\frac{1}{2}}},$$

$$f_2(p)=\frac{p}{(p^2+1)^{-n+\frac{1}{2}}};$$

then

$$f_1(p)\,.\,f_2(p)\,.\,\frac{1}{p}=\frac{p}{p^2+1}\doteq\sin x.$$

Hence, applying (17), we obtain

$$\frac{2^n\Pi(n)}{\Pi(2n)}\cdot\frac{2^{-n}\Pi(-n)}{\Pi(-2n)}\cdot\int_0^x(x-\xi)^n J_n(x-\xi)\,.\,\xi^{-n}J_{-n}(\xi)\,d\xi = \sin x,$$

which, after simplification and the use of

$$\Pi(n) \cdot \Pi(-n) = \frac{\pi n}{\sin \pi n},$$

becomes

$$\cos n\pi \cdot \int_0^x \left(\frac{x}{\xi} - 1\right)^n J_n(x-\xi) \cdot J_{-n}(\xi) \cdot d\xi = \sin x, \quad (44)$$

which is valid for $-\frac{1}{2} < n < +\frac{1}{2}$. Moreover, the expression (40) is well adapted for a derivation (with the aid of (8)) of the asymptotic series for Bessel functions, but we shall not enter into these details.

We now turn our attention to still another symbolic representation of Bessel functions, which will show us the close relation of these functions to spherical harmonics. Consider therefore again the fundamental differential equation (26). This time, however, we write $ix$ instead of $x$, and $n+\frac{1}{2}$ instead of $n$:

$$\frac{d^2z}{dx^2} + \frac{1}{x}\frac{dz}{dx} - \left(1 + \frac{(n+\frac{1}{2})^2}{x^2}\right) z = 0.$$

Substitute

$$z = y \cdot \sqrt{x},$$

which gives

$$x^2 \frac{d^2y}{dx^2} + 2x\frac{dy}{dx} - (x^2 + n(n+1))y = 0,$$

We now obtain again, with the aid of table (28), the differential equation for

$$X(p) = \int_0^\infty e^{-px} y(x)\, dx$$

as

$$(p^2-1)\frac{d^2X}{dp^2} + 2p\frac{dX}{dp} - n(n+1)X = 0,$$

which is the equation of the spherical harmonics.

We thus find, choosing the right harmonic and the right normalization,

$$\sqrt{\frac{2}{\pi}} \cdot p \cdot Q_n(p) \doteqdot x^{-\frac{1}{2}} \underset{n+\frac{1}{2}}{I}(x), \quad . \quad . \quad . \quad (45)$$

from which we may conclude at once with (1)

$$\int_0^\infty e^{-px} x^{-\frac{1}{2}} \underset{n+\frac{1}{2}}{I}(x)\, dx = \sqrt{\frac{2}{\pi}} \cdot Q_n(p), \quad . \quad (45\,a)$$

where the I-function is as usually defined by:

$$I_m(x) = e^{-\frac{1}{2}m\pi i} J_m(ix) = \sum_{r=0}^{r=\infty} \frac{(\frac{1}{2}x)^{m+2r}}{\Pi(r) \cdot \Pi(m+r)} *.$$

(45) shows the close relation between the Bessel function of imaginary argument and the Legendre functions, the latter being the operational representation of the former. In fact the familiar relations between Legendre functions on the one hand and those between Bessel functions (such as (30), (32), (33)) on the other are easily transformed into each other. *E.g.*:

$$\underset{n+1}{P'}(x) - \underset{n-1}{P'}(x) = (2n+1) \cdot P_n(x)$$

is transformed, with the aid of theorem (12), into

$$\underset{n-1}{J}(x) + \underset{n+1}{J}(x) = \frac{2n}{x} \cdot J_n(x),$$

and similarly for the others.

Leaving the spherical harmonics for the present, we now turn our attention to still another operational representation of Bessel functions. We therefore obtain from (26) (taking $u=x$) directly through the usual process the differential equation for

$$X = \int_0^\infty e^{-px} \cdot z(x)\, dx.$$

The result is

$$\frac{d}{dp}\left\{pX + (p^2+1)\frac{dX}{dp}\right\} - n^2X = 0,$$

of which the solution is

$$X = \frac{C}{\sqrt{1+p^2}}(\sqrt{1+p^2} - p)^{\pm n}.$$

Choosing the proper solution and the right integration constant, we thus find

$$\frac{p}{\sqrt{1+p^2}} \cdot (\sqrt{1+p^2} - p)^n = \frac{p}{\sqrt{1+p^2}} \cdot e^{-n \sinh^{-1} p} \doteqdot J_n(x), \qquad \text{. . . . (46)}$$

which expression we will study somewhat closer, as it gives us several properties of the Bessel functions in a very direct way.

* Watson, 'Bessel Functions,' p. 77.

(*a*) Writing $$\alpha = \sqrt{1+p^2} - p,$$

we have $$\frac{p}{\sqrt{1+p^2}} \cdot \alpha^n \doteq \mathrm{J}_n(x).$$

Further

$$\int_0^x \mathrm{J}_n(x)\,dx \doteq \frac{\alpha^n}{\sqrt{1+p^2}} = \frac{p}{\sqrt{1+p^2}} \cdot \frac{2\alpha^{n+1}}{1-\alpha^2}$$

$$= \frac{2p}{\sqrt{1+p^2}} \cdot \alpha^{n+1}(1+\alpha^2+\alpha^4+\ldots),$$

and hence

$$\int_0^x \mathrm{J}_n(x)\,dx = 2\sum_{r=0}^{r=\infty} \mathrm{J}_{n+1+2r}(x). \quad . \quad . \quad . \quad (47)$$

(*b*) Again take the series

$$\mathrm{J}_1 - \mathrm{J}_3 + \mathrm{J}_5 - \mathrm{J}_7 + \ldots \doteq \frac{p}{\sqrt{1+p^2}}(\alpha - \alpha^3 + \alpha^5 - \alpha^7 + \ldots)$$

$$= \frac{p}{\sqrt{1+p^2}} \cdot \frac{\alpha}{1+\alpha^2} = \frac{1}{2}\frac{p}{1+p^2} \doteq \frac{1}{2}\sin x. \quad . \quad (48)$$

(*c*) Further, another series,

$$-\mathrm{J}_0 + 2(\mathrm{J}_0 - \mathrm{J}_2 + \mathrm{J}_4 - \ldots)$$

$$\doteq \frac{p}{\sqrt{1+p^2}}\{-1 + 2(1-\alpha^2+\alpha^4-\alpha^6\ldots)\}$$

$$= \frac{p}{\sqrt{1+p^2}} \cdot \frac{1-\alpha^2}{1+\alpha^2} = \frac{p^2}{1+p^2} \doteq \cos x. \quad . \quad (49)$$

(*d*) Again, as for integer $n$

$$\mathrm{J}_{-2n}(x) = \mathrm{J}_{+2n}(x),$$

we easily find the sum

$$\sum_{n=-\infty}^{n=+\infty} \mathrm{J}_n(x) = \mathrm{J}_0 + 2\mathrm{J}_1 + 2\mathrm{J}_2 + 2\mathrm{J}_4 + \ldots$$

$$\doteq \frac{p}{\sqrt{1+p^2}}(1 + 2\alpha^2 + 2\alpha^4 + 2\alpha^6 + \ldots)$$

$$= \frac{p}{\sqrt{1+p^2}}\frac{1+\alpha^2}{1-\alpha^2} = \frac{p}{\sqrt{1+p^2}} \cdot \frac{\sqrt{1+p^2}}{p} \doteq 1, \quad (50)$$

as a matter of algebra.

(*e*) Next apply theorem (13) to (46). It follows that

$$\int_p^\infty \frac{\alpha^n}{\sqrt{1+p^2}}\,dp \doteqdot \int_0^x \frac{J_n(x)}{x}\,dx \qquad (n>0).$$

The left-hand member equals

$$-\frac{1}{n}\Big[\alpha^n\Big]_p = \frac{\alpha^n}{n} \qquad (n>0),$$

and we thus find the meaning of $\alpha^n$ as

$$\alpha^n = (\sqrt{1+p^2}-p)^n \doteqdot n\int_0^x \frac{J_n(x)}{x}\,dx \quad (n>0), \qquad (51)$$

and further,

$$p\alpha^n = p(\sqrt{1+p^2}-p)^n \doteqdot \frac{n J_n(x)}{x} \qquad (n>0). \quad (51a)$$

(*f*) Further, consider (46) in connexion with (17). Let us take as

$$f_1(p) = \frac{p}{\sqrt{1+p^2}}\cdot\alpha^n \doteqdot J_n(x),$$

$$f_2(p) = \frac{p}{\sqrt{1+p^2}}\cdot\alpha^{-n} \doteqdot J_{-n}(x).$$

Hence

$$f_1(p)\cdot f_2(p)\cdot\frac{1}{p} = \frac{p}{1+p^2} \doteqdot \sin x,$$

and thus we can write down at once the interesting result:

$$\int_0^x J_n(\xi)\cdot J^{-n}(x-\xi)\,d\xi = \sin x, \quad (-1<n<+1). \quad (52)$$

More generally we also have

$$\frac{p}{\sqrt{1+p^2}}\alpha^n\cdot\frac{p}{\sqrt{1+p^2}}\alpha^m\cdot\frac{1}{p} = \frac{p}{1+p^2}p\overset{n+m}{\alpha}\cdot\frac{1}{p},$$

which, interpreted with the aid of (51*a*), gives us the relation

$$\frac{1}{n+m}\int_0^x J_n(\xi)\cdot J_m(x-\xi)\cdot d\xi = \int_0^x \frac{\sin(x-\xi)}{\xi}\cdot J_{n+m}(\xi)\cdot d\xi$$
$$(n>-1, \quad m>-1, \quad n+m>0). \quad (53)$$

(*g*) Let us further inquire as to the meaning of $h(x)$, where

$$f(p) = \log\frac{1}{\alpha} = \sinh^{-1}p = \log(p+\sqrt{p^2+1}) \doteqdot h(x).$$

To this end we start again with

$$\frac{p}{\sqrt{1+p^2}} \doteq J_0(x).$$

Next apply (13 *a*), giving us

$$\int_0^p \frac{dp}{\sqrt{1+p^2}} \doteq \int_x^\infty \frac{J_0(x)}{x}\,dx,$$

or $$\sinh^{-1} p = \log(p+\sqrt{p^2+1}) = -\mathrm{Ji}(x), \quad . \quad (54)$$

where, analogous to

$$\mathrm{Ci}(x) = \int_\infty^x \frac{\cos x}{x}\,dx,$$

we define $$\mathrm{Ji}(x) = \int_\infty^x \frac{J_0(x)}{x}\,dx, \quad . \quad . \quad . \quad . \quad (55)$$

which function could be called integral Bessel function.

This function, which does not seem to have been much studied, will appear again later on.

(*h*) Finally, the application of (17) directly gives us some new and interesting relations, for we can write (46) as

$$\frac{p}{\sqrt{1+p^2}} \alpha^n . p\alpha^m . \frac{1}{p} \doteq \underset{n+m}{J}(x),$$

and thus we find, with the aid of (51 *a*), at once

$$m\int_0^x \frac{J_m(\xi)}{\xi} . J_n(x-\xi)\,d\xi = \underset{n+m}{J}(x) \quad (m>0, \ n>-1). \quad (55\,a)$$

A further interesting Frullani integral involving $J_0(x)$, and closely related to our Ji function, can also be easily evaluated by the operator method. Let it be required to find

$$\int_0^\infty \frac{J_0(x)-\cos x}{x}\,dx = \mathrm{Y}.$$

Here the application of our theorem (14) gives us at once the required result, for

$$\mathrm{Y} = \int_0^\infty \left(\frac{1}{\sqrt{p^2+1}} - \frac{p}{p^2+1}\right) dp = \log\left(\frac{p+\sqrt{p^2+1}}{\sqrt{p^2+1}}\right)\Bigg|_0^\infty = \log 2,$$

and hence

$$\int_0^x \frac{J_0(x)-\cos x}{x}\,dx = \log 2. \quad . \quad . \quad . \quad (53\,a)$$

### 6. *The Derivation of* $J_n(x)$ *with respect to* $n$.

In § 5 we obtained, among others, three operational representations of Bessel functions:

$$x^{\frac{n}{2}} . J_n(2\sqrt{x}) \doteqdot \frac{1}{p^n} . e^{-\frac{1}{p}}, \qquad (n>-1) . \quad . \quad . \quad (29)$$

$$x_n . J_n(x) \doteqdot \frac{2^n . \Pi(n-\frac{1}{2})}{\sqrt{\pi}} . \frac{p}{(p^2+1)^{n+\frac{1}{2}}}, \quad (n>-\tfrac{1}{2}). \quad (40)$$

$$J_n(x) \doteqdot \frac{p}{\sqrt{1+p^2}} . e^{-n \sinh^{-1} p}, \qquad (n>-1). \quad . \quad (46)$$

In order to obtain new expressions for $\frac{\partial J_n(x)}{\partial n}$, we differentiate all three expressions with respect to $n$. We thus obtain, respectively,

$$x^{\frac{n}{2}} \left\{ \frac{1}{2} \log x . J_n(2\sqrt{x}) + \frac{\partial J_n(2\sqrt{x})}{\partial n} \right\} \doteqdot - \log p . p^{-n} . e^{-\frac{1}{p}} .$$

$$. \quad . \quad . \quad (56)$$

$$x^n \left\{ \log x . J_n(x) + \frac{\partial J_n(x)}{\partial n} \right\} \doteqdot$$

$$\frac{2^n \Pi(n-\frac{1}{2})}{\sqrt{\pi}} . \frac{p}{(p^2+1)^{n+\frac{1}{2}}} \{ \log 2 + \psi(n-\tfrac{1}{2}) - \log(p^2+1) \}$$

$$. \quad . \quad (57)$$

$$\frac{\partial J_n(x)}{\partial n} \doteqdot - \sinh^{-1} p . \frac{p}{\sqrt{1+p^2}} . e^{-n \sinh^{-1} p} . \quad . \quad (58)$$

Now above we found already the three functions in (56), (57), and (58), namely,

$$- \log p \doteqdot \log x + C \quad . \quad . \quad . \quad (18\,g)$$

$$- \log \sqrt{1+p^2} \doteqdot \mathrm{Ci}(x), \quad . \quad . \quad . \quad . \quad . \quad (20)$$

$$- \sinh^{-1} p \doteqdot \mathrm{Ji}(x), \quad . \quad . \quad . \quad . \quad . \quad (55)$$

and therefore we are prepared to write the right-hand members of (56), (57), and (58) with theorem (17) as "produits de composition." The three equations thus yield, after some slight transformations, the following interesting relations:

$$\frac{\partial J_n(x)}{\partial n} = \log \frac{\gamma x}{2} . J_n(x) + \int_0^x \log\left(1 - \frac{\xi^2}{x^2}\right) . \left(\frac{\xi}{x}\right)^n J_{n-1}(\xi)\, d\xi,$$

$$(n>-1) \quad . \quad (59)$$

$$\frac{\partial J_n(x)}{\partial n} = \left\{ \psi(n-\tfrac{1}{2}) - \log \frac{x}{2} \right\} \cdot J_n(x)$$

$$+ 2 \int_0^x \mathrm{Ci}(x-\xi) \cdot \left(\frac{\xi}{x}\right)^n \cdot J_{n-1}(\xi)\, d\xi, \qquad (n > -\tfrac{1}{2}) . \quad (60)$$

$$\frac{\partial J_n(x)}{\partial n} = \int_0^x \mathrm{Ji}(x-\xi) \cdot J_n'(\xi) \cdot d\xi, \qquad (n>0). \quad . \quad . \quad (61)$$

All three relations are, as far as I know, new, and the ease with which they can be derived with the aid of the operators is remarkable.

### 7. *Legendre, Laguerre, and Hermite Polynomials.*

The familiar differential equation for the Legendre polynomials is

$$(1-x^2)\frac{d^2y}{dx^2} - 2x\frac{dy}{dx} + n(n+1)y = 0.$$

Substitution of

$$x = s+1$$

yields

$$(s^2+2s)\frac{d^2y}{ds^2} + 2(s+1)\frac{dy}{ds} - n(n+1)y = 0. \quad . \quad (62)$$

Applying the operational transformation on (62) gives us, with the aid of (28),

$$\frac{d^2f}{dp^2} - 2\frac{df}{dp} - \frac{n(n+1)}{p^2} f = 0,$$

where

$$f(p) \doteqdot y(s),$$

or, with the proper normalization, and for integral values of $n$, we obtain

$$\left.\begin{aligned} \mathrm{P}_n(x+1) &\doteqdot (-1)^n \left[ \sqrt{\frac{\pi p}{2}} \cdot e^p \, \mathrm{I}_{-(n+\frac{1}{2})}(p) \right] \\ &= p^{n+1} \cdot e^p \left( -\frac{1}{p}\frac{d}{dp} \right)^n \left( \frac{e^{-p}}{p} \right) \end{aligned}\right\} \quad . \quad . \quad (63)$$

Hence the operational representation of a Legendre polynomial is given by a Bessel function, in the same way as we found before that the operational representation of a Bessel function was given by a Legendre polynomial (see (45)). Obviously this symmetry is no accident and we will return to it later on. It is interesting to consider (63) in

relation to what has been found before in § 3 in connexion with the operational meaning of $e^{-\lambda p}$. Hence, if we multiply (63) by $e^{-p}$, we obtain

$$P_n(x) \doteqdot (-1)^n \left[\sqrt{\frac{\pi p}{2}} \cdot \underset{-(n+\frac{1}{2})}{I}(p)\right] = \left[p^{n+1}\left(-\frac{1}{p}\frac{d}{dp}\right)^n \frac{e^{-p}}{p}\right], \quad . \quad . \quad . \quad . \quad (63\,a)$$

where, as before, by the brackets [ ] is meant the omission of all positive powers of $p$ (the zero'th power excluded).

With the aid of (3) we therefore obtain the interesting integral

$$p\int_0^\infty e^{-px} P_n(x)\,dx = (-1)^n \sqrt{\frac{\pi}{2}} \left[p^{n+\frac{1}{2}} \underset{-(n+\frac{1}{2})}{I}(p)\right], \quad . \quad (64)$$

where in the result the negative powers of $p$ (zero'th power included) are to be retained only.

From (9) and (63) one can also find

$$\int_1^\infty P_n(x) e^{-px}\,dx = p^n \left(-\frac{1}{p}\frac{d}{dp}\right)^n \left(\frac{e^{-p}}{p}\right).$$

We now return to another consideration of the Legendre functions. If we change the independent variable of $\theta$, where

$$x = \cos\theta,$$

we obtain for the differential equation for $P_n(\cos\theta)$, which for short we write $P_n(\theta)$,

$$\sin\theta \cdot \frac{d^2P}{d\theta^2} + \cos\theta \cdot \frac{dP}{d\theta} + n(n+1)\sin\theta \cdot P = 0.$$

A further substitution of

$$\lambda = i\theta$$

yields

$$e^{+\lambda}\left(-\frac{d^2P}{d\lambda^2} - \frac{dP}{d\lambda} + n(n+1)P\right) + e^{-\lambda}\left(\frac{d^2P}{d\lambda^2} - \frac{dP}{d\lambda} - n(n+1)P\right) = 0. \quad . \quad (65)$$

In this case, where the coefficients contain exponentials, the usual transformation leads to a difference equation instead of a differential equation. In fact, we obtain

$$(p+n)(p-n-1)X_n(p-1) = (p-n)(p+n+1)X_n(p+1). \quad (66)$$

where, as before,

$$X_n(p) = \int_0^\infty e^{-p\lambda} \cdot P_n(\lambda)\,d\lambda.$$

From (66) the following solution follows at once

$$\underset{n-1}{\mathrm{X}}(p) \cdot \mathrm{X}_n(p) = \frac{-1}{n^2-p^2}, \quad . \quad . \quad . \quad . \quad (67)$$

and when we now return to the variable $\theta$ again, and therefore let $p$ relate to $\theta$, instead of to $\lambda$, (67) becomes

$$\underset{n-1}{\mathrm{X}}(p) \cdot \mathrm{X}_n(p) = \frac{1}{p^2+n^2}. \quad . \quad . \quad . \quad . \quad (68)$$

Now, writing

$$p\mathrm{X}_n(p) = \mathrm{Y}_n(p),$$

where, therefore,

$$\mathrm{Y}_n(p) \doteq \mathrm{P}_n(\theta),$$

(68) becomes

$$\underset{n-1}{\mathrm{Y}}(p) \cdot \mathrm{Y}_n(p) \cdot \frac{1}{p} = \frac{1}{n} \cdot \frac{pn}{p^2+n^2},$$

which expression can be regarded as a "produit de composition." Hence the application of (17) gives us immediately the interesting and apparently new relation

$$\int_0^\theta \underset{n-1}{\mathrm{P}}(\phi) \cdot \mathrm{P}_n(\theta-\phi)\, d\phi = \frac{\sin n\theta}{n} \quad (n = \text{integer}). \quad (70)$$

The directness with which this result is obtained with the use of the operator is again striking.

Returning to (69), and taking the integration constant of the difference equation (66) or (69), such that

$$\mathrm{P}_0(\theta) = 1,$$

we obtain as the operational expressions for the Legendre functions

$$\left.\begin{aligned}
&\mathrm{P}_0(\theta) \doteq 1, \\
&\mathrm{P}_1(\theta) \doteq \frac{p^2+0^2}{p^2+1^2} \\
&\mathrm{P}_2(\theta) \doteq \frac{p^2+1^2}{p^2+2^2}, \\
&\mathrm{P}_3(\theta) \doteq \frac{(p^2+0^2)(p^2+2^2)}{(p^2+1^2)(p^2+3^2)}, \\
&\mathrm{P}_4(\theta) \doteq \frac{(p^2+1^2)(p^2+3^2)}{(p^2+2^2)(p^2+4^2)}, \\
&\mathrm{P}_5(\theta) \doteq \frac{(p^2+0^2)(p^2+2^2)(p^2+4^2)}{(p^2+1^2)(p^2+3^2)(p^2+5^2)}, \\
&\quad . \quad . \quad . \quad . \quad . \quad . \quad . \quad . \quad . \quad . \quad .
\end{aligned}\right\} \quad . \quad . \quad (71)$$

Letting finally, in (69), $n \to \infty$, this expression becomes

$$\operatorname*{Lim}_{n\to\infty} Y_n^2(p) = \frac{p^2}{p^2+n^2},$$

or

$$\operatorname*{Lim}_{n\to\infty} Y_n(p) = \frac{p}{\sqrt{p^2+n^2}},$$

which second member, as we found before (see (41)), represents $J_0(n\theta)$, and hence we found

$$\operatorname*{Lim}_{n\to\infty} P_n\left(\cos\frac{\theta}{n}\right) = J_0(\theta). \quad . \quad . \quad . \quad . \quad (72)$$

Finally, we consider the differential equation for the Laguerre polynomials $L_n$:

$$x\frac{d^2L_n}{dx^2} + (1-x)\frac{dL_n}{dx} + nL_n = 0. \quad . \quad . \quad . \quad (73)$$

It transforms into

$$(1-p)\frac{d}{dp} + \frac{n}{p}f = 0,$$

where

$$f(p) \doteqdot L_n(x).$$

Hence, with the proper normalization, we find

$$L_n(x) \doteqdot n!\left(1-\frac{1}{p}\right)^n \quad (n=\text{integer}). \quad (74)$$

Similarly we obtain from its differential equation, as the operational expression for the Hermite's polynomials $He_n$

$$He_n\left(\frac{x}{2}\right) \doteqdot n!\left[\frac{e^{-p^2}}{p^n}\right] \quad (n=\text{integer}), \quad (75)$$

where [ ] means the retention of negative powers of $p$ only.

It is, further, a quite simple matter to obtain from (74) and (75) the properties of the Laguèrre's and Hermite's polynomials.

## 8. *Final Considerations.*

From the many examples discussed above of the operational transformation of a differential equation for $y(x)$ into another differential equation for $f(p)$, where $f(p) \doteqdot y(x)$, and also from a general consideration of the method, it follows that there exists a close analogy between the well-known Laplacian transformation and the transformation discussed above.

In a Laplacian transformation we express as an exponential integral :

$$y(x)=\int_a^b e^{qx}.\phi(q)\,dq, \quad . \quad . \quad . \quad . \quad . \quad (76)$$

while in our case we calculated

$$X(p)=\frac{1}{p}f(p)=\int_0^\infty e^{-px}y(x)\,dx. \quad . \quad . \quad . \quad (77)$$

As was pointed out in connexion with (3) and (4), with a suitable choice of the limits $a$ and $b$ in (76), or with a suitable choice of the path of integration in the complex plane,

$$\phi(s)=f(s), \quad . \quad . \quad . \quad . \quad . \quad . \quad (78)$$

or, in other words, the solution of a Laplace integral, considered as an integral equation, is again a Laplace integral. Hence many of the operational expressions $f(p)$ for functions $y(x)$ obtained above have exactly the same form as the integrand of the Laplace integral expression for $y(x)$. In fact (76), (77), and (78) can probably be considered to constitute a Fourier integral identity.

A very interesting list of Fourier integrals, published recently by G. A. Campbell * can therefore be considered also to be a list of operational representations of the functions examined.

The ultimate identity between the operational solution of a differential equation and the solution in the form of a Laplace integral clearly shows when the operational treatment of a problem has advantages over the normal analytical treatment. When, *e. g.*, functions such as Bessel functions occur, an operational treatment clearly is much simpler and very often much more direct than the normal way.

The above examples, which could easily be considerably extended, where many properties, known and new ones, *e. g.* of Bessel functions, could be derived in a most simple and direct way, were, in fact, intended to prove this statement. If, on the other hand, a physical problem would lead, say, to the function $y(x)$, where

$$y(x)=x^{-n}.e^{-x},$$

the operational method would lead to a Bessel function because this last expression is itself the operational representation of a Bessel function. In such a case the operational method would have no advantages. Hence the

* The Bell System Technical Journal, vii. p. 639 (1928).

operational way of solving physical or technical problems shows its full advantages in those problems where complicated functions occur which cannot be expressed directly by more elementary functions. It often happens that the operational representation of those complicated functions is given by rather elementary functions, as was demonstrated in many of the above examples, and in those cases the directness and simplicity with which the properties of those complicated functions can be studied is most remarkable.

Finally we wish to remark that several formulæ derived above are also valid outside the range mentioned. In fact, negative powers of $x$ (except negative integral powers) can be represented operationally by positive powers of $p$ (except positive integral powers). However, under these circumstances difficulty arises from the integral definition in § 3 of the $\Pi$ functions. In this case the $\Pi(n)$ functions have to be extended into the domain $n<-1$ (*e. g.*, by means of the Gauss limit of an infinite product).

In conclusion we wish to express our great indebtness in preparing this paper to the writings of Heaviside, especially volume ii. of his 'Electromagnetic Theory,' and to the late Dr. Bromwich of Cambridge and Dr. Le Corbeiller of Paris, and Professor Elias of Delft University, with whom I had the opportunity to discuss several of the questions treated in this paper. My thanks are also due to Dr. K. F. Niessen (of this Laboratory) for verifying most of the formulæ.

*List of some Operational Representations derived above and of some other Results obtained.*

$$p[1] \doteqdot \delta(x) \text{ (Heaviside's "impulsive" function } p[1] = \text{Dirac's } \delta(x)).$$

$$\frac{1}{2}\left(1+\coth\frac{hp}{2}\right) \doteqdot \text{"staircase" function of fig. 3.}$$

$$\frac{1}{2}\tanh\frac{hp}{2} \doteqdot \text{"meander" function of fig. 4.}$$

$$\cot^{-1}p \doteqdot \mathrm{Si}(x) \text{ (integral sine).} \quad . \quad . \quad (19)$$

$$-\log\sqrt{1+p^2} \doteqdot \mathrm{Ci}(x) \text{ (integral cosine).} \quad . \quad (20)$$

$$-\log(p-1) \doteqdot \mathrm{Ei}(x). \quad . \quad . \quad . \quad . \quad . \quad . \quad . \quad (21)$$

$$\frac{1}{p^n}\log\frac{1}{p} \doteqdot \frac{x^n}{\Pi(n)}\{\log x - \psi(n)\} \quad . \quad . \quad . \quad (18e)$$

$$\psi(n) = \frac{d}{dn}(\log\Pi(n)) \quad . \quad (18f)$$

$$\frac{1}{p^n} e^{-\frac{1}{p}} \doteqdot x^{\frac{n}{2}} \cdot \mathrm{J}_n(2\sqrt{x}). \quad (n > -1) \quad (29)$$

$$\left.\begin{aligned} \cos\frac{1}{p} &\doteqdot \mathrm{ber}\,(2\sqrt{x}) \\ \sin\frac{1}{p} &\doteqdot \mathrm{bei}\,(2\sqrt{x}) \end{aligned}\right\} \text{Kelvin's "ber" and "bei" functions.} \quad (29a)$$

$$\frac{2^n}{\sqrt{\pi}}\,\Pi(n-\tfrac{1}{2}) \cdot \frac{p}{(p^2+1)^{n+\frac{1}{2}}} \doteqdot x^n \cdot \mathrm{J}_n(x). \quad (40)$$

$$\sqrt{\frac{2}{\pi}} \cdot p \cdot \mathrm{Q}_n(p) \doteqdot x^{-\frac{1}{2}} \underset{n+\frac{1}{2}}{\mathrm{I}}(x). \quad (45)$$

$$\frac{p}{\sqrt{1+p^2}} \cdot e^{-n \sinh^{-1} p} \doteqdot \mathrm{J}_n(x). \quad (46)$$

$$p \cdot e^{-n \sinh^{-1} p} \doteqdot \frac{n}{x} \cdot \mathrm{J}_n(x) \quad (n > 0). \quad (51a)$$

$$-\sinh^{-1} p \doteqdot \mathrm{Ji}(x) = \int_{\infty}^{x} \frac{\mathrm{J}_0(x)}{x}\,dx \text{ (integral Bessel function).} \quad (54)$$

$$(-1)^n \left[\sqrt{\frac{\pi p}{2}} \cdot \underset{-(n+\frac{1}{2})}{\mathrm{I}}(p)\right] \doteqdot \mathrm{P}_n(x) \ (n = \text{integer}). \quad (63a)$$

$$n!\left(1-\frac{1}{p}\right)^n \doteqdot \mathrm{L}\,(x) \text{ (Laguerre's polynomials).} \quad (74)$$

$$n!\left[\frac{1}{p^n} e^{-p^2}\right] \doteqdot \mathrm{He}_n\left(\frac{x}{2}\right) \text{(Hermite's polynomials).} \quad (75)$$

---

$$\sum_{r=0}^{r=\infty} \frac{1}{\Pi(r)} \left(\frac{-a^2}{2x}\right)^r \cdot \underset{n-r}{\mathrm{J}}(x) = \left(1-\frac{a^2}{x^2}\right)^{\frac{n}{2}} \cdot \mathrm{J}_n(\sqrt{x^2-a^2}) \quad (x > a). \quad (34)$$

$$\sum_{r=0}^{r=\infty} \frac{1}{\Pi(r)} \left\{(1-y^2)\frac{x}{2}\right\}^r \cdot \underset{n+r}{\mathrm{J}}(x) = y^{-n} \cdot \mathrm{J}_n(yx) \quad (35)$$

$$\int_0^{\infty} e^{-\alpha x^2} \cdot x^n \cdot \underset{n-1}{\mathrm{J}}(2\alpha x)\,dx = \frac{1}{2\alpha} \cdot e^{-\alpha} \quad (\alpha > 0). \quad (37)$$

$$\frac{2^{m-n}}{\Pi(n-m)} \cdot \int_0^x (x^2-\xi^2)^{n-m} \cdot \xi^m \cdot \underset{m-1}{\mathrm{J}}(\xi)\,d\xi = x^n \cdot \mathrm{J}_n(x) \quad (n-m > -1, \quad m > 0). \quad (38)$$

$$\cos n\pi \int_0^x \left(\frac{x}{\xi}-1\right)^n . \mathrm{J}_n(x-\xi) . \mathrm{J}_{-n}(\xi)\, d\xi = \sin x$$
$$(-\tfrac{1}{2}<n<+\tfrac{1}{2}). \quad (44)$$

$$\int_0^x \mathrm{J}_n(\xi) . \mathrm{J}_{-n}(x-\xi)\, d\xi = \sin x$$
$$(-1<n<+1). \quad (52)$$

$$m \int_0^x \frac{\mathrm{J}_m(\xi)}{\xi} . \mathrm{J}_n(x-\xi)\, d\xi = \mathrm{J}_{n+m}(x) \quad (m>0). \quad (55\,a)$$

$$\int_0^\infty \frac{\mathrm{J}_0(x)-\cos x}{x}\, dx = \log 2. \quad . \quad . \quad . \quad . \quad . \quad (53\,a)$$

$$\frac{\partial \mathrm{J}_n(x)}{\partial n} = \log\frac{\gamma x}{2} . \mathrm{J}_n(x) + \int_0^x \log\left(1-\frac{\xi^2}{x^2}\right) . \left(\frac{\xi}{x}\right)^n \mathrm{J}_{n-1}(\xi)\, d\xi.$$
$$(n>-1). \quad (59)$$

$$\frac{\partial \mathrm{J}_n(x)}{\partial n} = \left\{ \psi(n-\tfrac{1}{2}) - \log\frac{x}{2} \right\} . \mathrm{J}_n(x)$$
$$+ 2\int_0^x \mathrm{Ci}(x-\xi) . \left(\frac{\xi}{x}\right)^n \mathrm{J}_{n-1}(\xi)\, d\xi. \quad (60)$$

$$\frac{\partial \mathrm{J}_n(x)}{\partial n} = \int_0^x \mathrm{Ji}(x-\xi) . \mathrm{J}_n'(\xi) . d\xi. \quad . \quad . \quad . \quad . \quad . \quad . \quad (61)$$

$$\int_0^\infty e^{-sx} . \mathrm{P}_n(x)\, dx = (-1)^n \sqrt{\frac{\pi}{2}} . \left[\frac{1}{\sqrt{s}}\, \mathrm{I}_{-(n+\frac{1}{2})}(s)\right]. \quad (64)$$
$$(n=\text{integer.})$$

$$\int_0^\theta \mathrm{P}_{n-1}(\cos\phi) . \mathrm{P}_n(\cos(\theta-\phi))\, d\phi = \frac{\sin n\theta}{n} \quad . \quad . \quad . \quad (70)$$
$$(n=\text{integer.})$$

$$\lim_{n\to\infty} \mathrm{P}_n\left(\cos\frac{\theta}{n}\right) = \mathrm{J}_0(\theta) \quad . \quad . \quad . \quad (72)$$

*Summary.*

§ 1 considers the earlier work on operators by Riemann, Heaviside, Pincherle, Carson, Lévy, and Bromwich. Bromwich's complex integral gives the solution of Carson's integral considered as an integral equation.

In § 2 some general theorems in connexion with the operational method, and formulated by Carson, are considered, and some new theorems are added. Heaviside's "impulsive" function $p\lfloor 1\rfloor$ is shown to be identical with Dirac's $\delta(x)$

function. The very fertile theorem (17) is considered as a "produit de composition" as defined by Volterra, and used by Borel in his "sommation exponentielle" of divergent series. It was known in physics as the Hopkinson–Boltzmann superposition principle for linear systems.

In § 3 some of the general operational theorems are considered in more detail, especially the meaning of $e^{-\lambda p}.f(p)$ by itself, and further, the meaning of the same expression after omission in its series development of all positive powers of $p$. The results are illustrated by figs. 1 and 2. Further, the "staircase" function of fig. 3 and the "meander" function of fig. 4 are found to be expressible in a very simple way with the aid of operators. Further, with the aid of the above theorems symbolic expressions are derived for $\mathrm{Si}(x)$, $\mathrm{Ci}(x)$, $\mathrm{Ei}(x)$, and $x^n \log x$.

§ 4 considers some examples of the solution of differential equations with constant coefficients, and a simple operational method is considered for finding the conditions for the elimination of transients in switching operations. It is further shown how the factor $(t-a)$ in $(t-a)(\dot{y}+y)=0$ fully destroys the effect of the initial condition after the instant $t=a$, thus leading up to

§ 5, where linear differential equations with variable coefficients are discussed. Starting from the differential equation for Bessel functions, the operational representation

$$p^{-n}.e^{-\frac{1}{p}} \doteqdot x^{\frac{n}{2}} \mathrm{J}_n(2\sqrt{x})$$

is derived. Several of the familiar relations existing between Bessel functions can at once be derived from (29). Similarly, the multiplication theorem of the argument of a Bessel function (35) can easily be found. Further, the operational relations

$$\mathrm{ber}\,(2\sqrt{x}) \doteqdot \cos\frac{1}{p} \quad \text{and} \quad \mathrm{bei}\,(2\sqrt{x}) \doteqdot \sin\frac{1}{p} \quad (29\,a),$$

are obtained, while the application of theorem (17) yields in a straightforward way the solution of some fairly complicated integrals involving Bessel functions. Next, another operational expression for $x^n \mathrm{J}_n(x)$ (40), is derived from the differential equation, which enables us to obtain several other interesting integrals containing a Bessel function. Further, a new operational representation,

$$x^{-\frac{1}{2}} \underset{n+\frac{1}{2}}{\mathrm{I}}(x) \doteqdot \sqrt{\frac{2}{\pi}}.p.\mathrm{Q}_n(p) \quad (45),$$

involving spherical harmonics is obtained, from which the analogy of the relations existing between the spherical harmonics are shown to be at once derivable from similar relations existing between Bessel functions. A further operational representation,

$$p(1+p^2)^{-\frac{1}{2}}(\sqrt{1+p^2}-p)^n \doteq J_n(x)$$

is found to lead easily to the derivation of several series and integrals involving Bessel functions.

Special attention is given to the function

$$\mathrm{Ji}(x)=\int_{\infty}^{x}\frac{J_0(x)}{x}\,dx,$$

which is formed in a similar way to $\mathrm{Ci}(x)$, and which plays an important part in an integral expressing $\frac{\partial J_n(x)}{\partial n}$. Next some Frullani integrals are shown to be easily solved with the aid of operators.

§ 6 discusses three new integral expressions for the derivation of a Bessel function $J_n(x)$ with respect to its order $n$. These three integrals contain log, Ci, and Ji functions respectively.

In § 7 operational expressions for Legendre, Laguerre, and Hermite's polynomials are obtained. Legendre polynomials, considered as a function of $\theta$, lead to a difference equation for its operational representative, from which an interesting and apparently new integral relation (70) containing Legendre polynomials can at once be derived. Similarly, the asymptotic behaviour of $P_n$ as a Bessel function when $n\rightarrow\infty$ is easily demonstrated.

§ 8 contains some general considerations on operators. It is shown that the operational representation of a function is closely related to its representation as a Laplace integral. It is further pointed out when in physical problems the operational solution is to be preferred to the ordinary solution. In those cases, which are many indeed, the operational solution leads to the desired result in a most remarkable and direct way.

At the end of the paper a number of operational expressions derived are summarized, together with some of the integral relations obtained.

Natuurkundig Laboratorium der
N. V. Philips's Gloeilampenfabrieken,
Eindhoven, July 1929.

## XCVI. *On the Damping of a Pendulum by Viscous Media.* *By* F. E. Hoare, *B.Sc., A.R.C.S.**

### *Introduction.*

THE following experiments were undertaken in an attempt to develop an alternative method for the measurement of viscosity. The torsional oscillation developed by O. Meyer, in which a horizontal disk, supported by a suspension wire, performs oscillations in its own plane, is well known, and although the theory is not above suspicion, the usual formula gives results for the viscosities of liquids which are in fair agreement with those obtained by other methods. The theory of this method was first developed by Stokes †, and in the same paper he gives the theory of a simple pendulum performing oscillations in a viscous medium.

The equation of motion of a pendulum consisting of a sphere attached to a fine wire and performing oscillations in a vertical plane, the sphere being immersed in a viscous medium of density $\rho$ and coefficient of viscosity $\eta$, can be written according to the classical theory ‡,

$$\mathrm{M}\frac{d^2x}{dt^2} = -(\mathrm{M}-\mathrm{M}')\frac{g}{l}.x. \\ -\mathrm{M}'\left(\frac{1}{2}+\frac{9}{4\beta r}\right)\frac{d^2x}{dt^2} - \frac{9}{4}\mathrm{M}'\sigma\left(\frac{1}{\beta r}+\frac{1}{\beta^2 r^2}\right)\frac{dx}{dt}, \quad (1)$$

where

$x$ = displacement at time $t$,

$\beta = \sqrt{\frac{\pi\rho}{\eta \mathrm{T}}}$,

$\sigma = \frac{2\pi}{\mathrm{T}}$,

$r$ = radius sphere,

T = periodic time,

M = mass of sphere,

M′ = mass of fluid displaced,

$l$ = length of pendulum,

$g$ = acceleration due to gravity.

* Communicated by Prof. F. H. Newman, D.Sc.

† Stokes, Camb. Phil. Soc. ix. p. 8.

‡ Lamb, 'Hydrodynamics,' p. 635.

This equation is formulated without taking into account either the resistance experienced by the wire, which will in general be small compared with that experienced by the sphere, or the finite arc of swing of the pendulum. Thus the equation will apply accurately only to infinitesimally small oscillations.

The solution of equation (1) may be written

$$x = e^{-\frac{M'9\pi k'}{4T(M+kM')}\cdot t} X \cdot \cos(\theta - \gamma), \quad . \quad . \quad . \quad (2)$$

where X and $\gamma$ are constants dependent upon the initial conditions, and

$$k = \left(\frac{1}{2} + \frac{9}{4\beta r}\right),$$

$$k' = \left(\frac{1}{\beta r} + \frac{1}{\beta^2 r^2}\right),$$

$$\theta = t \cdot \sqrt{\frac{(M-M')g}{(M+kM')l} - \frac{1}{4}\left\{\frac{M'\frac{9}{2}\frac{\pi}{T}k'}{M+kM'}\right\}^2}.$$

The second term under the root sign in the expression for $\theta$ is small and can be neglected in comparison with the first term. Hence the time of vibration is given by

$$T = 2\pi\sqrt{\frac{M+kM'}{M-M'}\cdot\frac{l}{g}}.$$

The periodic time, $T_1$, *in vacuo*, which is not greatly different from that in air, is

$$T_1 = 2\pi\sqrt{\frac{l}{g}},$$

and hence

$$\frac{T}{T_1} = \sqrt{\frac{M+kM'}{M-M'}}.$$

By substituting for $k$ and rearranging the terms, it will be seen that

$$\eta = \frac{1}{9\pi\rho T r^4}\left\{(M-M')\frac{T^2}{T_1^2} - \left(M+\frac{M'}{2}\right)\right\}^2. \quad . \quad (3)$$

If T and $T_1$ can be measured with sufficient accuracy this affords one method of finding $\eta$. The results obtained in this way will be given later.

The logarithmic decrement of the amplitude is, from (2),

$$\lambda = \frac{M' 9\pi k'}{8(M + kM')} \cdot \quad . \quad . \quad . \quad . \quad . \quad (4)$$

The quantities $k$ and $k'$ depend upon the periodic time T, but as this is independent of the amplitude according to the theory given above, $\lambda$ should be constant and its measurement would thus provide another method for finding the viscosity $\eta$.

If, when substituting for $k'$ in (4), $\frac{1}{\beta^2 r^2}$ is neglected in comparison with $\frac{1}{\beta r}$, and $2\lambda$ in comparison with $\pi$, the expression for $\lambda$ reduces to the simple form,

$$\lambda = \frac{9\pi M'}{4(2M + M')} \cdot \frac{1}{\beta r} \cdot \quad . \quad . \quad . \quad . \quad . \quad (5)$$

The relative magnitude of the terms $\frac{1}{\beta^2 r^2}$ and $\frac{1}{\beta r}$ can be readily estimated by assuming for water the following values as rough approximations :

$$\eta = \cdot 01 \text{ c.g.s.},$$
$$\rho = 1,$$
$$r = 2 \text{ cm.},$$
$$T = 3 \text{ sec.}$$

With these values, the approximate values of $\frac{1}{\beta^2 r^2}$ and $\frac{1}{\beta r}$ are

$$\frac{1}{\beta r} = \frac{1}{20},$$

$$\frac{1}{\beta^2 r^2} = \frac{1}{400}.$$

Consequently, no serious error for the present purposes will be made by neglecting $\frac{1}{\beta^2 r^2}$. From the results of the experiments performed, the error produced by neglecting $2\lambda$ in comparison with $\pi$ is about 2 per cent., which is equally negligible.

*Experimental.*

Originally it was proposed to determine the coefficient of viscosity by finding the period of a pendulum in air and then

immersed in water, using equation (3). For this purpose three brass spheres of diameter $1\frac{1}{2}$ inches, $1\frac{3}{4}$ inches, and 2 inches respectively—each accurate to two-thousandths of an inch—were obtained, and a fine german-silver wire of ·027 cm. diameter was fastened to each by drilling a small hole, heating the ball, and then filling the hole with soft solder and immersing a few millimetres of the carefully cleaned wire into the molten solder. It was found that the wires so fastened held very well and the method employed was not at all likely to disturb the sphericity of the balls. A large tank about 3 ft. 6 in. by 1 ft. by 1 ft. was used to contain the water in which the balls oscillated. Each ball was suspended so that when vibrating it was at a mean depth of about 5 inches below the surface of the water. It is necessary to employ a large tank, as in the development of the theory it is assumed that the fluid is of infinite extent and at rest at infinity, and, if a small tank is used wall effects would vitiate the results. By using a tank with the above dimensions it was considered that no correction would be necessary from this cause. Actually, of course, in calculating $\eta$ a correction should be made for the resistance experienced by the wire, but as the diameter of the wire was so small in comparison with that of the spheres employed, and only a short length was immersed, it was considered negligibly small, and consequently ignored in the calculations.

The chief experimental difficulty in measuring the periodic time of the pendulum when the ball is immersed in water is caused by the rapidity of decay of the oscillations, it being impossible to obtain more than about 70 vibrations. Preliminary experiments using a stop-watch to time the vibrations showed that much greater accuracy in measuring the time would be necessary before this method could be employed for finding $\eta$. Accordingly it was decided to use a chronograph capable of measuring 1/100 of a second, the instrument being controlled by a tuning-fork and the order of accuracy 1/100 sec. The results of preliminary experiments with the $1\frac{1}{2}$ inch sphere are given below.

| Temp. | Swings taken. | T. | $T_1$. | $\eta$ c.g.s. |
|---|---|---|---|---|
| 20° C. ..... | 60 | 2·9153 | ... | ·008 |
| | 100 | ... | 2·6595 | |
| 16° C. ..... | 65 | 2·8327 | ... | ·014 |
| | 100 | ... | 2·5794 | |

These results were considered too discordant to make the continuance of these particular experiments of any value, either as a test of the theory or as a method for finding the coefficient of viscosity, and it was decided to find $\eta$ by the measurement of the log. dec.

### *Logarithmic Decrement Experiments.*

In these experiments the log. dec. was measured for each sphere for two different lengths of wire suspending the ball. Errors arise in the log. dec. if forced oscillations are set up in the support, so a means of suspension which was at once rigid and easily adaptable was sought. The method finally adopted was to pass the wire to which the brass ball was attached through a fine drill chuck which could be screwed up tight, so that all four jaws were holding the wire. This drill chuck could be fastened, for the longer periods, into a bracket made of half-inch square brass screwed to a wooden beam in the ceiling, and for the shorter periods it was fitted into a bracket mounted on a solid cylinder of iron 2 in. in diameter which stood on a massive iron foot on a table. In neither case was it at all probable that appreciable forced oscillations would be set up.

The amplitudes were observed on one side only with a telescope containing a scale in the eyepiece situated $2\frac{1}{2}$ metres from the suspending wire. At this distance the image of the wire when properly in focus was fairly fine, and little difficulty was experienced in estimating to a tenth of a division in the eyepiece. The greatest angle through which the wire was displaced from the vertical in any experiment was less than 1·8°, and in every experiment the pendulum made several complete vibrations before any readings were taken.

According to theory the amplitudes should be in decreasing geometrical progression, and this was tested before proceeding further. The ratios of successive observed amplitudes were not sufficiently accurate for this law to be tested owing to the error of observation in each measurement, and it was therefore decided to find $\log \frac{\alpha_0}{\alpha_{11}}$ for a series of observations.

In the following table the amplitudes are given in eyepiece scale divisions and the last column gives $\log \frac{\alpha_n}{\alpha_{n+11}}$, the results being for the 2 in. sphere vibrating with a period of 3·58 sec.

| $a_n$. | $a_{n+11}$. | $\log \frac{a_n}{a_{n+11}}$. |
|---|---|---|
| 50·0 | 26·5 | ·6349 |
| 46·2 | 25·4 | ·5982 |
| 43·5 | 24·1 | ·5906 |
| 40·4 | 22·9 | ·5677 |
| 38·2 | 21·9 | ·5564 |
| 36·1 | 21·0 | ·5418 |
| 34·1 | 20·0 | ·5336 |
| 32·3 | 19·1 | ·5254 |
| 30·9 | 18·2 | ·5293 |
| 29·2 | 17·3 | ·5235 |
| 27·7 | 16·6 | ·5120 |

It will be seen that, except for one value of the logarithm, there is a progressive decrease in the third column showing that the assumption of successive amplitudes being in geometrical progression, and thus that the resistance experienced by the sphere is directly proportional to the velocity, is unjustifiable.

*Modified Theory.*

To account for the variation of the damping as found by experiment it was assumed that the decay of the amplitude could be resolved into two parts, one proportional to the velocity and the other to the square of the velocity. The differential equation for the variation of the amplitude can then be written

$$\frac{d\alpha}{dt} = -(A\alpha - B\alpha^2), \quad . \quad . \quad . \quad . \quad . \quad (6)$$

where $\alpha$ is the amplitude at time $t$, A and B being constants.

Integrating this equation, and substituting the end conditions,

$$\alpha = \alpha_0 \text{ at } t = 0$$

$$\alpha = \alpha_1 \text{ at } t = t_1,$$

we have

$$t_1 = \frac{1}{A}\log\frac{\alpha_0}{\alpha_1} - \frac{1}{A}\log\frac{A + B\alpha_0}{A + B\alpha_1}.$$

This solution involving constants in the logarithm is inconvenient for calculation, so the following method due to Stokes * was adopted.

Rewriting the equation (6) in the form

$$\frac{d\alpha}{\alpha} = -A\,dt - B\alpha\,dt,$$

we can substitute for $\alpha$ in the last term from the equation

$$\alpha = \alpha_0\left(\frac{\alpha_1}{\alpha_0}\right)^{\frac{t}{t_1}},$$

an approximation in the present case, but accurately true when the amplitudes decrease in geometrical progression.

Substituting, and integrating, we have

$$\log\frac{\alpha_0}{\alpha_1} = At_1 + Bt_1\frac{\alpha_0-\alpha_1}{\log\frac{\alpha_0}{\alpha_1}}.$$

This equation involving two disposable constants will represent the experimental results as was shown by one or two trials, and from it an equation for $\eta$ can easily be developed by the use of subsidiary hypotheses in the following manner.

The dimensions of the right-hand side must be zero, so assuming $\log\frac{\alpha_0}{\alpha_1}$ to depend only on the four quantities, $\eta$, T, $r$, $\rho$, where these symbols have the same meaning as before, it follows from a consideration of dimensions that $\log\frac{\alpha_0}{\alpha_1}$ must be of the form

$$\log\frac{\alpha_0}{\alpha_1} = K\left(\frac{\eta T}{r^2\rho}\right)^s$$

where $s$ is some as yet undetermined power. If the theory already given be assumed to hold as a first approximation, we find from equation (5) that

$$s = \tfrac{1}{2}.$$

Consequently, equation (7) becomes

$$\log\frac{\alpha_0}{\alpha_1} = K_1\sqrt{\frac{\eta T}{r^2\rho}} + B_1\eta T\frac{\alpha_0-\alpha_1}{\log\frac{\alpha_0}{\alpha_1}}, \quad . \quad . \quad (8)$$

* Stokes, *loc. cit.*

where $nT = t_1$,

$n$ = complete vibrations between $\alpha_0$ and $\alpha_1$.

The quantities $\alpha_0$ and $\alpha_1$ in equation (8) are the angular amplitudes. In the term $\log \frac{\alpha_0}{\alpha_1}$ the ratio will be the same if linear amplitudes or angular amplitudes are used, but for the term involving $\alpha_0 - \alpha_1$ the angular amplitudes must be obtained. This is easily done by setting up a metre scale in the same place as that in which the pendulum oscillates and reading off the number of centimetres corresponding to 100 scale divisions in the eyepiece. The mean result of several observations showed that 100 scale divisions corresponded with 5·2 cm. ;

$\therefore$ 1 scale div. = ·052 cm. deflexion of wire.

Also the angular amplitude corresponding to one scale division

$$= \frac{\cdot 052}{x},$$

where $x$ is the distance in cm. from the point of support to the point on wire where the amplitude is observed.

Hence, if "$a$" is the amplitude of an oscillation measured in cm., equation (8) can be written

$$\log \frac{a_0}{a_1} = K_1 \sqrt{\frac{\eta T}{r^2 \rho}} + \frac{B_2}{x} \frac{a_0 - a_1}{\log \frac{a_0}{a_1}}. \quad . \quad . \quad . \quad (9)$$

The method of testing this equation was to substitute in it the values obtained for $a_0$, $a_{10}$, and $a_{20}$ from a single experiment, using the 2 in. sphere vibrating with a period of 3·58 sec. and assuming the value ·0110 c.g.s. for the viscosity at 17° C., at which temperature the experiments were performed, and 1 for the density of water. Values were thus obtained for $K_1$ and $B_2$. The latter was next assumed to be some function of the periodic time, and the form of this function was obtained by considering the experiments with the same sphere, but vibrating with a shorter period. In this way it was found that $B_2$ could be written

$$B_2 = B_3 T^2.$$

Finally, a further assumption was made, viz., that $B_3$ was some function of the radius of the sphere. From the experiments on the $1\frac{3}{4}$ in. sphere vibrating with a period of 3·568 sec. it was found that

$$B_3 = K_2 \frac{T^2}{r^{3/2}}.$$

Rewriting equation (9), we now have

$$\log\frac{a_0}{a_1} = K_1\sqrt{\frac{\eta T}{r^2\rho}} + K_2\frac{T^2}{xr^{3/2}}\cdot\frac{a_0-a_1}{\log\frac{a_0}{a_1}}. \quad . \quad (10)$$

To verify all the assumptions the value of the viscosity $\eta$ was calculated from the results obtained with the three spheres, each vibrating with a long and a short period. For this purpose it does not matter if "$a$" is given in cm. or in scale readings, $K_2$ alone being affected by a constant factor. In the following table "$a$" is therefore given in scale deflexions, but the constants utilized in determining the results are in those appropriate units, so that "$a$" is in cm. to facilitate comparison with future work.

*Results.*

The mean value of $x$ was taken to the nearest cm. for the long and short pendulums.

For short pendulums..... $x = 84$ cm.

For long pendulums..... $x = 216$ cm.

Values used for calculating constants in equation (10) :

$\eta = \cdot0110$ c.g.s.

$\rho = 1.$

$T = 3\cdot58$ sec.

$r = 2\cdot54$ cm.

$a_0 = 50\cdot0$ divisions.

$a_{10} = 27\cdot7$ ,,

$a_{20} = 17\cdot3$ ,,

1 scale division = $\cdot052$ cm. deflexion of wire.

These values, when substituted, give the following values for the constants :

$$K_1 = 3\cdot86.$$
$$K_2 = 10\cdot04.$$

Hence, if "$a$" is measured in cm.,

$$\log\frac{a_0}{a_1} = 3\cdot86\sqrt{\frac{\eta T}{r^2\rho}} + 10\cdot04\frac{T^2}{r^{3/2}x}\cdot\frac{a_0-a_1}{\log\frac{a_0}{a_1}}.$$

The results are divided into Section A and Section B, the former relating to the 2 in. and $1\frac{3}{4}$ in. spheres which were used indirectly in finding the form of equation (10), and the

latter referring to these experiments on the $1\frac{3}{4}$ in. and $1\frac{1}{2}$ in. spheres which have not been used at all in the development of the equation for $\eta$.

SECTION A.

| Sphere. | T secs. | $a_0$. | $a_{10}$. | $\eta$ c.g.s. | Means. |
|---|---|---|---|---|---|
| 2 in. | 3·58 | 47·0 | 26·9 | ·0097 | |
| ,, | ,, | 49·0 | 27·1 | ·0116 | ·0105 |
| ,, | ,, | 49·5 | 27·8 | ·0101 | |
| ,, | 2·48 | 48·5 | 27·1 | ·0096 | |
| ,, | ,, | 48·2 | 26·9 | ·0099 | |
| ,, | ,, | 48·9 | 27·2 | ·0098 | ·0010 |
| ,, | ,, | 45·8 | 26·3 | ·0101 | |
| ,, | ,, | 47·9 | 26·8 | ·0098 | |
| ,, | ,, | 49·0 | 27·1 | ·0103 | |
| $1\frac{3}{4}$ in. | 3·568 | 49·0 | 25·4 | ·0098 | |
| ,, | ,, | 47·8 | 25·0 | ·0098 | |
| ,, | ,, | 48·4 | 25·2 | ·0097 | ·0101 |
| ,, | ,, | 46·3 | 24·1 | ·0106 | |
| ,, | ,, | 46·8 | 24·2 | ·0108 | |

SECTION B.

| Sphere. | T secs. | $a_0$. | $a_{10}$. | $\eta$ c.g.s. | Means. |
|---|---|---|---|---|---|
| $1\frac{3}{4}$ in. | 2·484 | 44·0 | 22·9 | ·0097 | |
| ,, | ,, | 46·0 | 23·2 | ·0125 | |
| ,, | ,, | 47·0 | 23·9 | ·0115 | ·0112 |
| ,, | ,, | 49·0 | 24·0 | ·0127 | |
| ,, | ,, | 48·2 | 24·3 | ·0105 | |
| ,, | ,, | 45·9 | 23·6 | ·0102 | |
| $1\frac{1}{2}$ in. | 3·553 | 46·8 | 21·0 | ·0125 | |
| ,, | ,, | 49·2 | 22·1 | ·0114 | |
| ,, | ,, | 45·9 | 20·7 | ·0110 | ·0116 |
| ,, | ,, | 50·0 | 22·2 | ·0118 | |
| ,, | ,, | 48·7 | 21·9 | ·0115 | |
| ,, | ,, | 48·7 | 21·9 | ·0115 | |
| ,, | 2·52 | 47·0 | 20·9 | ·0115 | |
| ,, | ,, | 47·5 | 21·0 | ·0105 | |
| ,, | ,, | 46·2 | 20·5 | ·0110 | ·0108 |
| ,, | ,, | 46·0 | 20·6 | ·0105 | |
| ,, | ,, | 47·1 | 20·9 | ·0104 | |

### *Conclusion.*

The results in Section B show a close approximation to the true result, viz., ·0110 c.g.s. units, and indicate that the theory accounts for the observed phenomena. The mean value of $\eta$ from the results in this section is ·0112 c.g.s. units, which is in remarkably close agreement with the true result when it is remembered that the accuracy of the constants $K_1$ and $K_2$ depends entirely upon the accuracy with which merely three readings of the amplitude have been made in the case of the 2 in. sphere.

It is suggested that the physical meaning of $K_1$ and $K_2$ may be found from further experiments with different liquids, and these are about to be undertaken.

---

## XCVII. *On Conditions near the Cathode of a Glow Discharge.*

*By* Nora M. Carmichael, *M.Sc.*, *and* K. G. Emeléus, *M.A. Ph.D., Department of Physics, The Queen's University of Belfast* *.

THE cathode dark space is not a simple unit of the glow-discharge, but includes, when fully developed, a number of partially distinct sections, there being encountered in turn, on proceeding out from the cathode, the primary dark space, the cathode glow, the cathode dark space proper, and the transition region between the dark space and negative glow. The present communication is a preliminary account of an investigation of the region of the cathode glow and primary dark space with an exploring electrode, for conditions not far removed from those of the normal cathode fall in potential †.

### I. *Experimental procedure.*

The form of tube used is shown in fig. 1. The cathode C consisted of a hollow, nickel-ended iron cylinder, with an iron tail T resting in the end-tube E ; with this construc-

* Communicated by the Authors.

† The work described was done early this year. Its completion has been unavoidably delayed, and although we hope to proceed again with it shortly, it is believed that the results already obtained are of sufficient interest to be published at this stage.

tion small changes were readily made in the position of the cathode with a magnet. The anode A was a nickel disk. The exploring electrode was a filament of tungsten, 0·09 mm. in diameter, or molybdenum, 0·107 mm. in diameter, strung across the tube in front of the cathode,

Fig. 1.

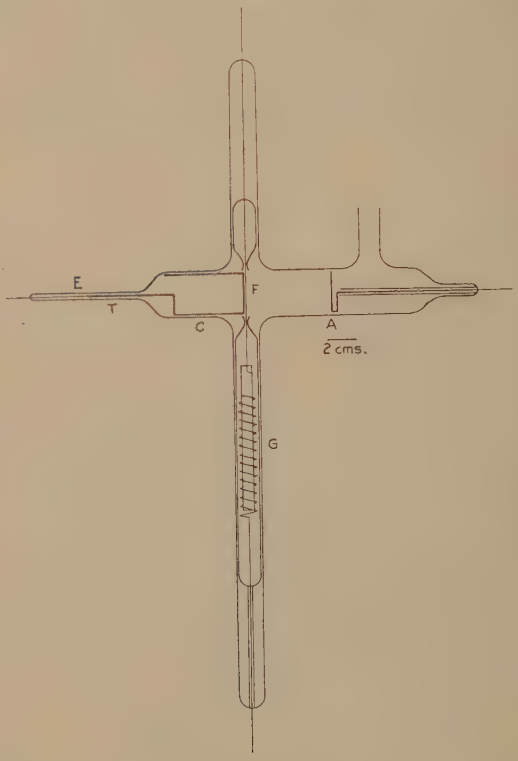


and kept taut by a 10 gm. piece of copper tube G. Care was taken that the glass sheath of F did not touch F for the last 6 mm. of its length on each side of the discharge, and that the filament was parallel to the surface of the cathode, although the latter precaution was found not to be of great significance. The metal parts were degassed in a vacuum furnace before assembly, and before admission

of any specimen of gas, the tube was baked out with a hand-flame at a pressure of less than $10^{-4}$ mm. Hg. That part of the surface of the cathode which was immediately opposite to the filament was also repeatedly subjected to electron bombardment from the latter. The gases used were oxygen, nitrogen, and neon, prepared as has been described elsewhere *, hydrogen, admitted through a palladium regulator, and technical argon, containing some 20 per cent. of nitrogen. Pressures were recorded by a McLeod gauge, and condensible vapours were kept from the tube by liquid-air traps.

Simultaneous measurements were made of the current to F ($i_e$); the current through the tube ($i_t$) as measured by the current to the anode; and the difference in potential between collector and cathode (V), and cathode and anode. The discharge was always allowed to pass for at least an hour before any readings were taken, and was then so steady that it was not necessary to correct $i_c$ for fluctuations in $i_t$. The potential applied between anode and cathode ranged from 250 volts to 450 volts, and the gas-pressures from 0·2 to 1·5 mm. Hg. The filament was always between 0·3 and 0·9 mm. from the cathode, and no change in its position was noticeable as its potential was varied. The results were not affected in their main features by change of the discharge conditions between these limits.

A typical collector characteristic is shown in fig. 2, in which a current below the axis of voltage is one in which there is a net flow of positive electricity from the gas to the filament. The zero of potentials is that of the cathode. The appearance of the curve is similar to that of the curve obtained when a collector in the negative glow is starting to act as a main cathode for the discharge †, but there are important differences in detail, the curve of fig. 2 exhibiting more or less sharp discontinuities of slope at the points A, B, and C (B is usually sharper than in this particular instance).

We are not sure that the discharge was not seriously disturbed locally when the filament was hot. Very small changes in $i_t$ also probably correspond to the breaks A, B, and C. Discussion of these two points is reserved for

* Emeléus and Beck, Phil. Mag. viii. p. 121 (1929).
† Emeléus and Brown, Phil. Mag. vii. p. 17 (1929).

a later paper. All data given in the present communication were obtained with F cold.

### II. *Interpretation of the Characteristic Curves.*

It is of fundamental importance to know if an ionic sheath forms round a collector in the cathode dark space. Theoretically, the problem is indeterminate, since in the usual integration of Poisson's equation it is necessary to know the field either at the surface of the collector or at some point in the sheath, supposed present, or at its

Fig. 2.

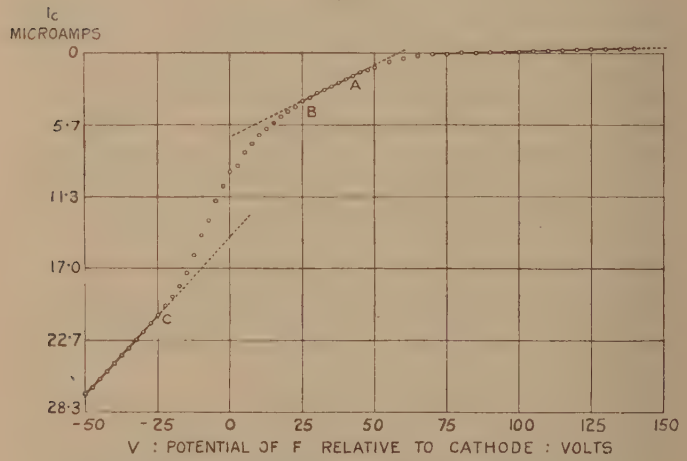


$i_e$=6·7*m*A. Tube voltage=310. F to cathode=0·6 mm. Gas-nitrogen. Thickness of cathode dark space=7 mms.

outer boundary; to assume a value for the field in the present case is tantamount to assuming the existence of the sheath. The problem can be approached directly in two ways from the experimental side; first, by visual observation, and, secondly, from the shape of the characteristic curves. Visual observation is impossible with the tubes that we have used, but has recently been made the subject of a special study by W. L. Brown and E. E. Thomson in this laboratory *. Their observations,

* See the following paper, p. 918

which are reported upon elsewhere, show that the well-known shadows thrown by obstacles in the cathode dark space can be used to find space-potentials, but are not conclusive as to the existence of sheaths like those formed in plasma-type discharges. We have thus to rely upon the form of the characteristic curves, and this appears to be irreconcilable with the existence of ordinary sheaths. There are several reasons for arriving at this conclusion. First, simultaneous observation of shadows and of collector currents in Brown and Thomson's apparatus, in the part of the cathode dark space in which we are now interested, has shown that the space-potential lies at or close to the break B. There is in this part of the characteristic no sign of the reception of the groups of slow electrons which produce a rise in the characteristic curve in other parts of the discharge at the space-potential, and, in spite of the large electric field in most of the cathode dark space, some of these slow electrons might be expected to be present near the cathode glow. Secondly, the position of the characteristic curve relative to the axis of voltage shows that, when insulated, the collector charges up positively to the surrounding space, as Aston suggested in his explanation of the reputed "Kathodensprung" in potential *. This shows that there are present large numbers of positive ions, or that the collector is emitting electrons, or that both of these effects, the latter of which certainly tends to destroy a sheath, are co-existent. Positive ions are, of course, known to be present in excess of electrons through most of the dark space, although the electrons may preponderate near the cathode. From such considerations we have come to regard the action of a collector in the dark space as more nearly like that of a grid wire in an evacuated thermionic triode, that is, its effect is not confined to a region bounded by a separate ionic sheath, but extends without existence of a definite boundary into the pre-existing space-charges of the cathode dark space, modified by the ionic shadows thrown by the collector.

Conditions appear to be too complicated to make a mathematical formulation of these ideas possible, but we can account for the course of the characteristic curves

* Aston, Proc. Roy. Soc. lxxxiv. p. 526 (1910).

qualitatively on lines indicated by Aston *. Fig. 3 *a*, which is taken from his paper, shows the probable trajectories of positive ions (thick lines) and electrons (thin lines) near a -positive—insulated collector F. We are concerned with what happens when F is made more negative than in this case, and it is evident that this will be accompanied by a gradual straightening of the lines until when F is at the space-potential, they run parallel to each other and perpendicular to the cathode. At this stage the space between the lines tangential to F will be

Fig. 3.

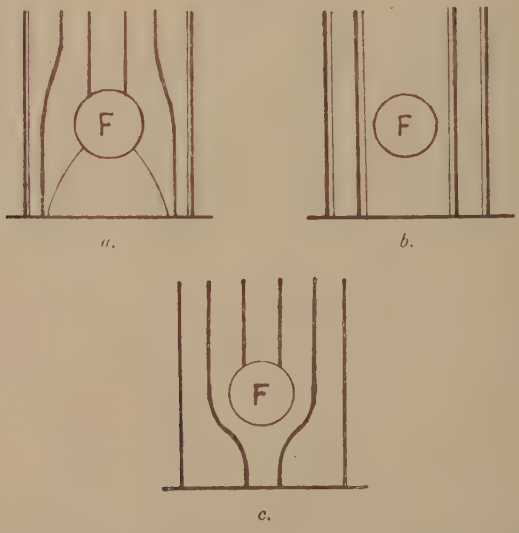


*a*. *b*. *c*.

shielded from the streams of ions and electrons and will appear as a shadow of these dimensions, this constituting Brown and Thomson's method for finding the space-potential. Meanwhile, only small and essentially steady changes will have been occurring in the current to the collector, so far as these ions and electrons are concerned. After passing the space-potential F will affect the positive ions which have passed it on their way to the cathode, so that their paths are more like the lines in fig. 3 *c*. The

* Aston, Proc. Roy. Soc. lxxxiv. p. 526 (1910).

positive ion current to F will commence to increase rather more rapidly than before, together with any secondary emission of electrons from F, and we might thus expect the net positive current to F from the gas to start to increase more rapidly after F has been made negative to the space, and so to give the discontinuous increase in slope that is observed to the negative side of B (fig. 2). As F is made still more negative, the positive current to F from the gas must increase more and more rapidly as the potential of F approaches nearer to that of the main cathode, whatever the precise nature of the processes which render an electrode capable of maintaining a discharge when cold. It is, of course, unlikely that conditions are quite so simple as this, but some such correlation of figs. 2 and 3 seems reasonable.

We have still to account for the breaks A and C. Of the two, C is the more pronounced, and might conceivably arise in at least three ways.

(i.) The region of the characteristic between B and C might correspond to the transition from a discharge of normal type on the collector to one of abnormal type, these terms being used to denote incomplete and complete utilization of the geometrical surface of the collector F; after the discharge is started, sputtering between F and the main cathode probably rapidly makes the two effectively of the same material, and so the fact that the break C, supposed to mark the onset of the normal discharge, is negative to the potential of the main cathode, could be supposed to be due to the fact that the collector F is a wire of large curvature. Against this view is the fact that a space-charge has already been established for F by the main discharge, and certain regularities in the position of C that are referred to again in section III.

(ii.) The point C might correspond to the closing in of the edges of the shadow behind F towards the main cathode until at this stage it ceased to reach to the main cathode.

(iii). The break at C is of a type which is usually associated with the reception of a group of fast electrons in a retarding field by a collector. Such a group could arise either from the gas, or from the surface of the cathode, being produced in the latter case photoelectrically, or by bombardment with excited atoms, or positive ions, or by some other process of the second kind taking place there. It is, of course, possible that fast electrons could come both

from the electrode and gas, but we should be inclined to favour the former source, particularly on account of the general similarity between our curves and those published by Oliphant for electrons liberated from a metal surface by metastable atoms *. On this interpretation of the curves, whatever the space-potential near F, the maximum energy of emission of the electrons from the cathode will be measured by the potential of C relative to the cathode, and many of the electrons would appear to have one half the maximum energy in the group. This form of apparatus is, however, not suited for study of slow electrons from the cathode, since these, unlike electrons emitted with a considerable initial velocity, will follow fairly closely the lines of the positive ions incident upon the cathode, and since the latter have escaped collection by F, the slow electrons liberated where the positive ions hit the cathode —but not necessarily *by* the positive ions—must likewise largely escape detection. There is, in fact, no upward break in the characteristic near the cathode potential. The break A may be very tentatively attributed to the failure of fast electrons liberated from F by a similar process to reach the main cathode in the field retarding their motion in that direction.

We are unfortunately unable at present to decide definitely between the alternatives II. and III.

Curves similar to that of fig. 2 were obtained by Aston † for a collecting electrode behind a hole in the main cathode, but are even less easy to interpret, both because of the disturbance of the main discharge by the aperture, and because there are rather too few experimental points to be sure of the existence of discontinuities in slope at B and A.

### III. *Results of Discussion.*

The interpretation of the characteristic curves remains much less satisfactory than could be desired. We may, however, indicate some of the consequences of assuming that the tentative conclusions of the last section are correct.

(*a*) The break B occurs at a potential consistently closer to that of the cathode than it would be if the fall in

* Oliphant, Proc. Roy. Soc. cxxiv. p. 228 (1929).
† Aston, Proc. Roy. Soc. xcvi. p. 200 (1920).

potential across the whole region between cathode and negative glow followed the parabolic law of Aston *, in general agreement with the results of Brown and Thomson.

(*b*) There are certain regularities in the position of the break C. In each gas there appears to be, on the interpretation iii. of the preceding section, a fairly definite maximum velocity for the electrons emitted from the cathode. In the cases of neon and argon, the break was double, the position of the more negative discontinuity corresponding to the position of the break in nitrogen; in these cases the less negative break has been assumed to be that for the inert gas itself. On the interpretation ii. this could be connected with the shadow reaching to the cathode at one stage, and to the primary dark space at

TABLE I.

| Gas. | No. of breaks measured. | Max. energy of electrons : volts. | Corresponding critical potential of gas in volts. |
|---|---|---|---|
| Nitrogen..... | 16 | 22 $\pm$5 | 28 : dissociation to two singly ionized atoms. |
| Hydrogen ... | 7 | 25·5$\pm$4 | 29·7 : process as for nitrogen. |
| Argon ..... | 9 | 13·5$\pm$3·5 | 15·5 : ionization of atom. |
| Neon ..... | 6 | 18·0$\pm$3·5 | 21·5 : ionization of atom. |

another. The data obtained for the maximum energies are collected in Table I., where the errors given against the energies are the root mean square departures from the mean. These errors are large, which points to the need for better control of the purity of the gas and electrodes than we have yet been able to attain. It may be significant, nevertheless, that the averages lie, as shown, a few volts below important critical potentials of the gas in each case †, and it is tempting to suppose that fast electrons are liberated from the cathode by the atomic processes in question taking place there, the electrons losing at least energy measured by the work-function of the cathode—4·4 volts

* Aston, Proc. Roy. Soc. lxxxiv. p. 526 (1910).

† Data from Geiger-Scheele, *Handb. d. Physik*, xxiii. article by Franck and Jordan for Ar, Ne, $N_2$, from Vencov, *Comptes Rendus*, clxxxix. p. 27 (July 1929), for $H_2$.

for nickel in vacuum *—in leaving it. The processes may then be identifiable with neutralization of the normal singly charged ions in neon and argon, simultaneous neutralization of two protons, with recombination of the latter to form $H_2$ in hydrogen, and neutralization of two atoms followed by recombination in nitrogen.

No breaks were found corresponding to C on five characteristics taken in oxygen.

## IV. *Summary.*

The characteristic curves for a collector very close to the cathode of a glow-discharge have discontinuities in slope. The most negative of these, which is always negative to the potential of the cathode, may be taken to indicate that there is a group of fast electrons leaving the cathode surface, where it is produced by some process of neutralization and recombination of the ions of the cathode dark space. The second, which is always positive to the cathode potential, is attributed to a change occurring in the mode of reception of the current at the space-potential, which, on this interpretation, is consistently more negative than if Aston's parabolic law held. The origin of the third, more positive break, is most uncertain, but it may indicate that there is an emission of fast electrons from the collector.

---

# XCVIII. *The Potential Distribution across the Cathode Dark Space.* *By* W. L. Brown, *M.Sc., Demonstrator, and* E. E. Thomson, *M.Sc., Musgrave Demonstrator, Physics Department, Queen's University, Belfast* †.

[Plate XVII.]

## *Introduction.*

THE chief contributions to the study of the electrical conditions in the cathode dark space of the glow discharge have been those of Aston ‡, Brose §, and Geddes ‖.

* Marx, *Handb. d. Radiologie*, iv. 3, p. 299.
† Communicated by Dr. K. G. Emeléus, M.A.
‡ Aston, Proc. Roy. Soc. lxxxiv. p. 526 (1911).
§ Brose, *Ann. d. Phys.* lviii. p. 731 (1919).
‖ Geddes, Proc. Roy. Soc. Edinb. xlvi. 2, p. 136 (1925–26).

Aston determined the electric fields at different points along the dark space in a wide tube, by passing across it a beam of cathode rays from a subsidiary tube kept at very low pressure. The deflexion of the beam at different distances from the cathode was used as a basis for the calculation of the electric field. It was not possible to take measurements right up to the cathode, but over the region investigated it was found that the field at any point was proportional to its distance from the negative glow. This means that the space charge is constant throughout that part of the dark space considered. The tube voltages varied between 265 and 610 volts.

Brose, using high voltages, 1000 to 4000 volts, in discharge-tubes of narrow bore, and with gases at low pressures, found the distribution of the field by measurement of the Stark effect. In common with Aston, he found a positive space charge throughout the main part of the dark space, but his results indicate that this is not constant, and also that there is a negative space charge in the region near the cathode.

Geddes applied Aston's method to discharges at high voltages. His results were similar to those obtained by Aston.

Many attempts have been made to measure the potential distribution across the dark space by introducing a third electrode, and measuring by means of an electrometer the potential taken up by it. These methods fail chiefly on account of the differences in mobility and concentration of electrons and positive ions, which prevent the wire from taking up the potential of the surrounding space *.

It was intended, on beginning the work described in the present paper, to take current-voltage characteristics of a collector or third electrode inserted in the cathode dark space of the glow discharge, and to attempt the analysis of these characteristics by some modification of Langmuir's method †. Previous work on the glow discharge has been concerned with the negative glow, Faraday dark space, and positive column, in which the characteristics obtained can be analysed by this method. The form of the characteristics in the cathode dark space is quite different from that obtained in other parts of the discharge, and the

* *Vide, e. g.*, Emeléus, 'Conduction of Electricity through Gases,' p. 39.

† Langmuir and Mott-Smith, Gen. Elect. Rev. xxvii. p. 554 (1924).

interpretation of the curves is difficult. The chief difference between the dark space and the rest of the discharge is the high value of the field in the dark space, almost the whole fall of potential applied to the tube taking place across it.

The data obtained were plotted in different ways and the resulting curves examined. The relation V against log (c +const.) gives a straight line with a break at a voltage between that of anode and cathode. This voltage approaches that of the anode as the collector is moved nearer the negative glow. We compared the values of this potential with observations taken by the method to be described later, but although agreement was very close near the cathode, it became less exact as the collector approached the negative glow.

The characteristics proving unsatisfactory, we turned our attention to another phenomenon. That there is a shadow cast towards the cathode by an obstacle placed in the cathode dark space has long been known. However, so far as we are aware, the effect of applying a potential to the obstacle has not been investigated. We carried out a series of observations, using obstacles (or *collectors*), of different shapes. Metals were used for all electrodes.

The effect of using a large circular collector, 8 mm. in diameter, mounted parallel to a cathode 2·5 cm. in diameter was very striking. When the collector was insulated, there was a circular patch cut out of the cathode glow underneath, and of greater area than the collector, while there was a very small circular patch cut out of the negative glow. On reducing the potential of the collector relative to the cathode, the cathode patch diminished while that in the negative glow increased in size, passing through the intermediate stage when both were equal in area to the collector, to the condition in which there was a large patch cut out of the negative glow, while the cathode glow was almost undisturbed.

The results of observations, using as collector a wire, 0·4 mm. in diameter, mounted parallel to the cathode surface, may be summarised as follows :—

(*a*) The potential applied to the collector by an external battery, necessary to maintain the shadow towards the cathode in the same form as when the collector is insulated, is always near the anode potential.

The form of the shadow is shown in Pl. XVII. fig. 1. It will be seen that the shadow is much wider than the wire.

(*b*) If the applied potential is reduced, the width of the shadow decreases. When the shadow to the cathode side has the same width as the wire, another shadow has appeared on the anode side, also of the same width as the wire. This is shown in Pl. XVII. fig. 2.

(*c*) Further reduction of the applied potential leads to the complete disappearance of the shadow to the cathode side, while the shadow on the anode side increases in size.

(*d*) As the potential approaches that of the cathode, a bright layer appears on the cathode side of the wire, while on the anode side the shadow is almost parabolic, with a bright layer round the edges. (Pl. XVII. fig. 3.)

The photographs shown were obtained in argon, with a tube voltage of 470 volts; the potential of the wire relative to the cathode was 228 volts in Pl. XVII. fig. 2 and 62 volts in Pl. XVII. fig. 3. In Pl. XVII. fig. 1 the wire was insulated. The dark space was 1 cm. in width in all cases. The photographs have all been enlarged two diameters, and only a small part of the cathode is shown.

The above facts can be explained qualitatively by considering that the potential of the collector when the shadows thrown to the two sides of it are equal is the potential of the surrounding space. This is reasonable, because the disturbance of the discharge, caused by the presence of the collector, appears to be least at this potential. Apparently positive ions moving towards the cathode, and electrons moving towards the anode, in paths parallel to the axis of the tube, are not deflected. When the potential of the wire is near that of the cathode, *i. e.*, negative to the surrounding space, we should expect electrons moving towards the anode to be deflected away from the collector and positive ions moving towards the cathode to be deflected towards it, so that the discharge would be more concentrated than normal between collector and cathode, and less concentrated on the other side of the

wire. The converse would be true when the potential of the collector was near that of the anode.

From such considerations, we have concluded that the potential of the collector, when the shadows thrown to the two sides of it are equal in width, is the potential of the surrounding space, and we have used this as a basis for measuring the potential distribution across the cathode dark space.

### *Preliminary Observations.*

Before considering the experimental arrangements for carrying out measurements of potential, it is of interest to mention some observations made in connexion with the shadow thrown to the cathode side of the collector. It was found that if the collector were charged to some potential at which a shadow was cast towards the cathode, and the discharge left running for a considerable time, perhaps an hour, the part of the cathode in shadow became sharply defined by a curious bluish marking, bounded by sharp lines. A photograph of markings on an iron cathode surface, obtained in this way, using a molybdenum collector, is shown in Pl. XVII. fig. 4.

The marking obtained was more intense with longer exposure to the discharge, and with higher current densities. If the potential of the wire is changed after a marking has been formed, so that there is no longer a shadow on the cathode side, the marking will disappear after a time.

It is well known that the glass surrounding the cathode of a discharge-tube becomes sputtered after a time depending on the intensity of the discharge, and the cathode material. This is due to atoms of the metal being liberated from the cathode by the impact of positive ions and being deposited on the neighbouring glass surfaces. We may attribute the marking described above to the same cause. Atoms of metal pass temporarily into the discharge, and most of these are returned to the cathode, the remainder depositing on the tube walls. We suggest that those atoms which deposit on that part of the cathode in shadow tarnish the surface, while atoms returning to the bright part of the cathode are prevented from tarnishing it by the continual bombardment of positive ions. This explanation is borne out by the fact that the

marking disappears when the discharge is allowed to fall on it.

We should also point out here that Oliphant * has obtained disintegration of the cathode, due to metastable helium atoms.

The form of the markings produced by using different types of collectors was studied next. In every case the shape of the marking corresponded roughly with that of the collector, small obstacles giving the most sharply defined markings.

The sharp lines on the edges of the markings (Pl. XVII. fig. 4) might possibly be due to a kind of focussing effect. There will be a tendency for positive ions to move across the dark space more or less perpendicularly to the cathode, under the influence of the large electric field. The path will, of course, be zigzag, but the main direction will be normal to the cathode. A positive ion moving in this direction, and passing near the wire when it is charged positively to the space, will be deflected away from the wire. If the number of collisions is fairly large, the path of the ion will rapidly return to a direction parallel to the original direction, and the effect of the wire will be merely to displace the particle sideways. Other positive ions passing the wire at greater distances will be displaced less, and this will tend to lead to a sharp line of demarcation between the shadow and the normal discharge. If the number of collisions is not large, we should expect a more diffuse edge to the marking.

An interesting case studied was that of a wire introduced from a side tube, and bent so that its free end was furthest from the cathode. The marking produced on the cathode surface is shown in Pl. XVII. fig. 5. It will be observed that the marking is not parallel sided, as in Pl. XVII. fig. 4. but has a maximum width, diminishing to a point towards the free end of the wire. We should expect that the point where the marking is the same width as the wire corresponds to that point of the wire which has the same potential as the space surrounding it. Bearing in mind the facts mentioned in the Introduction, it is clear that the part of the wire nearest the negative glow may not cast any shadow at all.

On the cathode of Pl. XVII. fig. 5 the marking was

* Oliphant, Proc. Roy. Soc. cxxiv. p. 228 (1929).

brown, the collector in this case being of copper-clad nickel iron, and the cathode of iron. The potential of the collector relative to the cathode was 240 volts.

Wehnelt * and Villard † found that the cathode became tarnished with a film of oxide on that part of it *exposed* to the discharge. They put this down to the oxidizing action of positive rays. The part of the cathode in shadow remained bright, while the edges of the deposit were not sharp. The differences between their results and those considered above must be due to the fact that they worked

Fig. 1.

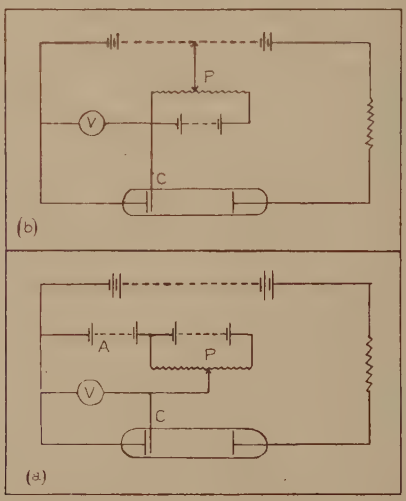


with an induction-coil discharge in air at low pressure, and a copper cathode.

### *Experimental Arrangements.*

The discharge-tube was run off a battery of small accumulators, capable of giving a maximum voltage of 660 volts. The first circuit used is shown in fig. 1. *a*. There was a wire resistance of 1100 ohms in series with the tube, to prevent the glow discharge from passing into an

* Wehnelt, *Ann. d. Phys.* lxvii. p. 421 (1899).
† Villard, *Comptes Rendus*, cxxvi. p. 1564 (1898).

arc. The potential applied to the collector C could be adjusted by varying the voltage of the battery A, and fine control was obtained by means of the potentiometer P, which had a maximum range of 60 volts. Voltages were read on the Weston high range voltmeter V. When taking current-voltage characteristics, Pye mirror galvanometers were brought into the circuit.

With this arrangement there was the difficulty that as the voltage available for the battery A was often less than half that of the main battery, there was a break in the series of readings when the voltage which was required for the collector was nearly half-way between anode and cathode potential. In order to avoid this, in some of the later work the battery A was abandoned, and the lead to it was taken to a plug, which could be connected to any desired point along the main battery (fig. 1, *b*). The potentiometer P was retained, and with this arrangement any voltage between anode and cathode potential could be applied to the collector.

The only possible objection to this arrangement was the fact that the tube and collector circuits were more closely coupled than when the first circuit was used. However, it was found that the results obtained with the two circuits showed no differences.

The discharge-tubes were exhausted by a Gaede steel mercury vapour pump, backed by a Hyvac pump. The tube section of the apparatus was cut off by a tap from the McLeod gauge and the pumps, and arrangements were made to introduce the different gases as required. Argon was purified by running an arc between calcium electrodes in a bulb sealed to the apparatus near the discharge-tube. For neon, this bulb was replaced by a liquid-air trap containing charcoal. The nitrogen used was generated by exploding sodium azide in a side reservoir, and was considered sufficiently pure without treatment. In all cases mercury vapour from the pump and the McLeod gauge, and hydrocarbon vapours from the taps, were kept out of the discharge-tube by means of liquid-air traps. Before making observations the discharge-tube and the glass-work near it were well baked by the gas flame for some hours. While observations were being made a liquid-air trap was always used.

These precautions allowed us to work with the gases in a fairly pure state. In the argon, after the calcium arc had

been running for several hours, no trace of nitrogen could be detected spectroscopically, although the Balmer lines of hydrogen were just visible. Both the neon and the argon showed a well marked primary dark space. The sample of neon used contained 2 per cent. of helium, other impurities being removed by the charcoal tube.

The discharge-tube, of soda glass, was 3 cm. in internal diameter. The cathode was a steel tube 4 cm. long, and fitted it fairly closely. The end of the steel tube was closed by a disk of iron or nickel, which acted as the cathode face. A small hole was drilled through this disk, as near the edge as possible, and through this was passed a thin glass rod, 4 cm. long; this rod carried the anode, which was made of light nickel sheet. The distance between the electrodes was therefore constant. The glass rod was so fine that it did not disturb the discharge appreciably.

The collector was a fine steel wire, 0·4 mm. in diameter, carried by a glass sheath which was introduced through a side tube. Steel was used as it was the only material at hand stiff enough to remain quite straight when supported only at one end.

The discharge-tube was set up with a slight tilt towards the cathode end of the tube. When a set of observations was being made, it was begun with the cathode as close to the collector as possible, so that after each reading had been taken, a slight tap on the tube caused the cathode to move a little farther from the collector. When a series of observations was completed the cathode could be brought back to its original position by means of an electromagnet. The distance between the cathode and the collector was measured with a travelling microscope, adjusted so that its axis was parallel to the collector.

### *Results.*

The observations of the potential at which the shadows on both sides of the wire were equal could be reproduced to within 5 volts throughout the dark space except near its cathode and negative glow boundaries, where the shadow on one side became so short that it was more difficult to determine the point of balance. This represents quite a high degree of accuracy when we consider that a wire 0·4 mm. in diameter placed in a field of 300 volts per cm.,

such as exists in the dark space, will be lying in a region across which there is a fall of potential of 12 volts.

When the collector approached close to the negative glow edge, it was found that not only did the shadows cast by the wire alter in form but the edge of the glow itself became somewhat distorted, as the potential applied to the wire was altered. However, in spite of this, no great difficulty was experienced in obtaining the balancing potential, since the glow assumed its normal outline when the shadows were balanced. By "normal outline," we refer to the contour of the glow before the collector was moved near.

Another point of some importance arises here. If the negative glow is not parallel to the cathode but presents a convex surface towards it, as is often the case at low voltages when the pressure is low, then we must consider that the equipotential surfaces across the section of the tube are curved also. In such cases the shadow cast by the wire will vary in width, and it is of importance to know the point of the wire for which we have balanced the shadows. On one occasion an accidental tap on the tube caused the glass sheath carrying the collector to move, so that its end passed into the path of the discharge. The shadow cast by it towards the cathode (it will be remembered that an insulated obstacle of any description casts a shadow towards the cathode) was wider than that cast by the wire when near the balancing potential. Although on the side of the tube remote from the eye, this shadow could be seen quite well in addition to that thrown by the wire. The shadow thrown by the glass may be seen in Pl. XVII. fig. 6.

In such cases the point of balance becomes rather indefinite, and the shadow of the same width as the wire seems to move along it as the potential is slightly altered; so that the shadows thrown by all parts of the wire influence the observer in deciding the balancing potential. That there is not any great deviation from plane equipotential surfaces in most cases, however, seems to be indicated by the parallelism of the marking on the cathode shown in Pl. XVII. fig. 4.

On completing a series of observations over the dark space by the shadow method, we usually estimated the space potential in the negative glow by moving the collector

into it and increasing the voltage applied until the electron current to the collector began to increase rapidly. Points on the curves which were thus obtained are marked with an L.

Data obtained with different gases under various conditions of pressure and voltage are given in Table I.

Fig. 2

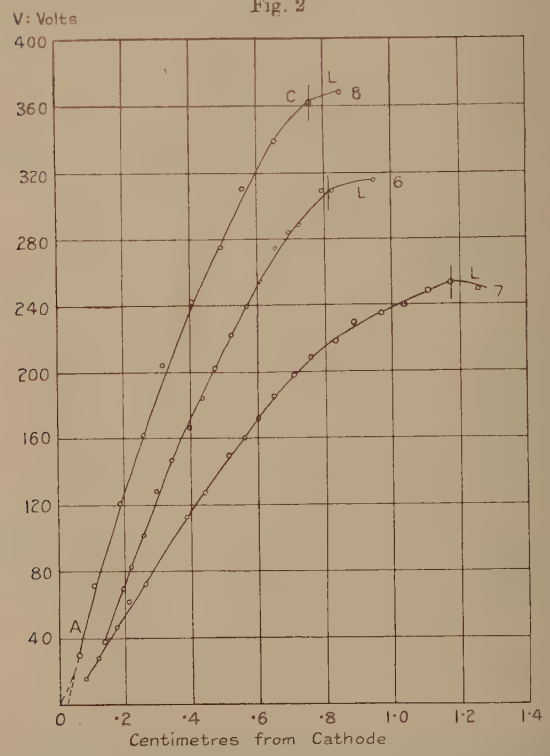


The vertical lines indicate the positions of the negative glow edge. Data for these curves will be found in Table I. Nos. 6, 7, and 8.

Some typical graphs drawn from these data are shown in figs. 2 and 3.

One of the curves in fig. 2 is lettered for the purpose of explanation. It rises smoothly to the point C, where the collector passes into the negative glow. The vertical line

through the curve indicates the position of the cathode edge of the negative glow. There is a break in the curve near its lower end, and the middle part, AC, when extrapolated, does not pass through the origin but cuts the axis at a distance of the order of half a millimetre from it. This initial part of the curve cannot be found accurately by the shadow method, as the cathode shadow here is so short; but the fact that AC does not pass through the

Fig. 3

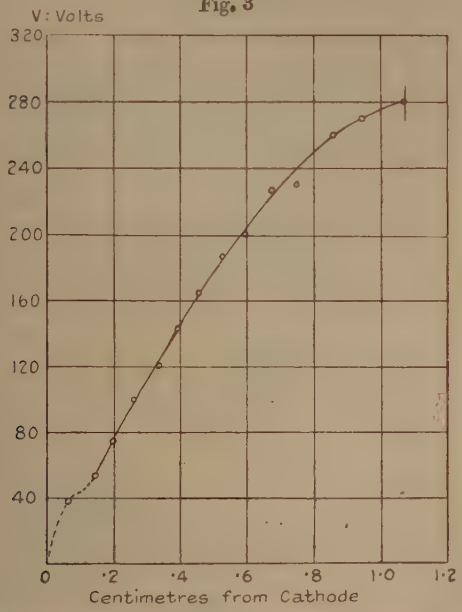


The vertical line indicates the position of the negative glow edge. Data for this curve will be found in Table I. No. 25.

origin confirms the supposition that there is a layer of negative space charge near the cathode surface, as shown by Brose's curves for strongly abnormal cathode fall, and that the effective cathode is the edge of this layer.

P. M. Morse * has recently given a comprehensive theory of the glow discharge, which is the most satisfactory yet proposed, and which it is desirable to test from these

* Morse, Phys. Rev. xxxi. p. 1003 (1928).

## Table I. a.

| No. | 5. | | 6. | | 7. | | 8. | | 9. | | 10. | | 11 | | 12. | |
|---|---|---|---|---|---|---|---|---|---|---|---|---|---|---|---|---|
| Tube Voltage. | 295 | | 314 | | 247·5 | | 373 | | 250 | | 300 | | 360 | | 410 | |
| C.D.S.† width. | ·9 cm. | | ·77 | | 1·16 | | ·74 | | ·98 | | 1·07 | | 1·07 | | 1·04 | |
| *x*. | V. | *x*. | V. | *x*. | V. | *x*. | V. | *x*. | V. | *x*. | V. | *x*. | V. | *x*. | V. |
| ·091 | 21 | ·137 | 38 | ·077 | 15 | ·061 | 50 | ·084 | 18 | ·066 | 27 | ·075 | 25·5 | ·100 | 38 |
| ·122 | 40 | ·197 | 70 | ·115 | 28 | ·106 | 72 | ·104 | 28·5 | ·090 | 40 | ·112 | 42 | ·170 | 78 |
| ·142 | 60 | ·217 | 83 | ·172 | 46·5 | ·186 | 121 | ·139 | 37·5 | ·120 | 47 | ·160 | 67·5 | ·225 | 116 |
| ·172 | 71 | ·257 | 102 | ·209 | 62 | ·256 | 162 | ·189 | 57 | ·146 | 60 | ·202 | 91·5 | ·295 | 159 |
| ·207 | 84 | ·297 | 128 | ·259 | 72·5 | ·316 | 204 | ·244 | 80·5 | ·188 | 76 | ·240 | 110 | ·365 | 195 |
| ·228 | 97 | ·342 | 147 | ·385 | 112·5 | ·406 | 242 | ·304 | 93 | ·218 | 90 | ·290 | 142·5 | ·445 | 225 |
| ·260 | 110 | ·397 | 166 | ·442 | 127 | ·496 | 275 | ·359 | 125 | ·244 | 104 | ·330 | 164 | ·495 | 249 |
| ·299 | 128 | ·437 | 184 | ·512 | 149 | ·561 | 310·5 | ·414 | 133 | ·275 | 117 | ·380 | 180 | ·560 | 281 |
| ·339 | 140 | ·472 | 202 | ·559 | 160 | ·656 | 339·5 | ·479 | 151·5 | ·303 | 129 | ·435 | 198 | ·620 | 304 |
| ·372 | 150 | ·522 | 222 | ·602 | 172 | ·761 | 362 | ·576 | 179 | ·338 | 144 | ·500 | 226 | ·675 | 313 |
| ·402 | 167 | ·567 | 239 | ·650 | 185 | ·85* | 369L | ·664 | 200 | ·361 | 150 | ·567 | 243 | ·735 | 332 |
| ·440 | 178 | ·612 | 254 | ·712 | 197·5 | | | ·819 | 228 | ·390 | 163 | ·640 | 265 | ·802 | 351 |
| ·455 | 190 | ·657 | 274 | ·762 | 208 | | | ·869 | 235 | ·433 | 177 | ·733 | 295 | ·855 | 369 |
| ·479 | 197 | ·697 | 284 | ·834 | 218 | | | ·929 | 243 | ·475 | 190 | ·830 | 317 | ·915 | 374 |
| ·550 | 220 | ·727 | 288 | ·890 | 229·5 | | | ·989 | 247·5 | ·502 | 201 | ·932 | 335 | ·975 | 394 |
| ·582 | 227 | ·797 | 309 | ·972 | 235 | | | 1·027 | 247·5 | ·564 | 215 | 1·020 | 353·5 | ·995 | 405 |
| ·600 | 239 | ·827 | 309 | 1·040 | 240 | | | 1·114 | 250 | ·625 | 235 | 1·400 | 358L | 1·095 | 406 |
| ·634 | 244 | ·955 | 314L | 1·112 | 248 | | | | | ·665 | 245 | | | | |
| ·692 | 261 | | | 1·160 | 253 | | | | | ·730 | 257 | | | | |
| ·722 | 263 | | | 1·25* | 248L | | | | | ·764 | 267 | | | | |
| ·782 | 283 | | | | | | | | | ·828 | 280 | | | | |
| ·826 | 287 | | | | | | | | | ·877 | 289 | | | | |
| ·882 | 291 | | | | | | | | | ·926 | 302 | | | | |
| | | | | | | | | | | ·975 | 306 | | | | |
| | | | | | | | | | | 1·069 | 308 | | | | |
| | | | | | | | | | | 1·22* | 298L | | | | |

*x* is the distance from the cathode in centimetres : V is the space potential in volts.

* These positions are approximate. L indicates that the value was obtained by Langmuir's method.

† The values for the width of the cathode dark space are necessarily approximate. Runs : 5–12 Argon.

TABLE I. B.

| No. | 17. | | 18. | | 19. | | 20. | | 21. | | 24. | | 25. | | 27. | |
|---|---|---|---|---|---|---|---|---|---|---|---|---|---|---|---|---|
| Tube Voltage. | 525 | | 460 | | 566 | | 225 | | 270 | | 372 | | 285 | | 314 | |
| C.D.S.† width. | 1·40 | | 1·55 | | 1·46 | | ·90 | | ·77 | | ·80 | | 1·05 | | ·93 | |
| | *x*. | V. | *x*. | V. | *x*. | V. | *x*. | V. | *x*. | V. | *x*. | V. | *x*. | V. | *x*. | V. |
| | ·050 | 30 | ·135 | 37 | ·065 | 14 | ·052 | 30 | ·075 | 60 | ·070 | 60 | ·065 | 39 | ·095 | 60 |
| | ·090 | 45 | ·190 | 70 | ·115 | 37 | ·087 | 48 | ·150 | 75 | ·130 | 81 | ·146 | 54 | ·165 | 75 |
| | ·130 | 75 | ·250 | 100 | ·170 | 67 | ·142 | 55 | ·210 | 98 | ·200 | 120 | ·201 | 75 | ·235 | 98 |
| | ·200 | 120 | ·310 | 128 | ·240 | 112 | ·200 | 75 | ·280 | 127 | ·257 | 150 | ·260 | 100 | ·311 | 135 |
| | ·275 | 157 | ·380 | 150 | ·305 | 163 | ·249 | 90 | ·360 | 150 | ·308 | 180 | ·335 | 120 | ·386 | 165 |
| | ·350 | 195 | ·460 | 180 | ·370 | 195 | ·332 | 110 | ·430 | 180 | ·354 | 202 | ·390 | 143 | ·448 | 186 |
| | ·535 | 280 | ·530 | 200 | ·450 | 228 | ·402 | 124 | ·530 | 200 | ·437 | 237 | ·453 | 165 | ·524 | 210 |
| | ·590 | 300 | ·630 | 228 | ·530 | 266 | ·432 | 135 | ·620 | 220 | ·495 | 265 | ·525 | 187 | ·575 | 230 |
| | ·675 | 330 | ·695 | 248 | ·620 | 295 | ·490 | 157 | ·686 | 233 | ·557 | 288 | ·595 | 200 | ·654 | 250 |
| | ·740 | 350 | ·765 | 270 | ·740 | 345 | ·590 | 165 | ·710 | 246 | ·620 | 315 | ·675 | 227 | ·712 | 270 |
| | ·840 | 380 | ·860 | 300 | ·860 | 385 | ·700 | 180 | ·775 | 255 | ·690 | 330 | ·752 | 230 | ·781 | 280 |
| | ·900 | 405 | ·920 | 328 | ·980 | 420 | ·780 | 198 | ·925 | 270 | ·735 | 345 | ·860 | 260 | ·860 | 300 |
| | 1·025 | 435 | 1·010 | 345 | 1·110 | 458 | ? ·768 | 210 | | | ·801 | 355 | ·945 | 270 | ·933 | 305 |
| | 1·086 | 457 | 1·100 | 360 | 1·250 | 505 | 1·030 | 210 | | | ·935 | 370 | 1·070 | 280 | | |
| | 1·135 | 467 | 1·175 | 374 | 1·375 | 535 | | | | | | | | | | |
| | 1·200 | 480 | 1·300 | 390 | 1·460 | 564 | | | | | | | | | | |
| | 1·235 | 488 | 1·370 | 400 | | | | | | | | | | | | |
| | 1·270 | 495 | 1·470 | 412 | | | | | | | | | | | | |
| | ?1·331 | 543 | | | | | | | | | | | | | | |

*x* is the distance from the cathode in centimetres : V is the space potential in volts.

† The values for the width of the cathode dark space are necessarily approximate.

Runs: 17–19 Nitrogen.
20–27 Neon.

data. Starting from Poisson's equation, and making use of Townsend's relation,

$$a = pNe^{-pNv/E} \quad . \quad . \quad . \quad . \quad . \quad . \quad (1)$$

he arrived at the equation

$$V = 4D(1-c) - 4D(1-c)e^{-2pNx^3} + 8DN(1-c)E_a px/3. \quad (2)$$

for the fall of potential across the cathode dark space.

In the above equations :

$a$ = the number of ions formed per cm. of path by an electron moving under a field E,

$p$ = pressure of gas,

$1/(1-c)$ = fraction of total discharge current carried by positive ions.

$v$ = ionization potential of the gas,

V = space potential at any distance $x$ from cathode,

D = diffusion coefficient,

$E_a$ = a constant.

Morse also gives the relation,

$$4D(1-c) = V' \text{ approximately}, \quad . \quad . \quad . \quad . \quad (3)$$

where V′ is the normal cathode fall of potential.

From (2) and (3),

$$V = V'(1 - e^{-2pNx/3} + 2NE_a px/3).$$

which may be written

$$V = V'(1 - e^{-kpx} + Kpx) \quad . \quad . \quad . \quad . \quad . \quad (4)$$

where $k = 2N/3$, and $K = kE_a$.

Hence,

$$S/V' = kpe^{-kpx} + Kp \quad . \quad . \quad . \quad . \quad . \quad (5)$$

where $S = dV/dx$.

When $x = 0$,

$$S/pV' = k + K = \sigma. \quad . \quad . \quad . \quad . \quad . \quad (6)$$

In the analysis of our curves on this basis, the main part of the experimental curve AC (fig. 2) has been extrapolated to cut the axis, and the point of section taken to be the effective cathode ($x = 0$). The slope of the tangent drawn at this point gives a value of S. By substituting this value in equation (6), the value of $k + K$ is found, $p$ and V′ being known.

Putting $V = V'$ in equation (4), we have

$$e^{-kpx} = Kpx.$$

The value of $x$ for $V = V'$ is found from the experimental curve and substituted in this equation. The values of $k$ and K can then be found, either by trial or graphically, by drawing the curve

$$\eta = \xi + e^{-\xi}, \text{ where } \eta = \sigma px \text{ and } \xi = kpx,$$

Fig. 4.

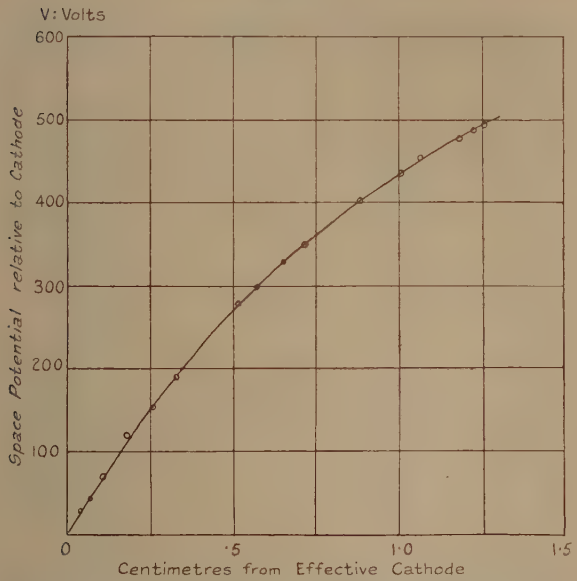


The distance between cathode and effective cathode is 0·02 cm.
The data for this curve will be found in Tables I. and II. No. 17.

$\sigma\ px$ is known, and so from the graph we can get $kpx$ and hence $k$. The values of k, K, V′, and $p$ are now all known, and are substituted in equation (4), and the curve of V against $x$ computed and drawn.

Owing to the nature of Morse's equation, involving as it does three terms including an exponential, there is some latitude in choosing the value of V′ (see below), and of course $k$ and K vary in consequence. This, taken in conjunction with the difficulty of drawing a tangent at the

effective cathode, rendered it necessary to test the values obtained in each case, by drawing the theoretical and experimental curves. If the agreement was not satisfactory the values were recalculated. In all cases excellent agreement was finally obtained between the calculated curve and the experimental points. One of the curves is shown in fig. 4, where the line is the computed curve, and the dots are the experimental values.

TABLE II.

| No. | V'. | $k$. | K. | $p$. | $E_a$. | Gas. |
|---|---|---|---|---|---|---|
| 5 | 270 | 15·6 | 4·5 | ·107 | ·288 | Argon. |
| 6 | 290 | 15·9 | 4·7 | „ | ·295 | |
| 7 | 227 | 14·0 | 3·3 | „ | ·235 | |
| 8 | 340 | 16·0 | 4·6 | „ | ·285 | |
| 9 | 230 | 26·3 | 7·7 | ·055 | ·293 | |
| 10 | 275 | 28·7 | 7·0 | „ | ·243 | |
| 11 | 330 | 34·0 | 4·5 | „ | ·132 | |
| 12 | 376 | 33·4 | 4·46 | „ | ·133 | |
| 17 | 480 | 48·8 | 7·3 | ·026 | ·149 | Nitrogen. |
| 18 | 385 | 46·4 | 7·6 | „ | ·163 | |
| 19 | 515 | 41·9 | 8·1 | „ | ·193 | |
| 20 | 206 | 17·1 | 1·14 | ·123 | ·067 | Neon. |
| 21 | 248 | 15·9 | 2·5 | „ | ·156 | |
| 24 | 341 | 22·5 | 5·4 | ·074 | ·239 | |
| 25 | 261 | 20·7 | 4·3 | „ | ·207 | |
| 27 | 288 | 21·7 | 4·5 | „ | ·206 | |

V' is in volts and $p$ in centimetres of mercury.

The cathode fall of potential can therefore be represented by Morse's equation between the effective cathode and the negative glow. At the cathode edge of the glow the equation breaks down *.

When several of the potential-distance curves for a given pressure and gas are drawn on the same scale, we find that,

* Morse gives the value of the field at the point of breakdown as $V'kp$. This is incorrect, as it involves the assumption that at the end of the dark space $e^{-kpx}$ is negligible, which we know (Table II.) is not the case.

as we should expect, the field at the end of the dark space decreases as the tube voltage decreases, the point of breakdown of the dark space curve on passing into the negative glow becoming less sharp as the cathode fall of potential approaches the normal fall for the material of the cathode (see, for example, fig. 2).

The values found for the quantities in the equation are given in Table II.

In the table the pressure $p$ is in centimetres of mercury and V′ in volts.

V′ is not the normal fall of potential, as it was found that the normal fall was too low to admit of the equation fitting the curves. The value used was 11/12 of the voltage across the tube, which was less than the actual fall across the cathode dark space as shown by Langmuir characteristics taken in the negative glow, but was greater than the normal cathode fall in all cases except those at very low voltage. The fraction 11/12 was found by trial to be a suitable value.

## *Discussion.*

From Table II. it may be seen that $k$ is nearly constant for a given gas at a fixed pressure. Beyond this there is nothing definite, but there are two possibilities. The first is that $kp$ is a constant for a given gas. For runs 5–8, $kp$ has an average value of 1·65, while for runs 9–12 the average value is 1·68. In nitrogen the average value of $kp$ is 1·19. The values of $k$ in neon, however, change very little with pressure.

The second possibility is that $k$ is nearly constant for a given gas, and almost independent of pressure. In this case we should have to assume that some impurity got into the gas when the pressure was changed between runs 8 and 9. It is highly probable that neither of the above suggestions is strictly true, but that, as is indicated below, $k$ is influenced considerably by both pressure and the degree of purity of the gas.

Since $k$ is nearly constant, the value of N ($=3k/2$) is also nearly constant for a given gas at a fixed pressure. According to Townsend, N is the number of ionizing collisions made by an electron per centimetre of path, in a field of 1 volt per cm., the pressure being 1 mm. of mercury. Since it is known that pressure influences the rate of

removal of excited atoms, we might expect some variation from Townsend's values *. N is also dependent on the purity of the gas.

The observed values of N, expressed in Townsend's units, are of the same order of magnitude as those given by him. Values for different gases are given in the following table :—

TABLE III.

| Gas. | Argon. | Nitrogen. | Neon. | Helium. |
|---|---|---|---|---|
| Townsend's value of N ... | 13·6 | 12·4 | — | 2·8 |
| Observed value of N ..... | 3·4 | 6·8 | 2·9 | — |

Observed values of N were obtained from average values of $k$ in Table II.

Townsend does not give a value for neon, but the value he gives for helium is close to that found for neon. Considering also that we measure the density of the gas only indirectly by means of the pressure, the agreement in this table is good evidence in favour of Morse's theory.

The value of K shows little regularity and is not of obvious theoretical significance. Its value is always considerably less than that of $k$, their ratio being roughly as 1 : 5. $E_a$ therefore does not vary a great deal from 0·21.

The total space charge per sq. cm. between two layers parallel to the cathode surface whose distance apart is $(a-b)$ can be determined from Poisson's equation.

Since

$$\frac{d^2V}{dx^2} = -4\pi\rho,$$

we have

$$\left[\frac{dV}{dx}\right]_b^a = -4\pi\int_b^a \rho.dx = \left(\frac{dV}{dx}\right)_a - \left(\frac{dV}{dx}\right)_b,$$

and therefore

$$\int_b^a \rho.dx = \frac{1}{4\pi}\left[\left(\frac{dV}{dx}\right)_b - \left(\frac{dV}{dx}\right)_a\right].$$

If we measure the slope of the potential-distance curve at two points distant $a$ and $b$ respectively from the cathode,

* Townsend, 'Electricity in Gases,' p. 295 (1915).

we can determine the mean space charge per c.c. between these points. The slope can be determined either from Morse's equation by differentiating and substituting the appropriate constants obtained from our experimental data, or directly by drawing a tangent to the experimental curve.

Referring again to figs. 2 and 3, it is evident that we can do no more than suggest the form of the curve between the cathode and the experimental points. For this reason it is impossible to measure the total space charge between the cathode and the negative glow, although the variation of space charge from the beginning of the experimental curve to the negative glow can be studied.

TABLE IV.

| | | | | | | | | | | |
|---|---|---|---|---|---|---|---|---|---|---|
| No. 5... | $x$ ..... | ·1 | ·2 | ·3 | ·4 | ·5 | ·6 | ·7 | | |
| | E..... | 510 | 454 | 402 | 362 | 324 | 294 | 270 | | |
| | $\rho$ ..... | ·169 | ·143 | ·121 | ·102 | ·087 | ·073 | ·062 | | |
| No. 11... | $x$ ..... | ·1 | ·2 | ·3 | ·4 | ·5 | ·6 | ·7 | ·8 | ·9 |
| | E..... | 594 | 508 | 436 | 373 | 323 | 284 | 247 | 221 | 198 |
| | $\rho$ ..... | ·254 | ·210 | ·175 | ·145 | ·120 | ·100 | ·083 | ·069 | ·057 |
| No. 17... | $x$ ..... | ·1 | ·3 | ·5 | ·7 | ·9 | 1·1 | 1·3 | | |
| | E..... | 629 | 509 | 413 | 341 | 283 | 240 | 206 | | |
| | $\rho$ ..... | ·181 | ·140 | ·109 | ·084 | ·065 | ·051 | ·039 | | |
| No. 21... | $x$ ..... | ·1 | ·2 | ·3 | ·4 | ·5 | ·6 | ·7 | ·8 | ·9 |
| | E..... | 476 | 404 | 347 | 300 | 258 | 226 | 201 | 179 | 161 |
| | $\rho$ ..... | ·164 | ·135 | ·111 | ·091 | ·075 | ·062 | ·051 | ·042 | ·034 |

$x$ is in centimetres. E in volts per cm. $\rho$ in e.s.u. per c.c.

From Morse's equation we have, by differentiating,

$$\mathrm{E}=\frac{d\mathrm{V}}{dx}=\mathrm{V}'(kpe^{-kpx}+\mathrm{K}p) \quad . \quad . \quad . \quad . \quad (5)$$

and

$$-4\pi\rho=\frac{d^2\mathrm{V}}{dx^2}=-\mathrm{V}'k^2p^2e^{-kpx}.$$

When the appropriate values of V′, $k$, K, and $p$ are substituted in the above equations, we can draw up a table showing the variation of field and space charge as $x$ is increased. Such a table of values obtained from the data for several of the given curves is shown in Table IV.

Values of field obtained by measuring a series of slopes on the experimental curve for run 17 are plotted against the distance from the cathode in fig. 5 *a*. In the same figure, curve (*b*) shows the corresponding space charge distance curve, the data for which were obtained by measuring the slopes at different points on curve (*a*). Leaving out of consideration the region between cathode and effective cathode, it will be observed that the field has its maximum value a short distance out from the

Fig. 5.

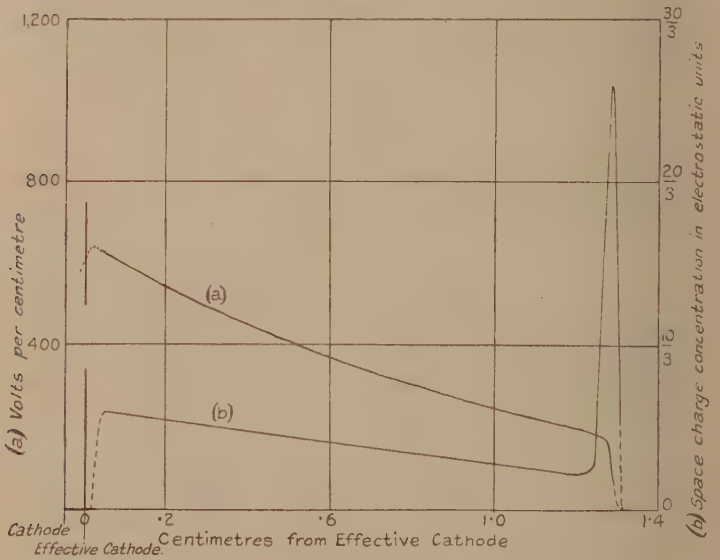


cathode, and falls gradually to less than one-third of this value at the cathode edge of the negative glow, when it drops rapidly to zero in the negative glow. Curve (*b*) indicates that the positive space charge concentration prevailing throughout the greater part of the dark space decreases almost uniformly to less than half its initial value between the effective cathode and the negative glow edge. Between this point and the middle of the negative glow the positive space charge varies rapidly, at first increasing to from 4 to 6 times its average value over the dark space, and then falling to zero.

Regarding the space between the cathode and the effective cathode, it is evident that there must be at least one point of inflexion on the potential distance curve; that is, the space charge curve must pass through zero. This is indicated by the dotted line. There may, of course, be two points of inflexion, giving a positive space charge on the cathode surface, with a negative space charge farther out, and then the main dark space. This is discussed later.

The sudden change in space charge concentration in curve (*b*) marks the point where Morse's equation ceases to hold. It is impossible to mark off the boundaries of this layer of high positive space charge accurately in many cases since the point where the curve turns over to run parallel to the distance axis is not very definite. The average estimated thickness of the layer is 1 mm., while the space charge concentration in it is approximately three times the mean space charge over the region to which the equation is applicable.

Miss N. M. Carmichael * in some recent work in this laboratory, has shown that on the cathode side of the negative glow maximum, and between it and the feeble luminosity in the cathode dark space, there exists a dark layer. This dark space has not yet been observed in any gas other than oxygen. Voltage-current characteristics taken near this dark space show a change in form as the collector is moved through it. It is probable that if a similar dark space should subsequently be found in other gases, it will correspond in position to the breakdown of the cathode dark space potential-distance curve.

Emeléus and Carmichael † have given reasons for supposing that there is a positive space charge on the cathode surface. Now a positive space charge is indicated when the potential distance curve is concave to the distance axis. If this is so, consideration of the curves for argon in fig. 2 shows that the curve between the cathode and the experimental points should have two points of inflexion. All the curves drawn from the observations in neon, of which fig. 3 is an example, show at least one point, that nearest the cathode, which does not lie on the smooth line through the others.

* Carmichael, Phil. Mag. viii. p. 362 (1929).
† Emeléus and Carmichael, Phil. Mag. v. p. 1039 (1928).

The dotted lines in figs. 2 and 3 show the most obvious ways of drawing the curves between the cathode and the experimental points, taking into consideration only the actual distribution of the points themselves. At first sight it would appear that the observations in neon would justify us in drawing the initial parts of the curves in such a way as to be in accord with the idea of a positive space charge immediately in front of the cathode surface. The absence of a corresponding point in argon and nitrogen would, however, be difficult to account for.

Again, when we consider the difficulty of making an observation of balancing potential close up to the cathode surface, a task which, while troublesome in all cases, is especially so in the case of neon, in which a primary dark space is visible (for example, Pl. XVII. fig. 6), we are inclined to attribute the position of the first point to an experimental error. The presence of the primary dark space means that the shadow to the cathode side of the collector is shorter by the width of the dark layer, with the result that the first reliable reading, other things being equal, is somewhat farther from the cathode in cases where a primary dark space is visible. On the other hand, the point always appears on the same side of the main curve, seeming to indicate that any experimental error in determining its position is not of great account.

Taking into account all these facts, we do not think our results in this region afford decisive evidence either for or against the existence of a positive space charge on the cathode surface.

The presence of a layer or layers of space charge near the cathode surface must almost certainly be associated in some way with the production of the Aston or primary dark space. From the fact that the effective cathode had to be taken at some distance out from the cathode in most cases, whether a primary dark space was present or not, we think we are justified in supposing that some, at least, of the conditions necessary for the production of a primary dark space must obtain in all glow discharges. Provided that a similar argument holds in the case of the dark space near the negative glow, it appears that the potential-distance curve can be expressed in the form of the equation given by Morse, if we consider only that part of the cathode dark space proper lying between these two more intensely dark regions. The effective cathode is not, however, at

the cathode potential, and so there must be some modification of the curve in the transition region between the primary dark space and the main dark space.

The sheath surrounding the collector in neon is very interesting, as it is the first indication we have had of anything resembling the ordinary positive ion sheath in the cathode dark space. The characteristic curve affords no evidence either for or against the existence of a positive ion sheath round a collector in the dark space, for, although the curve obtained at potentials negative to that of the surrounding space has a form compatible with the presence of such a sheath, we know that the grid characteristic of a valve, in which the grid is not limited in its influence by a positive ion sheath, has a similar form. A photograph taken in neon, when the collector potential was negative to the surrounding space, is shown in Pl. XVII. fig. 6. A further investigation of sheath formation in the dark space is contemplated.

To summarize our results: by means of the shadow method, a continuous distribution of potential has been found from close upon the cathode to the negative glow. This in itself is important, as we do not have to account for an anomalous distribution of potential of the type of the "Kathodensprung" either near the cathode or at the boundary between the cathode dark space and the negative glow, where our curve passes continuously into the Langmuir curve of potentials for the negative glow itself. Although, as indicated previously, there is some latitude in the choice of the values of V′, $k$, and K in Morse's equation, yet the agreement of the values of N with those obtained by Townsend is strong evidence in support both of the substantial accuracy of Morse's theory of the dark space and of our methods of observation. Nevertheless, owing to the complex nature of the problem of the cathode dark space, we have thought it best to give in detail a large part of the data obtained, so that, should any further theory be worked out, a preliminary test will be available.

## *Summary.*

1. Details are given of some markings observed on the cathode when an obstacle, or collector, is placed in the cathode dark space.

2. A new method of determining space potentials in the cathode dark space is put forward, based on the behaviour of shadows thrown by a wire inserted in it. Values of the potential obtained in the dark space by this method and in the negative glow by Langmuir's method give a continuous curve from near the cathode potential right into the negative glow, for cathode falls in potential between 220 volts and 560 volts.

3. The results obtained conform to a theoretical expression given by P. M. Morse, connecting space-potential and distance from the cathode, provided we measure distance from an "effective cathode," about half a millimetre from the cathode surface, and choose suitable constants.

4. The constants in Morse's equation involve N, the number of ionizing collisions of an electron per centimetre of path under given conditions. Values of N obtained from our data are shown to be of the same order as Townsend's values.

5. Space-charge and electric field conditions over the dark space are discussed.

We are indebted to Dr. K. G. Emeléus for suggestions made during the course of the investigation, and for help in the preparation of this paper.

## *Key to Plate* XVII.

Figs. 1–3 show the form of shadows thrown by a wire inserted in the cathode dark space of the glow discharge and charged to different potentials.

The photographs were obtained with argon, with a tube voltage of 470; the potential of the wire relative to the cathode was 228 volts in fig. 2 and 62 volts in fig. 3. In fig. 1 the wire was insulated. The dark space was 1 cm. in width. The photographs have been enlarged two diameters and only a small part of the cathode is shown.

Figs. 4 and 5 show markings produced on that part of the cathode in shadow. In fig. 4 the molybdenum wire causing the shadow was parallel to the cathode surface and at a distance from it of 0·48 cm. The cathode dark space was 0·7 cm. in width. The wire was charged to a potential 380 volts positive to the cathode, while the tube voltage was 440 volts. The diameter of the wire was 0·01 cm. and the width of the marking 0·11 cm.

In fig. 5 the wire was of copper-clad nickel-iron and was inclined to the cathode surface at an angle of 30°. The potential applied to the wire was 240 volts, while the tube voltage was 490.

Fig. 6 shows a bright sheath round the wire formed when its potential was negative to the surrounding space. The discharge in this case was in neon and shows a well-marked primary dark space.

# XCIX. *Problems of determining Initial and Maximum Stresse in Ties and Struts under Elastic or Rigid End Constraints*

*By* W. H. Brooks, *B.Sc., Ph.D.(Eng.) Lond.**

## *Introduction.*

IN practice it may often be very desirable to know the minimum and maximum stresses to which any particular tie or strut may be subjected when forming part of a given structure and consequently stressed by irremovable dead loads.

The stresses taken in designing the tension and compression members of many framed structures are commonly based upon the assumptions of pin-jointed ends and negligible deformation of the configuration of the structure when loaded, but faulty workmanship, coupling adjustment, or a slight alteration or configuration, due to the loads or to the subsidence of a support, may set up stresses only determinate by direct experiment, and in extreme cases of subsidence, even reversals of stresses in certain members may result.

Methods for determining the stresses in thin wires and slight swaged rods—as the bracing wires and raf-wires of aeroplanes—are known [1] to [6], but the application is limited to members whose transverse dimensions are small as compared with their lengths. Instruments are in use [7] to [10] which are applicable to members of larger cross-sectional area; but these indicate only incremental stresses by the direct measurements of strains in the usual cases where the initial loads cannot be reduced to zero, which fact often appears to be overlooked.

The objects of the author are (*a*) to show how, by using any suitable one of the three methods introduced later, it is possible to find the stress (due to irremovable loading) existing in a tie or strut of uniform cross-section having its ends constrained by hinges or clamps; (*b*) to indicate by Stress Charts how most of the equations established may be readily solved; and (*c*) to experimentally verify some of the cases discussed.

The following methods are confined to the determination of initial direct stress, set up by a longitudinal end load $P$,

* Communicated by the Author. Section of Thesis approved for the Degree of Doctor of Philosophy in the University of London. (Copies of the complete Thesis are deposited in the University Library, South Kensington.)

to which—at any particular cross-section—would be added any secondary bending stresses due to lateral loading or to eccentricity of end load, both of which may co-exist with P. Methods for calculating such secondary stresses are fully discussed in standard books on materials.

The direct stress $f_d$ at any section $= \frac{P}{A}$, where A is the cross-sectional area, and $f_d$ will have its minimum or maximum values according as P has its initial and lowest value $P_a$ or its highest value when increased by incremental temporary loading ;

$$i.e.,\ f_d \text{ min.} = \frac{P}{A},$$

$$f_d \text{ max.} = (P_a + \text{incremental P})/A.$$

In this latter expression the magnitude of the second term may be determined by the strain gauges in use ; hence, when $P_a$ is known, $f_d$ max. is also known. Alternatively, $f_d$ max. may be found direct by the application of one of the following methods to the member under maximum load conditions.

### *Principles and Preliminary Argument.*

The underlying principles herein involved in the determination of these direct stresses are briefly as follows :—

The member, whether tie or strut, is very slightly flexed by the temporary application of either lateral known forces or known couples of magnitude sufficient to give the smallest deflexions or slopes that can be accurately measured. The test readings taken are then treated as described under "General Procedure."

These deflexion and slope effects are known to be proportional to the disturbing causes in the isolated cases of members having their ends either simply supported or *encastré* with no end load. They are also proportional—as will be seen from the equations established later—when the end load remains of constant magnitude during the flexing of the member. When, however, the end loads are applied through strong end constraints, the process of flexing may be expected to result in altered reactions of the constraints with consequent alteration of the direct stress induced in the member, and, if the initial end load is large (in the case of a tie it may be many multiples of the crippling load for the

same member when used as a strut), this effect may be apparent for comparatively very small deflexions.

Consider a tie A, B under initial tension $= P_a$ (fig. 1), caused by the reaction of elastic end constraints, for which the springs A, C and B, D are simple substitutes. C and D are at a fixed distance apart. When a slight flexing is given to A, B, as shown exaggerated in fig. 2, the effect will be a reduction of the original length to, say, $(l - \delta l)$, so forcing the springs to slightly elongate, and thereby increasing $P_a$ to, say, $P_a + \delta P = P$ in fig. 2.

Thus, in the case of a tie under end loads applied through elastic constraints, the effect of flexing is increased tension. Conversely, in the case of a strut, the effect of flexing is reduction in compression, as may readily be seen by replacing A, C and B, D by compression springs.

Fig. 1.

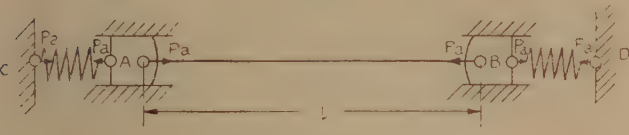


Fig. 2.

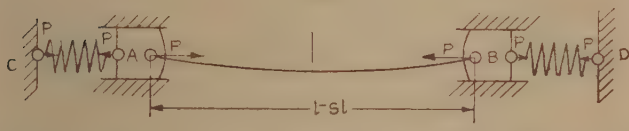


In the case of a tie or strut having its ends fixed by rigid constraints, the flexed axis length is greater than the length ($l$) of the unflexed axis, and, assuming the yield of the end clamps to be negligible, it may be shown that the longitudinal strain of the flexed axis is *increased* by

$$\frac{1}{2l}\int_0^l \left(\frac{dy}{dx}\right)^2 dx,$$

with consequent *increase* in the *tension*, or *decrease* in *compression*, according to whether the member is a tie or a strut:

$$= \frac{EA}{2l}\int^l \left(\frac{dy}{dx}\right)^2 dx,$$

where the symbols have their usual meaning, and the origin is taken at one end of the member.

In all cases it should therefore be assumed at the outset that, directly a member is flexed, the initial end load will be altered in some unknown varying manner, and the problem is to find the magnitude of the initial load that exists before any temporary alteration is induced by flexing.

*General Procedure and Further Argument.*

The general experimental procedure is as follows:—A few values of either the disturbing force or the disturbing couple are chosen as independent variables "X," and the corresponding values of "Y," either of the deflexion or of the slope at a particular point, are experimentally determined, tabulated, and plotted, as indicated by the curve B, $B_1$ in fig. 3.

Fig. 3.

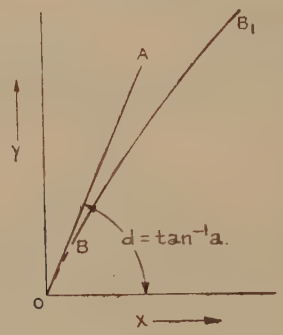


Now the ratio $\frac{Y}{X}$, established in each of the various cases dealt with later, is a function of the end load P (assumed variable with flexure), and holds for all values of P.

When the initial value of $P = P_a$ required, $Y = 0$ and $X = 0$; or the initial magnitude of the ratio $\frac{Y}{X} = \frac{0}{0}$, and is a definite value = "$a$," say, for each set of conditions.

The value of "$a$" is given by the slope of the curve B, $B_1$ when extended backward to the origin, as shown by the broken line in fig. 3; *i.e.*, "$a$" = $\tan \widehat{AOX}$, and may be calculated from the curve B, $B_1$ or approximately determined graphically.

Having determined this value of "$a$"—*which hereinafter*

*will for each case treated be referred to as "the initial derivative of the* X, Y *graph," or more shortly as "the* X, Y *derivative,"*—it is substituted for $\frac{Y}{X}$ in the equation for the particular method used, and the equation is then solved for $P_a$ by approximation or by graph. (For graphical solution methods, see Stress Charts later.)

For example, in the case of a tie with pinned ends flexed centrally through distance $\delta$ by a central load W (as dealt with in case A and illustrated in fig. 4, *quod vide*), the general equation is

$$Y/X=(L-\tanh nL/n)/2P$$

and "$a$" $=(L-\frac{1}{n_a}\tanh n_aL_a)/2P_a$. (*Tie equation* $A_5$.)

Fig. 4.


To facilitate its solution by Stress Chart I., this equation is written

$$2Pa=L-\tanh nL/n,$$

the suffix (small $a$) being suppressed for simplicity.

In the equations, $P_a$ is expressed for simplification in terms of

$$n_a=\sqrt{P_a/EI},$$

where EI is the flexural rigidity of the member at right angles to the plane of flexing, and should be made the smaller possible value if the member be not of circular cross-section.

Thus $P_a$ required $=n^2{}_aEI$, and during bending $P=n^2EI$, where $P \gtrless P_a$ according as the member is a tie or a strut.

### *To determine Expressions for* Y/X *for Ties flexed by various Methods.*

*Method* 1 A :—

Consider a straight uniform tie A, B of length $2L_a$ pin-jointed at the ends and strained by an initial end load $P_a$.

When a concentrated lateral load W is applied at mid-span to produce a small deflexion in a transverse direction, assume $P_a$ to be increased by elastic constraints at A and B to a value P, and the unflexed span to be slightly decreased to 2L, as shown in fig. 4.

Taking an origin O at mid-span on the line of action of P, and considering the deflexion $y$ at $+x$ from O as negative, and therefore the bending moment for the curvature shown as of positive sign [11],

$$M_x = W(L-x)/2 + Py = EI\frac{dy^2}{dx^2}, \quad . \quad . \quad . \quad (1)$$

where the symbols have their usual meaning.

Let $$P/EI = n^2.$$

Then $$d^2y/dx^2 - n^2y = WL/2EI - Wx/2EI. \quad . \quad . \quad (2)$$

The general solution to equation (2) is

$$y = A\cosh nx + B\sinh nx + Wx/2P - WL/2P. \quad . \quad (3)$$

From equation (3) it follows that

$$\delta \text{ max. at } C = W(L - \frac{1}{n}\tanh nL)/2P \text{ as measured} \quad . \quad (4)$$

or $$\delta/W = (L - \frac{1}{n}\tanh nL)/2n^2EI \quad . \quad . \quad . \quad . \quad (5)$$

Here $\delta = Y$ and $W = X$ referred to in the "General Procedure."

Thus initially, when $\delta = 0$ and $W = 0$, equation (5) becomes

$$0/0 = a = L_a - \frac{1}{n_a}\tanh n_aL_a)/2n_a^2EI. \quad (\textit{Tie equation } A_\delta.)$$

(where $L_a$ is the initial unflexed half-length),

or $$2n_a^2EI \,.\, a \,. = L_a - \frac{1}{n_a}\tanh n_aL_a). \quad . \quad . \quad . \quad (6)$$

Equation (6) when solved for $n_a$ by trial or graph yields $P_a = n_aEI$, which is sought.

Graphical equations to equation (6) may be readily obtained from the wide range of "A values" given in Chart I.

To obtain a solution from this chart, the curves plotted from generating equation A are used—which is equation (6), wherein the suffix $a$ is suppressed for simplicity. Having obtained experimentally the "initial derivative $a$," the corresponding value of $EIa$ is located along the A values up the ordinate through $n^2=0{\cdot}05$ on the abscissæ and the polar ray drawn—preferably on tracing-paper—through the point to the origin. The intersection of this ray with the appropriate L curve, interpolated from the vertical scale on the

CHART I.

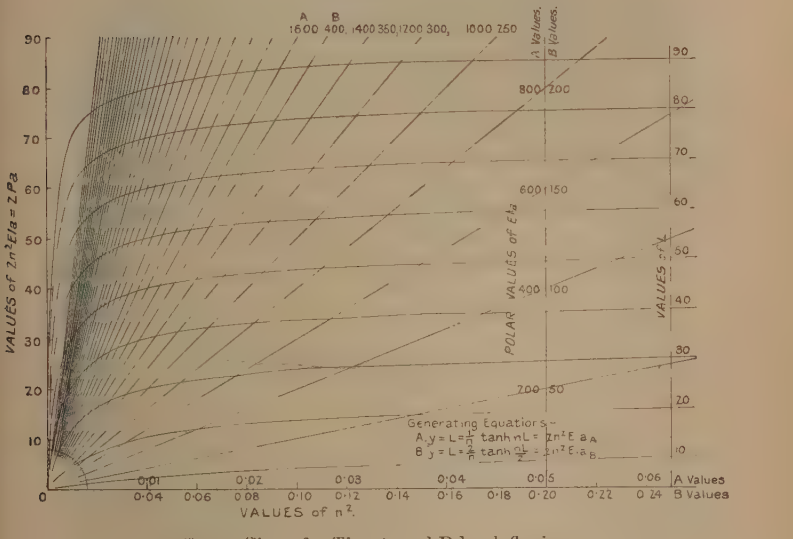


Stress Chart for Ties A and B by deflexion.

extreme right of the chart, locates a point vertically above the value of $n_a^2$ sought along the abscissæ scale of A values.

The initial direct stress ($f_d$) is thus found, since

$$f_d = P_a/A = n_a^2 E K^2,$$

where K is the radius of gyration of the cross-section of the member.

A simpler expression which may be used for an approximate solution is obtained by writing equation (6) as

$$2n_a^2 EIa = (L_a - 1/n_a) \quad . \quad . \quad . \quad . \quad . \quad (7)$$

since $\tanh n_a L_a$ rapidly approaches unity for values of $n_a L_a >$ about 4 ; and this value will be easily exceeded in ties of fair length and cross-section under moderate stresses: *e. g.*, for a tie-rod of mild steel 1 inch in diameter in which $f_a = 10{,}000$ lb. per square inch, $E = 30 \times 10$ lb. per square inch, and $L = 60$ inches,

$$nL = 4{\cdot}392.$$

For $\frac{3}{4}$ in. tie-rod of the same length under the above stress,

$$nL = 5{\cdot}850.$$

It should perhaps be here observed that the equations obtained in the foregoing case, and in all the following cases with hinged ends, are based upon the assumption that no friction couples exist about these transverse axes of constraint, and that results arising from this theoretical condition may, of course, be easily obtained in experimental work where friction slipping about the pins occurs, by taking two series of Y values : one series for increasing values of X, the other for decreasing values of X, so that the effect of friction may be neutralized by plotting the series of mean Y values against the one series of X values.

Fig. 5.


*Method* 1 A. *Alternative* :—

If, instead of measuring the deflexion at C, the slope $(dy/dx)$ be measured at either end, as shown at B in fig. 5, we shall get

$$dy/dx = \theta(\text{say}) = W(\tanh nL \,.\, \sinh nL - \cosh nL + 1)/2P$$
$$= W(1 - \operatorname{sech} nL)/2P = W(1 - \operatorname{sech} nL)/2n^2EI, \quad (8)$$

or

$$d\theta/dW \text{ (initially)} = a = (1 - \operatorname{sech} n_a L_a)/2n_a^2EI.$$

(*Tie equation* A ) ;

$$i.e., \; 2n_a^2EIa = 1 - \operatorname{sech} n_a L_a. \quad . \quad . \quad . \quad (9)$$

Here "$a$" is found by treating $\theta$ as Y, and W as X, as described in the "General Procedure." A graphical solution for $n_a$, and hence for $P_a$, may then be found by the aid of Chart II.

To use this chart, the experimental value of "$a$" having been found, the polar value of $1000\ EIa/L^2$ is next located up the ordinate through $n^2L^2=20$, or located along the top of the chart where these polar values are extended: then the polar ray is drawn. The point of intersection of this ray with the "A curve," projected on to the abscissa scale, gives the solution to $n^2L^2$, and thus to the solution of P.

Now, as $n$L increases, such $n$L rapidly decreases from

CHART II.

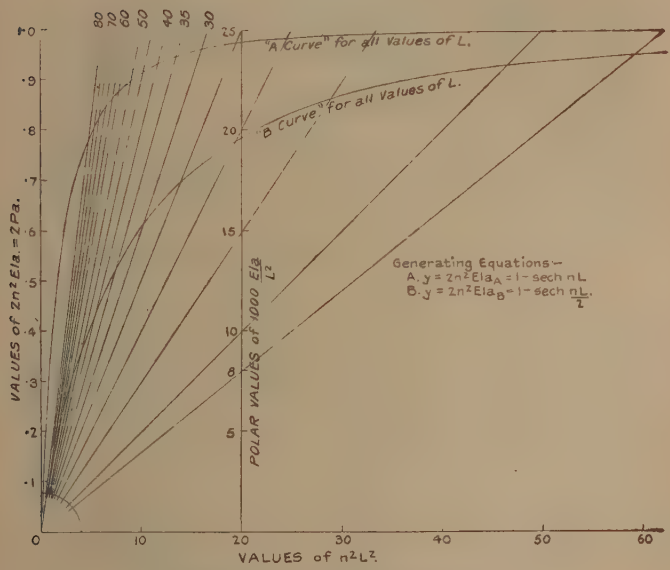


Stress Chart for Ties A and B by slope.

unity to a very small fraction, and, when $n$L > about 6, equation (9) may be written

$$a \doteqdot 1/2n_a{}^2EI \doteqdot 1/2P_a, \quad \text{or} \quad P_a \doteqdot 1/2a. \quad . \quad . \quad (10)$$

This is clearly shown by the "A" curve of Chart II.

*Method* 1 B :—

As in Method 1 A, but with ends constrained by fixing couples M, M in the line of action of P, instead of being pin-jointed. (See fig. 6.)

Using the same sign conventions as in Method 1 A, the bending moment at $+x$ from the origin O=

$$M_x = W(L-x)/2 + P.y - M = EId^2y/dx^2, \quad . \quad (11)$$

or $$d^2y/dx^2 - n^2y = (WL/2 - M)/EI - Wx/2EI. \quad . \quad (12)$$

The general solution to equation (12) is

$$y = A\cosh nx + B\sinh nx + Wx/2P + M/P - WL/2P \; . \; (13)$$

Fig. 6.


From this it follows that numerically at C, remembering that $y$ is negative,

$$\delta = -y_0 = W(L - 2n \,.\, \tanh nL/2)/2n^2EI \; ; \quad . \quad (14)$$

*i. e.*, initially,

$$\delta/W = 0/0 = a = \frac{1}{2n_a^2EI}\left(L_a - \frac{2}{n_a}\tanh n_aL/2\right). \; . \quad (15)$$

(*Tie equation* B$\delta$.)

Graphical solutions to this equation are given by the B values of Chart 1. In this case the solution to $n^2$ is located along the abscissa scale of B values by interpolation from the appropriate polar ray of EI$a$(B) values, and the curve of L as described for the corresponding Method 1 B.

Fig. 7.


As in Method 1 A, equation (15) will be found to reduce to a simpler approximate expression; for when

$$n_aL/2 > \text{about } 5, \quad \tanh n_aL/2 \doteqdot \text{unity},$$

and the above equation becomes

$$2n_a^2EIa \doteqdot (L - 2/n_a). \quad . \quad . \quad . \quad . \quad (16)$$

*Method* 1 B. *Alternative*:

By measuring the slope $\theta$ at L/2 from the origin, instead of the deflexion $\delta$ at the middle. (See fig. 7.)

From equations (11) and (13) we get

$$M_x = W(\tanh \frac{nL}{2} \cosh nx - \sinh nx)/2n \quad . \quad . \quad (17)$$

$$= 0 \text{ when } x = L/2 ;$$

*i.e.*, the point of inflexion and therefore of maximum slope $= \theta$ occurs at $\frac{1}{4}$ span from either end.

Also from equation (13)

$$dy/dx = \frac{W}{2P}(\tanh \frac{nL}{2} \sinh \frac{nL}{2} - \cosh \frac{nL}{2} + 1) = \theta$$

$$= W(1 - \operatorname{sech} nL/2)/2P. \quad . \quad . \quad . \quad . \quad . \quad . \quad (18)$$

Thus "$a$" here $= d\theta/dW$ (initially) $= (1 - \operatorname{sech} n_a L_a/2)/2n_a^2 EI.$

(*Tie equation* $B_\theta$). . . . . (19)

Graphical solutions to equation (19) may readily be found from the B curve of Chart II., which has been drawn to cover a very wide range. A solution to $n^2L^2$ is obtained from this chart by the intersection of the "B" curve for all values of L, with the polar ray given by the determined value of "$a$" in a similar way to that described for Method 1 A. Alternative.

In passing, it may be noted that for values of $nL >$ about 12, $\operatorname{sech} nL/2$ is a very small fraction, and therefore equation (19) becomes

$$a \doteqdot 1/2P_a \quad \text{or} \quad P_a \doteqdot 1/2a \text{ as in Method 1 A.}$$

It is important to observe that in all cases, only the the smallest possible measurable values of Y and X are necessary for the determination of the XY derivative, so that the range of cases as regards rigidity to which these flexing methods are applicable is controlled by the problem of accurate measurement or magnification.

The complete Thesis contains detailed descriptions of flexing apparatus designed by the author to test the applicability of the theoretical expressions established here, and others of much more general utility established later. The results obtained therefrom show that remarkable agreements exist between the theoretical and the practical results.

### *Units.*

It will be observed that throughout the series of stress charts (there are twelve in the complete series) units of force and of length are suppressed thereon. The reason for this

suppression lies in the fact—as a moment's consideration will show—that the charts hold for any system of consistent units whatsoever, and, since the quantity E is compounded of units of both force and length, the particular units applicable to any experimental determination will be those taken for E. Thus, if E is taken in pounds per square inch, length values (L) must be read off in inches, load values (P) in pounds, stress values ($f_d$) in pounds per sq. inch, and second moment of area values (I) in inches$^4$, or radius of gyration values (K) in inches. If E is taken in kilograms per square millimetre, L must be read off in millimetres, P in kilograms, $f_d$ in kilograms per square millimetre, I in millimetres$^4$, or K in millimetres.

In this way, and by a judicious choice of units—although on some of the charts only a few curves for L have been drawn,—these curves may be used for a number of actually different lengths by the expedient of altering the units of length to suit a chosen curve, thereby considerably extending the range of the chart used.

### *References.*

(1) "Tension Meters.—II." By Dr. A. H. Stuart. 'Model Engineer and Electrician,' p. 245, Feb. 28, 1924.
(2) "An Acoustic Tension Meter." By Dr. A. H. Stuart. Journal of the Royal Aeronautical Society, Feb. 1923, vol xxvii. no. 146.
(3) "Tensiometer for measuring Tautness of Airplane Wires and Cables." Miscellaneous Publications of the Bureau of Standards, no. 26, pp. 38–40, April 1, 1921.
(4) "Mechanical Testing.—I. and II.' By Batson & Hyde. D. U. Technical Series. Chapman & Hall.
(5) "Apparatus for measuring the Tension in Taut Wires.—Tautness Meter." Cambridge & Paul Instrument Co. P. 429 in ref. 4 above.
(6) "The Larson Tautness Meter." Developed by L. J. Larson. P. 430 in ref. 4 above.
(7) "The Tudsbery Stress Indicator." C. F. Casella & Co., Ltd., London.
(8) "Bureau of Standards' Telemeter for recording Strains in Bridges." 'World Power,' p. 254, May 1924; and Journal of Soc. of Automotive Engineers, p. 582, June 1924.
(9) "Measurement of Movements and Stresses in Structures," chap. xviii. Bib. 4, above.
(10) "The Fereday-Palmer Stress Recorder." 'Notes on the Analysis and Testing of Bridges.' By Mr. Fereday.
(11) "Sign Conventions applied to Flexing Problems." By the author. Philosophical Magazine, vol. v. April 1928.

(To be continued.)

C. *Oscillations in Low Pressure Discharge-Tubes.* *By* E. W. B. Gill, *B.Sc., M.A., Fellow of Merton College, Oxford* *.

MANY observers have noticed the occurrence of oscillations when direct current discharges pass in gases at low pressures ; but as no systematic investigation appears to have been made of the phenomenon the following experiments leading to a simple theory were carried out.

The discharge-tube T in the figure, contained two small circular electrodes, about 1 cm. in diameter, whose distance

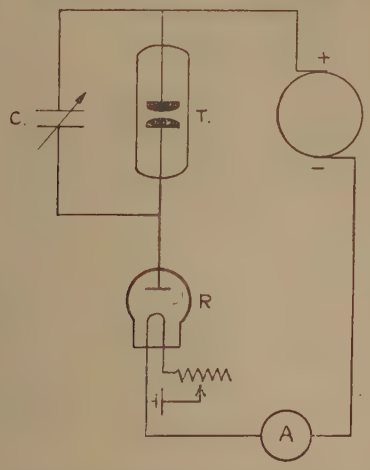


apart could be varied from a fraction of a mm. to about 1 cm. The tube contained air at a low pressure. A standard adjustable air-condenser C was connected externally across the electrodes, and a discharge was passed through the tube from a direct current high voltage dynamo. This current was maintained at any desired value by the insertion in one of the leads to the dynamo of a 2-electrode valve R. The discharge current had to pass across the valve and could therefore be adjusted to any desired value by controlling the temperature of the valve filament.

* Communicated by Prof. J. S. Townsend, F.R.S.

In this arrangement the potential across the discharge-tube is that necessary for the particular current passing, and the remaining potential of the dynamo falls across the valve. It was found that up to a limiting current of the order of 2 or 3 milliamps this discharge, over a very large range of pressures, produced oscillations varying in frequency according to circumstances from a few per second to about 150,000 a second.

The oscillations were detected and their wave-length determined by a single valve self heterodyning wireless receiver graduated in wave-lengths. This receiver was placed a few yards from the discharge-tube, which emitted quite enough energy to produce a loud signal.

The waves emitted were extremely rich in harmonics, and care was necessary not to confuse the fundamental with some of the louder harmonics.

### *Experimental Results.*

In what follows the fundamental wave-length $\lambda$ was found to depend on the following factors :—

1. The pressure $p$ of the air in the discharge-tube measured in mm. of mercury.
2. The distance $d$ between the electrodes.
3. The current $i$ flowing through the tube.
4. The capacity C of the condenser.

The results of varying one only of these factors keeping the remainder constant were as follows :—

1. *Pressure.*—Oscillations were examined from $p = 85$ to $p = 2$. It is difficult to get oscillations below $p = 2$, but they can be produced for much higher values than $p = 85$. The general effect of a reduction in pressure is a reduction in the wave length but the variation is not large.

2. *Distance between the Electrodes.*—The wave-length $\lambda$ increases rapidly as the distance is increased: thus for $p = 25$, $i = 2$ m.a. & C = 110 cm.; when $d = \cdot 7$ mm. $\lambda = 2700$ metres; $d = 1 \cdot 1$ mm. $\lambda = 4200$; and $d = 1 \cdot 5$ mm. $\lambda = 6800$. As the wave-length gets inconveniently large for the larger values of $d$ most of the measurements were made with small gaps.

3. *The Current.*—The current magnitude has a much greater effect upon the wave-length than any of the other factors. Thus for $p=25$ mm. C=110 cm., $d=\cdot 7$ mm. the corresponding values of $i$ and $\lambda$ are given below.

| $i$. | $\lambda$. | $\lambda i$. |
|---|---|---|
| ·5 m.a. | 10400 | 5·2 |
| ·75 | 6850 | 5·14 |
| 1 | 5250 | 5·25 |
| 1·25 | 4250 | 5·31 |
| 1·5 | 3500 | 5·25 |
| 1·75 | 3000 | 5·25 |
| 2 | 2700 | 5·4 |
| 2·25 | 2400 | 5·4 |
| 2·5 | 2100 | 5·25 |

The last column gives the product of $i$ and $\lambda$ and shows that very approximately $i\lambda$=constant; for small values of $i$ the oscillations are of audible frequency. A large number of sets of observations were made for various values of C and $d$, and in all cases $i\lambda$ was approximately constant in each set.

4. *The Capacity.*—As the capacity is increased the wave-length increases and the curve giving the relation between C and $\lambda$ is very accurately a straight line. The line does not pass through the origin and is given by the equation

$$\lambda=k\,(\mathrm{C}+c'),$$

where $k$ and $c'$ are constants; $c'$ is small and depends on the current, being larger for the larger currents.

For example, with $p=6\cdot 7$ $d=1\cdot 1$ mm.; when the current is ·21 m.a. the wave-length increases uniformly, being 8200 metres for C=15 cm. and 12,600 metres for C=40 cm.; here $c'=30$ cm.

For a current of 1·35 m.a. $\lambda$ increases from 2500 metres for C=15 to 6000 metres for C=100: in this case $c'=45$.

The final experimental result is therefore that

$$\lambda=\frac{k(\mathrm{C}+c')}{i};$$

$k$ depends only on $d$ and $p$ and increases if either is increased. $c'$ is small and depends chiefly on $i$ and decreases if $i$ is increased.

The following theory appears to be adequate to explain the experimental results:—Suppose that the valve filament is first of all heated to the temperature necessary to allow a current $i$ to pass the valve. At the moment when the external E.M.F. is applied practically all of it falls across the valve owing to its very small capacity. The current $i$ thus commences to flow instantaneously through the valve, and, provided the external E.M.F. is large enough, this current $i$ remains constant whatever happens in the rest of the system.

At the outset the tube insulates, the potential across it being low, and all the current $i$ flows into the condenser, and the potential across it and the tube increases until the sparking potential is reached. At this stage the tube begins to conduct and the current through it begins to grow from zero value; but as the constant current $i$ is still flowing into the combination a portion of it will still flow into the condenser until the discharge current has grown to the value $i$. At the instant, therefore, when current ceases to flow into the condenser the potential across it and the discharge-tube *is slightly above the sparking potential*, say $\nu_1$.

For air this state of affairs is essentially unstable; as the sparking potential is higher than that required to maintain a current, the potential cannot remain at $\nu_1$, the condenser begins to discharge through the tube, and the current through the tube begins to exceed $i$.

The relation between E.M.F. and current in a discharge-tube is that for zero current the E.M.F. is the sparking potential, and that as the current is increased the E.M.F. falls till it reaches a certain value $\nu_2$ corresponding to a current $i_2$, after which, however much the current is increased, the E.M.F. remains practically the same.

The superposition of the condenser discharge current upon the current $i$ flowing through the tube runs the potential across the tube down to this value $\nu_2$ and the condenser then ceases to discharge, as the P.D across it can fall no further. If $i$ is less than the critical value $i_2$ the discharge must go out, as the potential $\nu_2$ at this instant across the tube will only maintain currents equal to or greater than $i_2$. If $i$ is equal to or larger than $i_2$ the

discharge current remains constant, the condenser has no further effect, and no oscillations occur, which explains why no oscillations could be found unless the current was small.

For the small currents the discharge goes out and the current again all flows into the condenser, charging it from $\nu_2$ to $\nu_1$, at which point it again discharges, after which the process repeats itself indefinitely. The time for the charging is

$$C\frac{(\nu_1-\nu_2)}{i},$$

and if the time for discharge is $t_0$ the total time for one cycle is $C\frac{(\nu_1-\nu_2)}{i}+t_0$. But $\lambda$ is proportional to the total time of one cycle, and since $\lambda i$ was found to be constant if C is fixed, this shows, as might have been expected, that $t_0$ is indefinitely small; for $\nu_1$ and $\nu_2$ are constant and independent of $i$. Thus far, then, it has been proved that

$$\lambda \propto \frac{C}{i}.$$

It remains to account for the constant $c'$.

At first sight it might appear that stray capacities and the capacity of the electrodes might account for this, but these corrections cannot be more than a few electrostatic units while $c'$ is about 30.

It must be remembered, however, that when the potential across the condenser reaches its maximum value $\nu_1$ the gap is discharging, and its capacity is not solely due to the electrodes but is very much increased by the space charges. That this is the correct explanation is borne out by the fact that $c'$ increases if $i$ is increased.

Finally, therefore,

$$\lambda \propto \frac{(\nu_1-\nu_2)(c+c')}{i};$$

$\nu_1-\nu_2$ is the difference between the sparking potential and the minimum maintenance potential. This difference is increased if we increase the distance between the electrodes or raise the pressure, which is in accordance with the observed facts.

A simple experiment verified the deduction that $t_0$ is very small. A hot wire ammeter was placed to read the

current flowing into and out of the condenser. There is no possibility of resonance on the wave-lengths emitted, and the condenser current cannot therefore exceed the current flowing into the system. But when 1 m.a. was flowing through the 2-electrode valve the hot wire ammeter read as much as 30 m.a. This can only occur if the discharge current reaches momentarily a very high value causing the AC instrument to give a reading greater than the DC instrument.

The impurity of the emitted wave is evident from a consideration of the process occurring. The potential across the condenser rises uniformly from $\nu_2$ to $\nu_1$ and falls instantaneously to $\nu_2$ each cycle.

An application of Fourier's analysis indicates that in such a case the amplitude of the $n$th harmonic is $\frac{1}{n}$ of the amplitude of the fundamental.

The presence of the external condenser is not essential for the production of oscillations, the capacity of the electrodes magnified, as explained by the presence of the space charges, being sufficient to produce oscillations.

It appears, therefore, that any discharge-tube is in a state of oscillation provided that the sparking potential is higher than the maintenance potential and that the current is less than that at which the maintenance potential is independent of the current. At the higher pressures there is a fair range of currents over which oscillations occur, but at pressures of 2 or 3 multimetres they only occur if the current is a very small fraction of a milliampere.

It is scarcely necessary to add that the existence of oscillations in no way depends on the particular method of limiting the current by a valve. If the current is controlled instead by a large resistance oscillations occur equally well, but the calculations are not quite so simple.

Professor Townsend, in whose laboratory the experiments were made, has most kindly given me much advice and assistance.

---

(*a*)

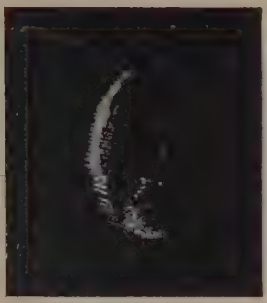

(*b*)

(*c*)

(*d*)

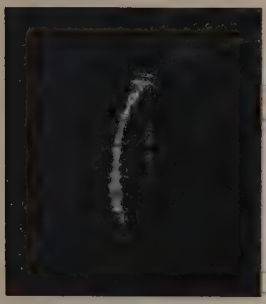

(*e*)

(*f*)

(g)

(h)

(i)

(j)

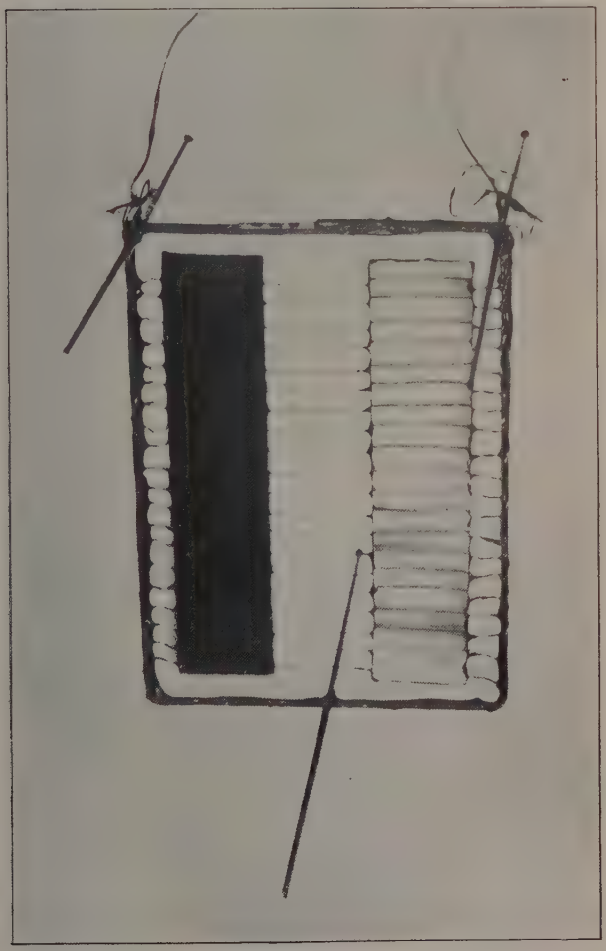

Radiation Instrument.

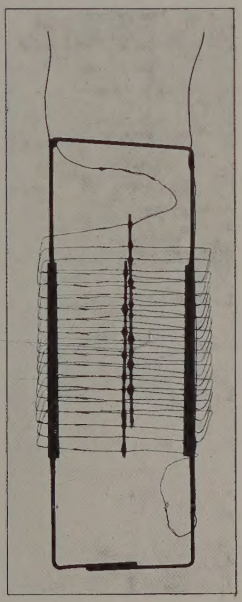

Convection Instrument.

Fig. 1.

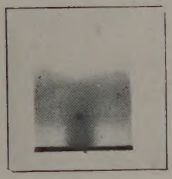

Fig. 2.

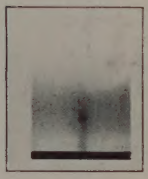

Fig. 3.

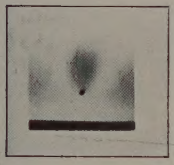

Fig. 4.

Fig. 5.

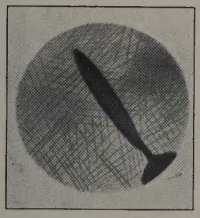

Fig. 6.